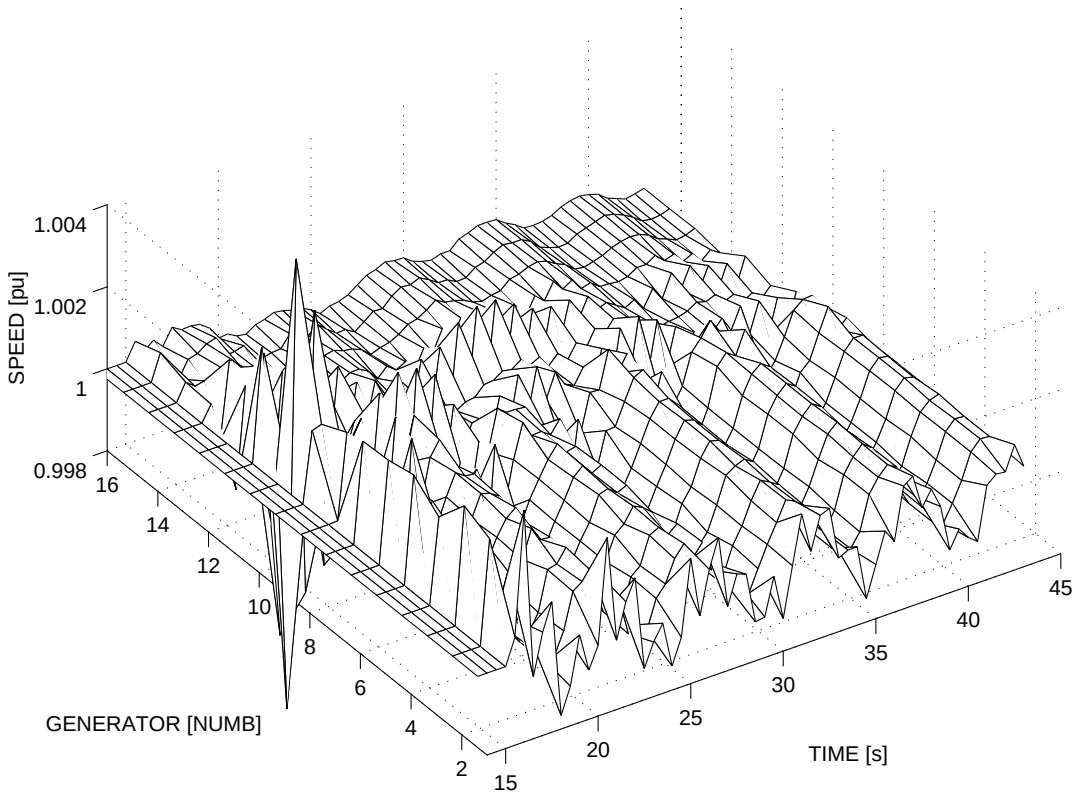

Protection Strategies to Mitigate Major Power System Breakdowns

Mattias Jonsson

Department of Electric Power Engineering
CHALMERS UNIVERSITY OF TECHNOLOGY
Göteborg, Sweden 2003

THESIS FOR THE DEGREE OF DOCTOR OF PHILOSOPHY

Protection Strategies to Mitigate Major Power System Breakdowns

by

MATTIAS JONSSON

Department of Electric Power Engineering
Chalmers University of Technology
Göteborg, Sweden 2003

Protection Strategies to Mitigate Major Power System Breakdowns
MATTIAS JONSSON
ISBN 91-7291-293-6

Doktorsavhandlingar vid Chalmers tekniska högskola
Ny serie nr 1975
ISSN 0346-718X

School of Electrical Engineering
Chalmers University of Technology
Technical Report No. 447
ISSN 1651-498X

Department of Electric Power Engineering
Chalmers University of Technology
SE-412 96 Göteborg
Sweden
Telephone: +46 (0)31 - 772 1660
Fax: +46 (0)31 - 772 1633

Cover: Inter-area modes in the 68 bus NPCC system.

Chalmers bibliotek, Reproservice
Göteborg, Sweden 2003

Abstract

This thesis deals with new methods to improve the performance of power system protection in the case of voltage- and transient instability. These methods are designed primarily to mitigate power system breakdown. Relay algorithms are proposed where conventional distance protection is combined with additional relay criteria. In case of voltage instability the criteria are based on the derivative of the voltage whereas the rate of change of the phase angle of the current is used for transient instability. For generator coherency determination a method based on wide area generator speed measurements and Fourier analysis is proposed. Using this method a concept for a System Protection Scheme addressing inter-area events is introduced. Finally, an emergency scheme based on conventional distance relays is proposed to avoid a complete system collapse in the case of severe voltage instability.

The performance of these new methods has been compared with conventional methods based on simulations using different test systems.

The proposed relay algorithms improve the relay security with respect to voltage instability whereas the reach of the distance protection is not restricted. Neither the line length, different swing frequencies or faults having a slowly decreasing impedance will affect the performance of the proposed schemes as may be the case when using conventional Power Swing Detectors. The fault clearing will also not be blocked as with conventional PSD applications. The proposed method for establishing generator coherency leads to almost identical results if compared with off-line methods as modal analysis or generator speed. Results obtained from phasor measurements however showed deviations. This work also demonstrates that, taking initial transient distortion after a contingency into account, a reliable coherency is faster obtained by the proposed technique than by methods using pure speed or generator voltage angle measurements. It has been demonstrated that the proposed emergency scheme can save part of the system from a voltage collapse. Black-start can then be avoided and the restoration time can be reduced.

Keywords: Distance protection, Generator coherency, Out-of-Step Protection, Power Swing Detectors, Voltage instability, System Protection Schemes, Transient instability, Wide Area Protection.

Acknowledgements

I owe my deepest gratitude to my advisor Professor Jaap Daalder. First for accepting me as a student, then for the support and help he has given me throughout the project. Finally for what I appreciate the most, that he has given me the feeling that his ”door is always open” when I had any kind of problem.

Dag Holmberg at Svenska Kraftnät is acknowledged for his efforts in arranging the financial support for this project. The members of my steering group Magnus Danielsson, Leif Koppari, Lars Wallin and Kenneth Walve are acknowledged for their valuable contributions. All group members are with Svenska Kraftnät. Additional staff at Svenska Kraftnät that I would like to thank for their help and support are Anders Edström, Anders Fransson (nowadays with Svenska Energihuset), Dag Ingemansson, Bertil Kielén, Allan Lundberg, Thomas Thor and Karl-Olof Jonsson. I also would like to thank the management of Svenska Kraftnät for funding the ARISTO computer.

ABB Power Systems are acknowledged for providing SIMPOW free of charge. Special thanks go to Sune Sarri, Lars Lindkvist and Jonas Persson for their valuable help with SIMPOW. In addition I would like to thank Stefan Arnborg, Svenska Kraftnät for being so generous with his ”dsl models” when I started to work with SIMPOW.

I am deeply grateful to Magnus Akke, Lars Messing and Daniel Karlsson, all with ABB Automation Technology Products AB, for their unrestrained way of sharing their great expertise in the area.

I would like to sincerely thank Associate Professor Miroslav Begovic at Georgia Institute of Technology, Atlanta, USA for accepting me as a visiting scholar in his research group during the spring and summer, 2002.

Annika, Arne, Jan-Olov and Valborg thank you for all help with various practical things, I really appreciate it.

Many thanks to all the staff and former colleagues at the Department of Electric Power Engineering for the pleasant working atmosphere and your friendship.

Finally, I owe my deepest gratitude to Jenny-Ann and my parents, for understanding, encouragement and love throughout this project.

LIST OF PUBLICATIONS

This thesis is based on the work reported in the following papers.

A Jonsson M, Daalder J, “An adaptive scheme to prevent undesirable distance protection operation during voltage instability”, Accepted for IEEE Transactions on Power Delivery.

B Jonsson M, Daalder J, “A new protection scheme to prevent mal-trips due to power swings”, IEEE/PES Transmission and Distribution Conference and Exposition, October 28 - November 2, 2001, Atlanta, USA. Proceedings Vol. 2, pp. 724 - 729.

C Jonsson M, Daalder J, ”A distance protection scheme to prevent mal-trips during abnormal power system conditions”, Cigré Study Committee 34 Colloquium and Meeting, September 10 - 14, 2001, Sibiu, Romania. Proceedings paper 113.

D Jonsson M, Begovic M, Daalder J, “A new method suitable for real time generator coherency determination”, Submitted to IEEE Transactions on Power Systems.

E Jonsson M, Daalder J, Begovic M, “A system protection scheme concept to counter inter-area oscillations”, Submitted to IEEE Transactions on Power Delivery.

F Jonsson M, Daalder J, Walve K, “An emergency strategy scheme based on conventional distance protection to avoid complete system collapse”, Accepted for IEEE/PES Transmission and Distribution Conference and Exposition, September 7 - 12, 2003, Dallas, USA.

Contents

Chapter 1 Introduction

1.1 Background and Motivation

At about 13.00 hrs. on Tuesday December 27, 1983, the Swedish electrical power system experienced the most severe disturbance of the last 30 years. The blackout resulted in a number of projects by the utilities and universities where different aspects of the collapse were investigated. Several projects analysed the behaviour of different power system elements such as generators, transformers and loads while other projects were addressing numerical methods intended to analyse events similar to the collapse.

These investigations of the 1983 blackout indicated that the performance of the relay protection system might had been deficient. At the same time developments in computer and communication technologies have significantly enhanced the potential for improved protection systems. As a result the project *Protection Strategies to Mitigate Major Power system Breakdowns* was initiated by Svenska Kraftnät[1] in co-operation with Chalmers University of Technology. The aim of the project has been to investigate the performance of the existing relay protection during abnormal operating conditions and to improve protection methods in order to avoid extensive system breakdowns.

The NORDEL system in Fig. 1.1 is a synchronous system involving Finland, Norway, Sweden and the part of Denmark east of the Great Belt. This system is connected to surrounding synchronized systems by HVDC interconnections. There are also two HVDC interconnections within the Nordel system; one from the middle part of Sweden to the south part of Finland and one from the Swedish mainland to the island of Gotland. The installed generation capacity for the NORDEL system amounts to about 80 000 MW. Approximately 50 % is hydro generation and 50 % thermal generation (oil, coal and nuclear).

In the Swedish electrical power system the main load centres are located in the central and south regions while a significant part of the generation is located in the north. The regions are separated by hundreds of km and thus the Swedish bulk power system involves

1. Regulator of the Swedish bulk power system.

large power transfers over long distances. Deregulation resulting in the decommission of (small) power plants in the south part of Sweden has further enhanced the radial characteristic of the system. The possibilities for local generator support in the case of abnormal operating conditions have obviously been reduced. In addition an increased variation of power flow directions has been experienced during recent years. As a result the main constraints for the NORDEL system are represented by power system stability issues.

The main ambition in this project has been to improve the protection performance during power system instability without jeopardizing fault clearance. During the first part of the project which was concluded by the licentiate degree, focus was given to local area protection schemes. Furthermore, in the second part concluded by the Ph.D degree focus was given to extensive protection systems involving large areas.

1.2 Outline of the Thesis

This dissertation is organized into two parts. The first part gives a background to the relevant topics while the second part includes six papers in which the main technical contributions from this project are presented.

The background and motivation for the thesis are given in Chapter 1 while Chapter 2 summarizes power system instability phenomena. Chapter 3 and Chapter 4 discuss the relevant relations between power system instability and power system protection. Chapter 3 treats local area protection while Chapter 4 discusses System Protection Schemes. Chapter 5 briefly introduces the papers enclosed in the second part of this dissertation. Finally, the conclusions and suggestions for future work are presented in Chapter 6.

At the end of part 1 an appendix and the references of the six first chapters are included.

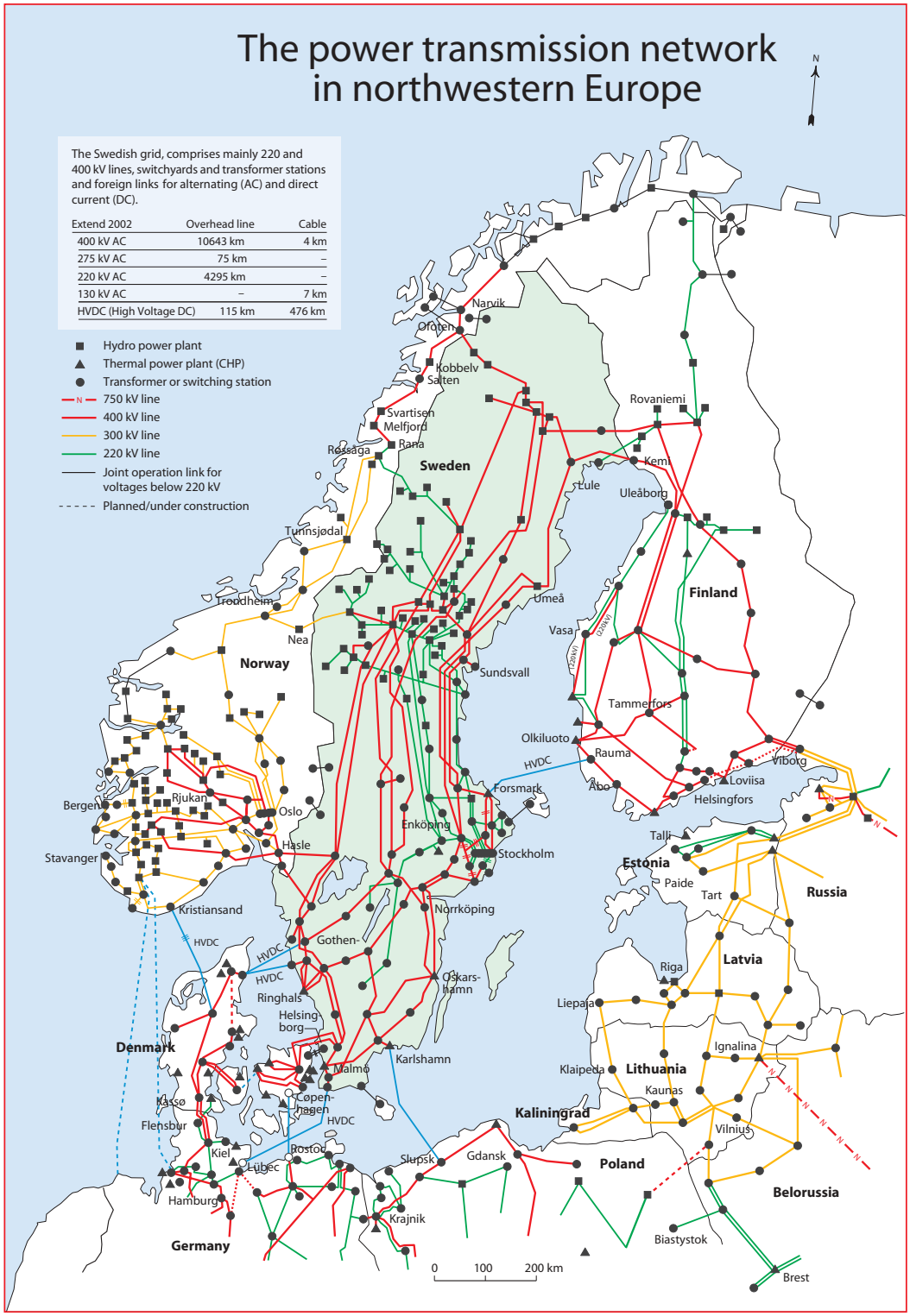

Figure 1.1 The NORDEL system.

Chapter 2 Power System Instability

In this section a brief summery of power system instability is given. The different types of power system instability are further described by Kundur [1] while attention here is given to instability aspects relevant to power system protection. In particular the focus is on the relation between grid configuration and system instability due to its importance in the case of protection applications. For simplicity the different types of power system instability are discussed separately. During a severe disturbance some of these phenomena may occur simultaneously though.

2.1 Angle Instability - Power Oscillations

The fundamental phenomena appearing in a power system in case of angle instability are power oscillations. Depending on their severity and origin they are categorised as transient angle instability or small-signal angle instability.

Generally power oscillations can be divided into three different categories; **1)** *local plant mode oscillations or inter machine oscillations with a frequency range of 0.7 - 2 Hz (6 Hz),* **2)** *inter-area oscillations, where groups of generators are swinging against each other in the frequency range of 0.4 - 0.7 Hz* and **3)** *large sub-systems oscillating against each other where the swinging frequency usually is in the order of 0.1 - 0.3 Hz.*

2.1.1 Transient Angle Instability

According to Kundur transient stability is the ability of the power system to maintain synchronism when subjected to a severe disturbance such as a fault on transmission facilities, loss of generation, or loss of a large load [1]. Usually this type of disturbances leads to large excursions of generators angles and significant changes in active and reactive power flows, bus voltages, system frequency and other system variables. Accordingly both the customers and the power system are confronted to these features where they have a more or less developed transient characteristic. In case appropriate counteractions are not taken transient instability may result in extensive power system blackouts.

Loss of synchronism may include one single generating unit, a power plant represented by multiple generators, a region of the network or several interconnected regions. The loss of synchronism may occur during the first swing after the disturbance or after a number of divergent oscillations. In the first case the mismatch between the electrical and mechanical torque is considered to be the main issue while insufficient damping is associated to loss of synchronism after a few swings.

Lightly meshed networks, large power flows and long distance power transport are features which contribute to transient angle instability. Accordingly tie-lines, bottlenecks and weak interconnections (between different countries) are typical sources of transient instability. As transient instability includes large voltage and power variations, fast tripping of power system devices may be initiated due to undesirable protection operation. This is especially true for some generator and line protection [2].

2.1.2 Small-Signal Angle Instability

Small-signal stability is the ability of the power system to maintain synchronism when subjected to small disturbances. In this context, a disturbance is considered to be small if the equations that describe the resulting response of the system may be linearized for the purpose of analysis [1]. Such disturbances happen all the time due to small variations in loads and generation. The physical response of the system may be a steady increase in rotor angle due to lack of synchronizing torque or rotor oscillations of increasing amplitude due to lack of sufficient damping torque. Important to observe is that although the initial phase can be described by linear behaviour the consequences of these oscillations could be non-linear.

Measures to counteract small-signal instability are usually based on closed-loop controls. These devices provide dynamic control of electric quantities of the power system. Typical examples of closed-loop control devices include generator excitation control, power system stabilizers (PSS), Static Var Compensators (SVCs) and series capacitors with a closed-loop controlled varying capacitance. Closed-loop control devices are not included here as they fall outside the scope of the project.

Normally, power oscillations associated with small-signal stability have amplitudes which are non-relevant to protection applications. Consequently, in this report we will exclusively discuss the interaction

between transient instability and protection applications. However, in case small-signal instability results in power oscillations relevant to protection applications the fundamental principles and relevant issues applicable to transient instability are also true for small-signal instability.

2.2 Voltage Instability

Voltage stability is concerned with the ability of a power system to maintain acceptable voltages at all buses in the system under normal conditions and after being subjected to a disturbance. A system enters a state of voltage instability when a disturbance such as an increase in load demand or a change in system conditions causes a progressive and uncontrollable decline in voltage. The main factor causing instability is the inability of the power system to meet the demand for reactive power [1]. According to the time duration of load response, voltage instability can roughly be divided into two different categories; short-term and long-term voltage instability. Induction motors restore their active power consumption within one second (short-term) while Load Tap Changers (LTCs) will restore voltage dependent loads within one to several minutes (long-term). Also thermostatically controlled loads have a recovery time in the range of minutes. In case of long-term voltage instability generator current limiters may be activated to protect the generators from thermal stresses. When current limiters are activated the operating condition of the power system is often seriously aggravated. Particularly armature current limiter activation often leads to blackouts. In many situations the distinction between voltage and transient instability is diffuse as aspects of both phenomena may exist for a single disturbance.

Voltage instability may be caused by a variety of single and/or multiple contingencies. Typical initiating events are heavy load pick-up and grid weakening. Obviously generator tripping also contributes to voltage instability; especially tripping of generators located close to the loads supporting the voltage control in that area. Generator tripping can be the event which initiates voltage instability, but it may also be an accelerating element when it occurs some time into a voltage instability event.

In case of short-term voltage instability the system may collapse within a few seconds after the disturbance if no curative measures are taken.

For short-term voltage instability the fault clearing time may be essential as an induction motor dominated load, e.g air conditioning, may become unstable if the fault is present for a longer period.

During long-term voltage instability the power system normally reaches a quasi-stable low voltage operating point after the initial disturbance. Because of the voltage drop LTCs will start to restore the voltage on regional transmission and distribution levels. In turn the loads recover which leads to increased system loading. Consequently the voltage will further decline and the LTCs will operate again to restore the loads. This interaction between LTCs and increased system loading continues while the voltage on the transmission level declines continuously. The reactive power demand of the system is continuously increasing as the voltage is decreasing. Eventually the reactive power demand cannot be supplied by the generators and their current limiters operate. At this moment the voltage decay accelerates significantly, which in turn leads to generator tripping due to low voltage and cascading line outages due to overload. The voltage decay due to LTCs is obviously restricted to the operating range of the tap-changers.

In case of a heavy load pick-up in a highly meshed network the crucial aspect with respect to voltage stability will initially be related to whether local generators manage to meet the increased load demand without hitting their limits. As when the local units hit their limits, stability will depend on the capability of the surrounding system to provide active and reactive power. If the surrounding system is strong it will be able to support the highly loaded area successfully. However, if the surrounding system is weak a sufficient support will most likely not be given and the situation may aggravate to a voltage collapse. Generally speaking the more circuits and the shorter the lengths of the circuits in the grid, the stronger the network.

When a long distance separates a load centre from a significant amount of supply, a grid weakening between the two areas may lead to voltage instability. The remaining grid may not have the capability to transport the required power at a sufficient voltage level, which in turn increases the reactive power demand from the system and the tap-changer interaction as discussed above. Moreover this may lead to generators hitting their limits, cascading lines outages because of (distance) relays operating on overload and eventually to a collapse.

The case where generators located close to loads are tripped is similar to the case of a heavy load increase. Also in this case the stability will be decided by the capability of the surrounding system to provide active and reactive power to the area lacking generation.

To summarize, voltage instability is especially likely for system configurations where large amounts of power have to be transported long distances in a lightly meshed network as in the case for weak interconnections between remote generation areas and load centres.

In addition to the network configuration also the following aspects are important as far as voltage stability is concerned:

- Active and reactive power reserves. For example, generators, synchronous condensers and SVCs. Both the amount of available reactive power and the location are important.
- Passive reactive power reserves such as capacitors.
- System loading levels. High loading levels are critical.
- Low power factor.
- Load characteristics. Especially the load recovery due to LTC operation as discussed above (or thermostatic heating).

2.3 Frequency Instability

Frequency stability describes the ability of a power system to maintain the system frequency within an acceptable range during normal operating conditions or after a severe disturbance. Thus frequency instability occurs when there is a mismatch between load and supply and the system cannot compensate for this mismatch before the frequency reaches an unacceptable value. Typical events which may lead to frequency instability are major outages of generating units and splitting of the system into isolated areas.

In case normal frequency control measures fail to maintain the frequency within an acceptable range, it is still important to limit frequency excursions. Especially generators are sensitive to fairly small frequency deviations. Normally generators can operate within a band of ±0.5 Hz related to nominal frequency (50 and 60 Hz systems) without any restrictions. Additionally generators can operate outside

these values for a limited time period given by manufacturing constraints.

Publication [3] refers to an example of typical steam turbine limitations during abnormal frequency conditions where the worst case limitations have been specified by five turbine manufactures with respect to 60 Hz operation [4]. The example indicates that operation between 58.5 and 57.9 Hz is permitted for ten minutes during the generator life time before turbine blade damage is probable. Note that steam turbines may be considered to be the weakest link with respect to low frequency operation. In Sweden thermal power units are tripped around 47.5 Hz to protect the steam turbines against detrimental vibrations. The hydro units in operation are more robust and can handle operating frequencies down to 45 Hz [5].

Due to its nature protection applications responding to frequency instability are normally rather straightforward. For example, unit devices protecting equipment from damage in the case of frequency excursions should respond to a certain frequency deviation present for a specified duration. Accordingly, simple frequency relays with settings relevant to the current application can be used. Similarly the process for System Protection Schemes responding to frequency instability is also straightforward, although extensive setting procedures in order to obtain the optimal curative measures may be required. Hence, no further attention is explicitly given to frequency instability in this dissertation. Still there is a close relationship between frequency- and transient instability and as far as undesirable distance protection performance is concerned, the discussion in section 3.2 is also relevant to events involving frequency instability.

2.4 The Relation Between Network Configuration and System Instability Phenomena

As indicated above the network configuration where large amounts of power have to be transported long distances over weak interconnections is vulnerable with respect to power system instability. In Table 2.1[1] a rough classification has been made with respect to the relation between network configuration and the different power system instability phenomena. The different system structures can roughly be

1. The table was originally introduced in [3].

divided into densely meshed transmission systems with dispersed generation and demand or lightly meshed transmission systems with localised centres of generation and demand. Furthermore the coupling of the local sub-system to the surrounding system can also be given a classification. The first characteristic includes transmission systems which are parts of larger power networks. The second characteristic includes transmission systems that are not synchronously interconnected with neighbouring systems or the largest partner in the current power network.

Table 2.1: The relation between network configuration and power system instability phenomena.

	Densely meshed system with dispersed generation and demand	**Lightly meshed system with localised centres of generation and/or demand**
Sub-system being a part of a large power network	Small-signal instability Thermal overload No large frequency variations	Transient instability Small-signal instability Voltage instability
Separate systems not synchronously interconnected to other systems. Systems by far the largest sub-system in a power network	Thermal overload Large frequency variation	Transient instability Voltage instability Large frequency variation

Chapter 3 Power System Instability and Local Area Protection

During a power system instability the presence of negative or zero sequence currents is usually limited. Therefore, protection schemes responding to unbalanced operation should be unaffected by instability events. Most relays respond to a quantity directly linked to the safe operation of the particular system component protected by the relay unit. Irrespective of the surrounding system status, the relay should operate when the relay criteria reach the tripping level(s) in order to avoid equipment damage. Also this type of protection devices is of less importance as far as power system instability is concerned. Finally, there is a class of relays responding to the impedance calculated from measured voltages and currents. Distance protection belongs to this class and is mainly used as line protection, but can also be utilized for generators. For generators the impedance protection is used against internal short circuit- and/or loss of excitation. Generator impedance protection is of less concern with respect to power system instability due to limited reach and its reverse characteristic. However, in the case of strong transmission networks the concerns associated to transient instability and line distance protection may be more relevant to the generator protection. In this chapter the focus is on line distance protection as all relevant phenomena are then included. At the same time identical fundamental concepts can be applied on any relevant issue involving generator impedance protection.

3.1 Distance Protection and Voltage Instability

Here the performance of distance protection during *long term* voltage instability is discussed. The behaviour of distance protection during short term voltage instability is similar to the performance during transient instability. For the relation between short term voltage instability and distance protection the reader is referred to section 3.2.

3.1.1 Distance Protection may Contribute to Voltage Instability

One can define 10 distinct types of possible short circuit faults in a three phase power system [6]. In order to calculate the correct fault distance for all types of faults, different voltage and current signals are used by the distance relay. Basically two types of equations are applied. For three phase faults and phase to phase faults (3.1) is used

where L1 and L2 are the faulted phases. Equation (3.2) is valid for phase to ground fault involving phase L1.

$$\overline{Z_r} = \frac{\overline{U}_{L1} - \overline{U}_{L2}}{\bar{I}_{L1} - \bar{I}_{L2}} \tag{3.1}$$

$$\overline{Z_r} = \frac{\overline{U}_{L1}}{\bar{I}_{L1} + \frac{\overline{Z_0} - \overline{Z_1}}{\overline{Z_1}} \cdot \bar{I}_0} \tag{3.2}$$

$\overline{U}_{L1}$, $\overline{U}_{L2}$: Phase voltages at the relay location.

$\bar{I}_{L1}$, $\bar{I}_{L2}$: Phase currents at the relay location.

$\bar{I}_0$: Residual (zero sequence-) current at the relay location.

$\overline{Z}_1$: Positive sequence impedance for the primary protected circuit.

$\overline{Z}_0$: Zero sequence impedance for the primary protected circuit.

$\overline{Z}_r$: the apparent impedance as seen by the distance relay.

Voltage instability is a phase symmetrical phenomenon. Hence no zero sequence component is present and the phase voltages and currents are symmetrical. Thus the apparent impedance $\overline{Z}_r$ as seen by a distance relay during voltage instability is given in (3.3). Here $\overline{U}$ is the line to line voltage and P and Q are the injected active and reactive power at the location of the relay.

$$\overline{Z_r} = \frac{\overline{U}_{L1}}{\bar{I}_{L1}} = \frac{\left|\overline{U}\right|^2 \cdot (P + jQ)}{P^2 + Q^2} \tag{3.3}$$

In case $\overline{Z}_r$ remains within the area of one of the pre-defined tripping zones during a time exceeding the setting of the timer associated to the zone, the relay will operate. Low system voltages and high (reactive) power flows are typical for voltage instability events. It follows from (3.3) that these events will lead to a reduced apparent impedance which in turn may result in undesirable relay operation. This behaviour is normally devastating as the system already is in a critical operating condition.

Case **a** in Fig. 3.1 corresponds to a short circuit fault while case **b** corresponds to a scenario where the zones of operation are slowly (seconds to minutes) approached from outside as the voltage decreases and/or the reactive power increase. Undesirable relay operations due to voltage instability will then mainly be initiated by the zone with the longest reach. Normally this is the zone used for remote back-up protection; i.e zone 3. In some applications start elements are applied which have a longer reach than the zone 3. However, they can usually not trip the line but only activate the tripping elements.

The sensitivity for mal-trips due to voltage instability is depending on the length of protected lines, the relay characteristic, the devices used to prevent load encroachment, the safety margins concerning overload and the robustness of the system. Also the *protection philosophy* in the setting process of the distance relay with the longest reach is important; is dependability or security emphasized?

Paper A proposes a method to avoid incorrect distance relay tripping in the case of voltage instability.

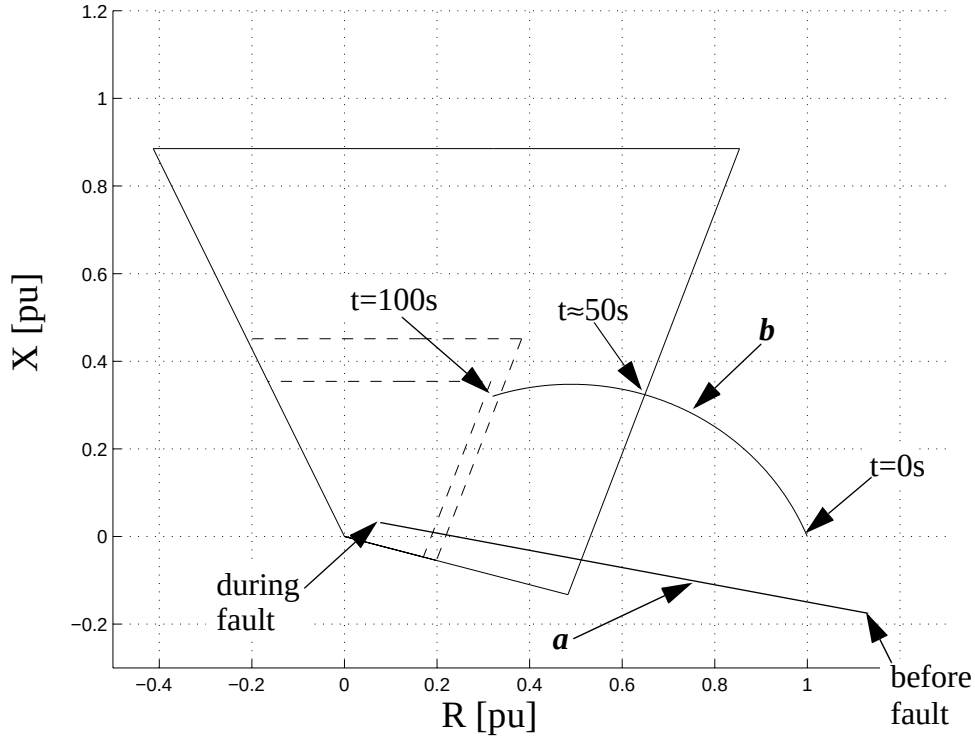

Figure 3.1 Apparent impedance as seen by a distance relay during different power system events. ***a***: Short circuit fault involving the primary protected circuit. ***b***: A case where the voltage linearly decreases from U=1 pu to U=0.8 pu and the reactive power linearly increases from Q=0 pu to Q=1 pu during a time interval of 100 s. The injected active power is held constant at P=1 pu.

3.1.2 Worldwide Experience on Voltage Collapse Related to Distance Protection

Undesirable distance protection operations during long term voltage instability have contributed to blackouts worldwide. About 52 seconds after the initiating event in the Swedish blackout in 1983 [7-11], at a voltage level of approximately 300 kV, a distance relay located in the receiving end of the long distance transmission line between Kilforsen and Hallsberg operated. Roughly 1 second later cascading outages followed and almost instantaneously south Sweden experienced a blackout. About 65% of the pre-fault load was lost. As distance protection usually is directional it may seem a bit remarkable that the relay in the receiving end of the line between Kilforsen and Hallsberg operated. However the relay was operated in such a way that when the apparent impedance remained within the start zone for a time longer

than 3.2 seconds without relay operation, the start element alone initiated tripping. In such a case the relay behaved as a non-directional unit with a long reach having a circular impedance characteristic, where operation due to load encroachment was not obstructed.

On July 2, 1996 the WSCC system was operated within its transfer limits and only a few facilities were out of service [12-14]. Due to a single phase to ground fault resulting in remedial actions, and incorrect relay operation as a result of mechanical failure the system was significantly weakened. About 24 seconds after the initial fault an important 230 kV line tripped through its zone 3 relay due to moderate overload and moderate voltage depression. Cascading outages resulted and approximately 10 seconds later the system had separated into five electrical islands. About 2 million customers were affected by the disturbance. Furthermore, a zone 3 distance relay operated incorrectly during the restorative process due to load encroachment and delayed the restoration of the system.

On March 11, 1999, Brazil [15] faced the most severe power interruption in its history. About 72 % of the pre-disturbance load amounting to 34 200 MW was affected. The initiating event of the blackout was a phase to ground fault in a substation which led to the loss of five incoming 440 kV lines. The system survived this contingency and recovered to a quasi stable operating point. About 12 seconds after the phase to ground fault another line tripped. Cascading outages followed and approximately 18 seconds later the entire network collapsed. The tripping of the line after 12 seconds was initiated by the start unit of the distance protection. The start unit had the longest reach of all zones of operation to provide remote back-up for all adjacent lines which are much longer than the given line. The start unit had been given a setting corresponding to a very long reach with an associated time delay of 1.5 seconds. Hence, when the line loading increased after the initial fault and likely in combination with an increasing reactive power demand throughout the entire system, the apparent impedance entered the start zone and the relay operated.

Further examples where undesirable (zone 3) distance protection operations have contributed to blackouts include the ¨November 9, 1965 Northeastern U.S/Canada disturbance and the August 22, 1987 Western Tennessee U.S blackouts [16].

3.2 Distance Protection and Transient Instability

Power oscillations are inherent to power systems. They may result from any power system event such as line switching, short circuit faults, generator tripping or load shedding. During normal operation the magnitude of the oscillations are usually small and quickly attenuated. However, during abnormal operation the oscillations can be severe and are in some cases of an increasing nature. In this section the relation between power oscillations and distance protection is examined.

3.2.1 Distance Protection During Transient Instability

Referring to the frequency range of power oscillations given in 2.1 power oscillations may be the source of incorrect relay behaviour as the cycle times of the oscillations are in the same time range as the timer settings of the protection devices.

The two machine system in Fig. 3.2 can be used to analyse the performance of distance protection during power oscillations. The machines are interconnected through a 200 km long transmission line and they are represented by voltage sources with constant magnitude behind their transient reactance. By studying the apparent impedance as seen by a relay located at C for different transfer angles the effect of power oscillations can be examined. The analysis made in this section is similar to the one given by Kundur in [1].

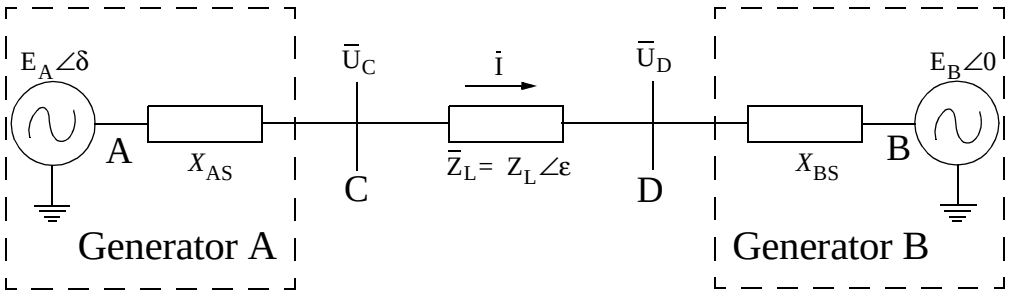

Figure 3.2 Two machine system.

In Fig. 3.2, $\overline{E}_A$ and $\overline{E}_B$ are the internal voltages of the machines and X_{AS} and X_{BS} are the transient reactances. $\overline{E}_B$ is assumed to be the reference phasor and δ represents the angle by which $\overline{E}_A$ leads $\overline{E}_B$. Hence the current $\bar{I}$ is given in (3.4) and the voltage $\overline{U}_C$ in (3.5).

$$\bar{I} = \frac{E_A\angle\delta - E_B\angle 0}{jX_{AS} + \bar{Z}_L + jX_{BS}} \tag{3.4}$$

$$\overline{U}_C = E_A\angle\delta - jX_{AS}\bar{I} \tag{3.5}$$

The apparent impedance as seen by the relay at C during phase symmetrical operation can be determined when (3.4) and (3.5) are inserted into (3.6).

$$\bar{Z}_C = \frac{\overline{U}_C}{\bar{I}} = \frac{E_A\angle\delta}{\bar{I}} - jX_{AS} \tag{3.6}$$

$$\bar{Z}_C = -jX_{AS} + (jX_{AS} + \bar{Z}_L + jX_{BS}) \cdot \frac{E_A\angle\delta}{E_A\angle\delta - E_B\angle 0} \tag{3.7}$$

Fig. 3.3 shows the locus of $\overline{Z}_C$ as a function of the transfer angle δ in the RX-diagram when different ratios of the magnitude of the internal voltages of the generators are applied in (3.7). The zones of operation of the relay are set to cover 80%, 120% and 200% of the line length, respectively.

During a power swing the transfer angle δ will vary. For a stable swing, δ gradually increases until the maximum value is reached where the trajectory shifts direction and δ decreases until the minimum value is reached where the trajectory ones again shifts direction. This sequence of events is repeated until the oscillations are damped out. If the trajectory of δ reaches beyond 180 degrees the swing can be considered to be unstable.

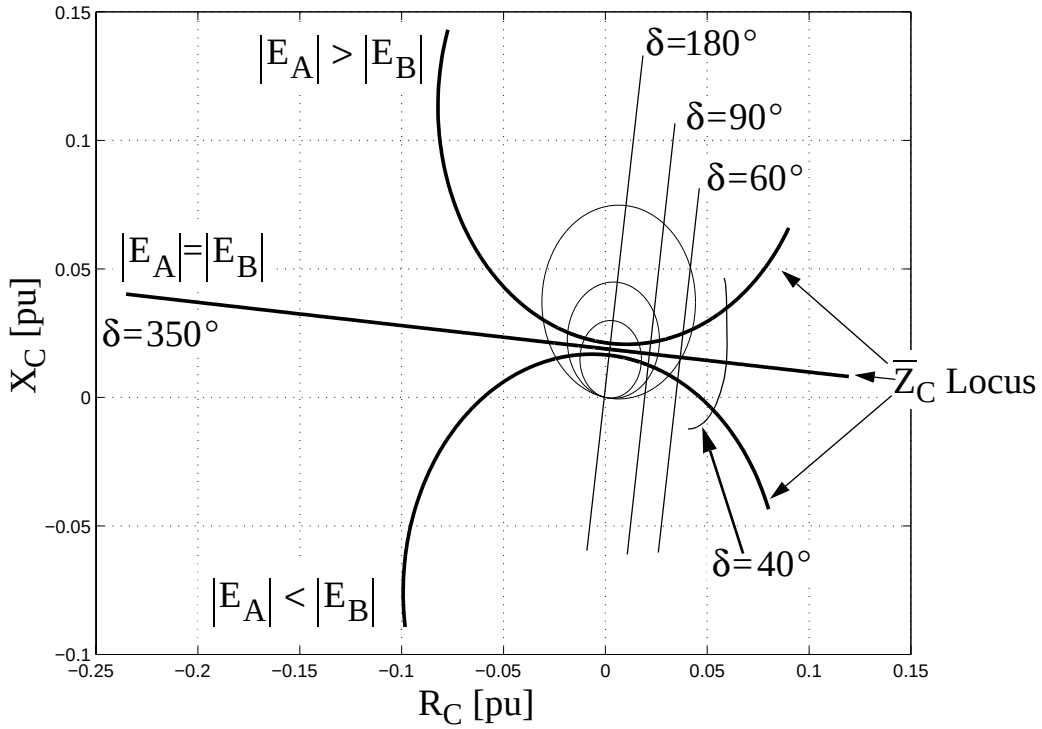

Figure 3.3 The locus of $\overline{Z}_C$ (bold curves) for different values of the ratio $|E_A|/|E_B|$ when δ is increased from 20° to 350°. Specific values of $\overline{Z}_C$ at a given transfer angle δ are given by the intersection of the locus of $\overline{Z}_C$ and the characteristic for constant δ. In addition the three zones of operation of the relay are indicated.

For the transfer angle δ=0, the current $\bar{I}$ in (3.4) is zero and thus the apparent impedance $\overline{Z}_C$ is infinite. As the transfer angle increases the apparent impedance $\overline{Z}_C$ moves towards, and enters the zones of operation eventually. Fig. 3.4 shows that the point where the locus crosses the total system impedance corresponds to a transfer angle of 180 degrees. If the angle reaches 180 degrees loss of synchronism occurs (a pole is slipped for generator A). Unless the system is separated by protective devices the initial pole slipping will be followed by repeated pole slips in rapid succession. During pole slipping the voltages and apparent impedances at points near the *electrical centre*, i.e the intersection point between the system impedance and the δ trajectory, oscillates rapidly. Furthermore, the voltage at the electrical centre is zero for a transfer angle of 180 degrees. Consequently the relay at C will actually see a three phase fault at the electrical centre. In case of identical internal voltage magnitude the locus of $\overline{Z}_C$ is a straight line. The impedance loci are

circles with their centres on the extensions of the impedance line AB in case the internal voltage magnitude differ. For $|E_A| > |E_B|$ the electrical centre will be above the impedance centre while it will be below when $|E_A| < |E_B|$.

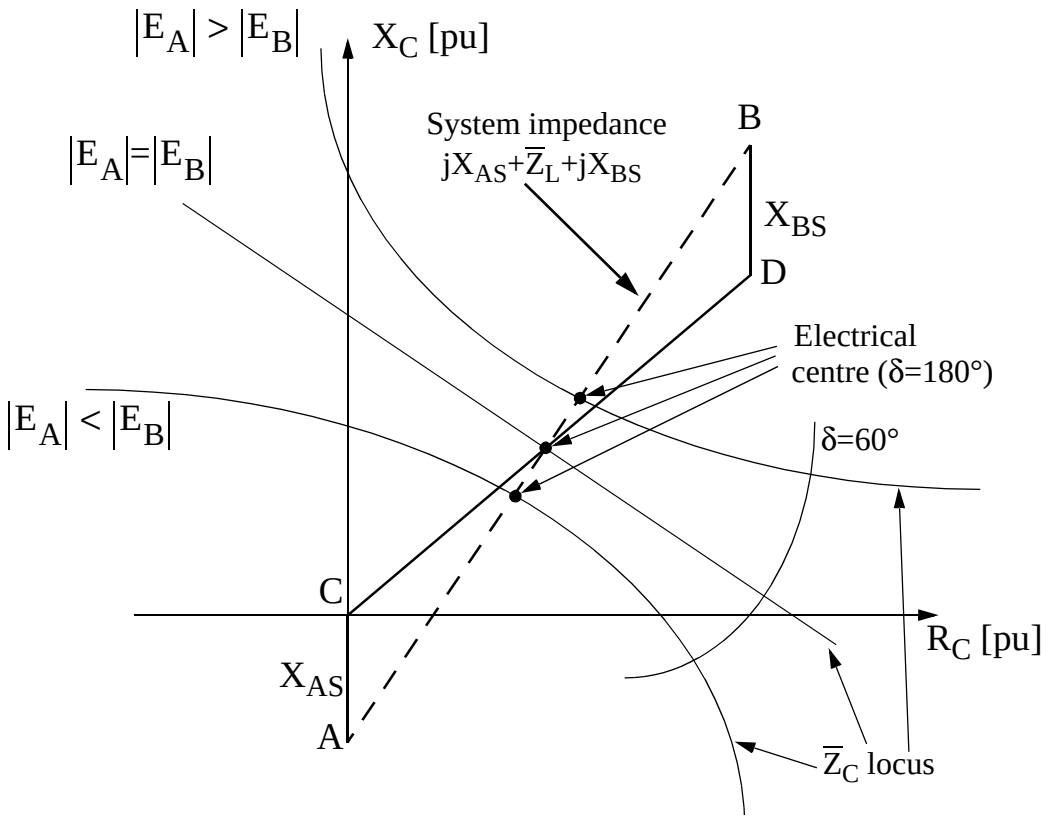

Figure 3.4 The electrical centre for the two machine system in Fig. 3.2.

Fig. 3.3 indicates that when a power swing with a given cycle time reaches a certain angle the apparent impedance will remain within a tripping zone during a certain time period. The timer of the zone may expire and consequently the relay operates. In this way the distance relay may operate undesirably for a stable power swing. The relay type strongly influences the sensitivity for this type of mal-trips. Numerical relays usually reset the associated timer when the apparent impedance leaves the tripping zone. This means that the impedance must remain within the area of the tripping zone during the entire timer setting period to initiate a tripping signal. For relays supervised by a start element, the apparent impedance must not always remain within the tripping zone during the entire timer setting period to initiate tripping. As the timers usually are not reset until the impedance leaves the start zone. Hence, as long as the impedance remains within the area

associated to the start element the impedance can enter, leave and re-enter the zones of operation unlimited times and the timer will in any case continue to count. This means that a tripping signal is generated immediately when the zone of operation is entered after the timer has expired. If the start element has a shape which surrounds all the tripping zones the area which decides the likelihood for mal-trips due to power swings has increased. Therefore it is very important to take this effect into account when power oscillations are considered with respect to undesirable distance protection operations.

Fig. 3.3 and Fig. 3.4 illustrate the impedance trajectories for a relay located in the sending end of a line. The trajectories for the receiving end are identical but reversed.

Observe that the assumption made above where the internal machine reactance and voltages are given fixed values is a rough reflection of the system behaviour suitable for illustration. In real operation the electrical centres are non-fixed points as the internal machine impedances and voltages will vary during dynamic conditions.

Distance protection should not operate for stable swings. However, in the case of unstable power swings the protection system should operate to divide the system into stable sub-systems or to separate the ”sick” part of the system from the ”healthy” parts. The issue is further discussed in the next section.

3.2.2 Power Swing Detectors - Out-of-Step Protection

Different approaches for Power Swing Detectors and Out-of-Step Protection have been suggested throughout the years. In [17] a method to avoid mal-trips due to high frequency (above 6 Hz) power swings is proposed based on the phase angle of the voltages at the line terminals and at the fault location. The method is restricted to avoid zone 1 mal-operations due to power swings. Another indicator is proposed in [18-20] where tripping is prevented if the rate of change of an electric quantity exceeds a threshold value. In [21] decision trees are used to classify a transient swing on the basis of real-time phasor measurement. Furthermore, neural networks are used in [22] to detect power swings. An adaptive out-of-step relay is proposed in [23,24] which uses the equal area criterion and GPS technology. Also the algorithm introduced in [25] applies the equal area criterion to assess the stability of the generators and determine when pole-slipping will occur. In [26] circle fitting and parameter estimation are applied to discriminate power swings from faults. However, the most common

method used for Power Swing Detectors and Out-of-Step Protection is based on the transition time through a blocking impedance area in the RX-diagram.

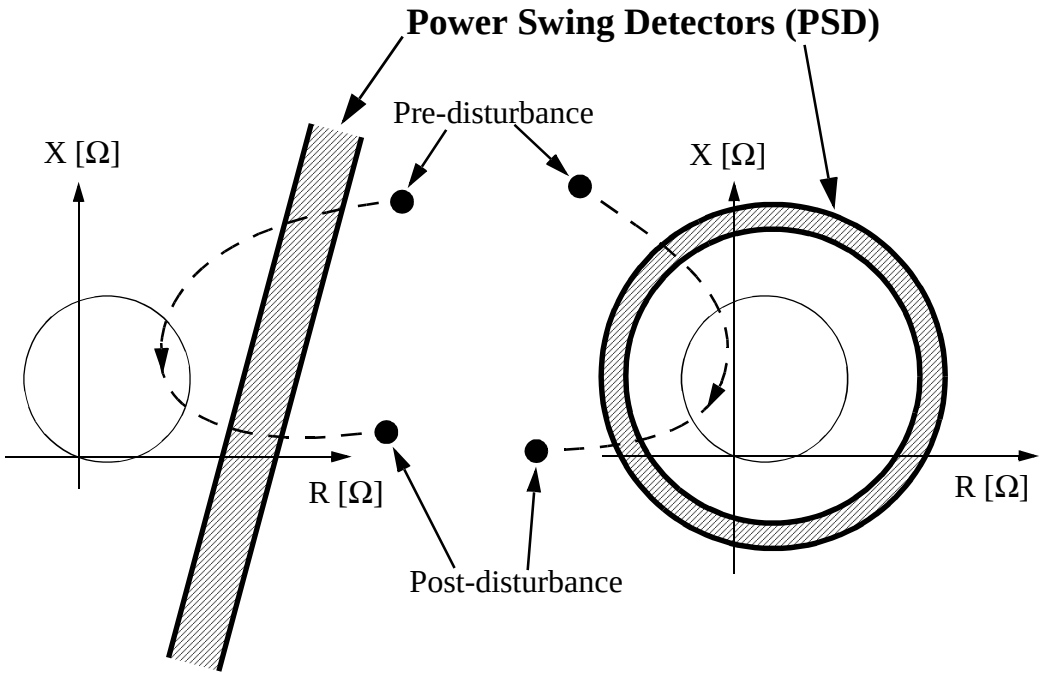

Figure 3.5 Vertical and circular characteristics for Power Swing Detector schemes. The dashed lines indicate trajectories for the apparent impedance during a power swing. The left scheme is operated at the sending end of a line and the right scheme is located at the receiving end of a line.

Basically the method uses the feature that the movement of the apparent impedance during power swings is slow as compared to its movement for short circuit faults. Fig. 3.5 shows two different characteristics of Power Swing Detector (PSD) schemes. When the apparent impedance penetrates the outer circle or line of the PSD schemes a timer is started. If the impedance crosses the grey area very rapidly the PSD determines a short circuit fault and tripping is permitted. If the transition time for the apparent impedance through the grey area exceeds the pre-set timer value, the tripping function is blocked during a certain time. Usually the pre-set value for the timer amounts to about 80 ms and tripping is blocked during a couple of seconds.

A circular PSD device is discussed in [27] where the inner circle is composed by the outermost zone of operation i.e zone 3. In order to cater for the fastest possible swings the outer circle is normally set with a reach as large as possible and consistent with load discrimination. However, to achieve satisfactory performance the reference asserts that the outer circle should have a diameter of at least 1.3 times the diameter of the outermost zone of operation.

In some protection schemes the PSD is used alone. This means that the distance relays will not operate due to stable power swings but neither the unstable power swings will be controlled. Thus some device is needed as a supplement to the PSD to distinguish stable power swings from unstable ones so that adequate relay action can be obtained. This can be achieved by adding an additional circle (mho relay) or line (blinder) to the characteristics in Fig. 3.5. If the PSD has detected a power swing, the Out-of-Step Characteristic (OSC) is activated to decide if the swing is stable or unstable. The location of the line and circle related to the OSC in Fig. 3.6 is usually determined by simulating numerous power swing cases [6]. The impedance trajectory as seen by the distance relay for each of the stable cases is analysed. It will be found that all stable swings come no closer than a certain minimum distance from the origin in the RX-diagram. In order to detect unstable swings the OSC is usually given a position at a shorter distance from the origin than the minimum distance obtained from the simulations. When the PSD in Fig. 3.6 detects a power swing the distance relay waits for the apparent impedance to pass the OSC. If the swing is stable the OSC is not passed and the relay is inactivated while if the swing is unstable the OSC will be penetrated and the relay initiates tripping.

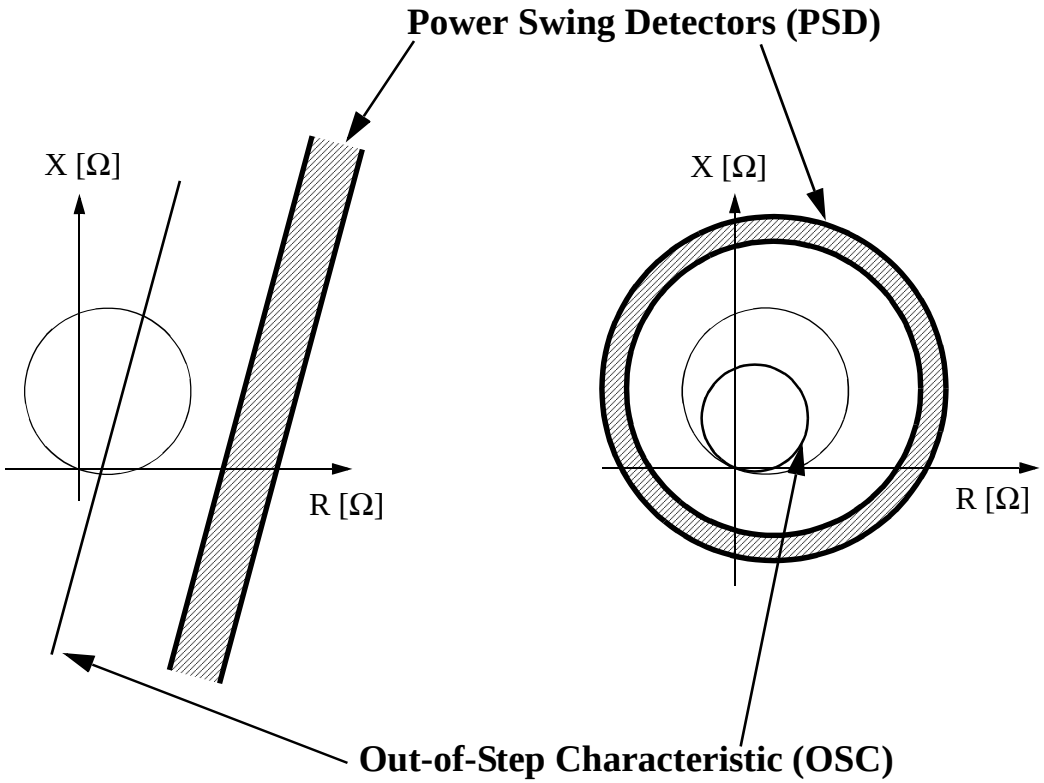

Figure 3.6 Power Swing Detectors and Out-of-Step scheme for relays located at the sending end.

Sometimes the inner circle or the inner line of the PSDs in Fig. 3.5 is applied as the boundary for stable swings. When the apparent impedance passes the outer circle or line the timer is started. If the inner circle or line is penetrated shortly after the timer is started the device declares a short circuit fault. Alternatively, if the inner circle or line is not passed the device declares a stable swing while in case the inner line or circle is penetrated after the timer has expired the device signals an unstable swing. However, depending on the system configuration nearby the relay this solution may not be acceptable with respect to line length, fault clearing, load discrimination and the nature of possible power swings.

If the line flow may occur in both directions the PSD and the OSC must be duplicated; one application for sending and one for receiving operating conditions. The application for the receiving operating condition looks similar as for the devices in Fig. 3.6 but is located on the opposite side of the tripping characteristic.

The system in Fig. 3.7 can be used to study the influence of the source impedance on the apparent impedance as seen by a relay located at bus T during power swings. In the system one generator is connected to an infinite system through a single transmission line. In Fig. 3.8 two different swing loci as seen by the relay are illustrated where the ratio between the impedance of the transmission line and the source impedance is varied.

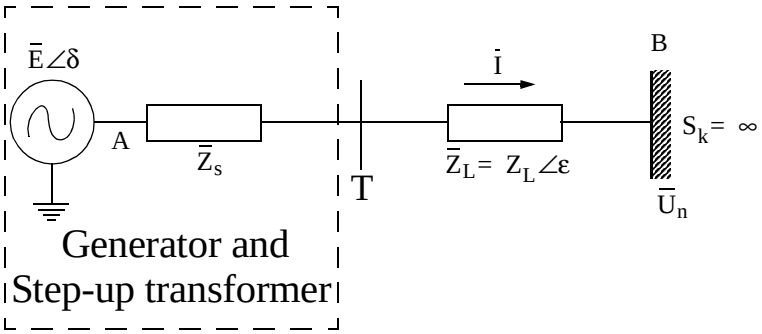

Figure 3.7 A generator connected to an infinite system through a transmission line.

Fig. 3.8 indicates that for generators connected to the main grid through a weak interconnection (large line impedance) the electrical centre may appear on the transmission line. However, for generators connected via a strong grid the electrical centre will be in the step-up transformer or in the generator itself. Although power oscillations are mainly relevant in the case of weak connections, they may also be present in strong line configurations. Consequently, the Power Swing Detector and the Out-of-Step Characteristic included in the line protection may be incapable to detect swings in the case of this type of line configurations. To cope with the phenomenon the Generator Out-of-Step Protection is introduced. The Generator Out-of-Step Protection [28] operates similar to Out-of-Step Protection for transmission lines and is used to clear unstable swings when the electrical centre is within the generator or step-up transformer. Note that line protection schemes may be unaffected by the phenomenon as certain (mho) distance relays inherently adjust their tripping zones with respect to the source impedance [29].

In addition to the source impedance also a low excitation level tends to contribute to an impedance trajectory through the step-up transformer or the generator. See the case $|E_A|<|E_B|$ in Fig. 3.3.

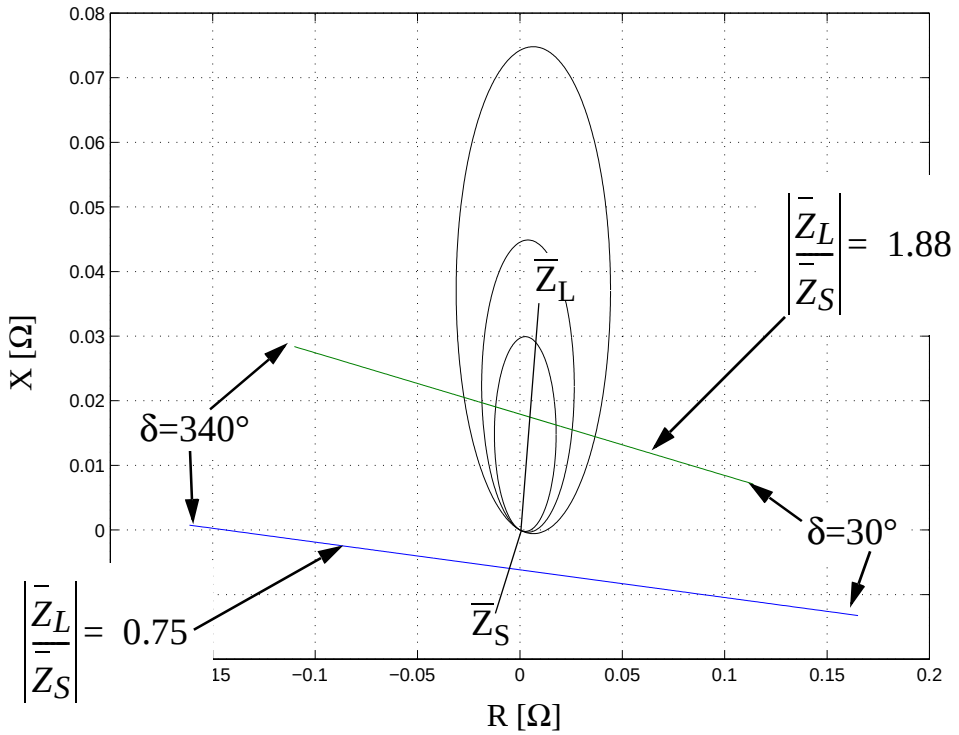

Figure 3.8 The apparent impedance trajectories as functions of the transfer angle δ for two different ratios of the relation between the line impedance and the source impedance as seen by the relay located at T in Fig. 3.7.

As intimated in the beginning of this section many approaches of Power Swing Detectors and Out-of-Step schemes have been proposed throughout the years. One reason is that the conventional schemes described in this section have their limitations and thus sometimes operate unsatisfactory. The limitations involve reduced availability in the case of long lines, setting conflicts with respect to different oscillation-frequencies, blocked fault clearing and incorrect operation in case of slowly decreasing fault resistances. In ***Paper B*** a proposal for a PSD is discussed which avoids most of those setbacks.

3.2.3 Worldwide Experience on Distance Protection and Transient Instability

In this paragraph a few relevant events are briefly discussed. The data presented were obtained from a survey carried out by CIGRÉ WG 34.09. On July 27, 1989 in Portugal a Power Swing Detector failed to operate and on August 24, 1993, in Spain three distance relays operated due to power swings as the swings had a higher frequency than the effective range of the blocking unit. Furthermore, on July 18, 1995 the WSCC system was subjected to incorrect out-of-step blocking during non-three phase faults. The location of the out-of-step protection was the main reason for inadequate performance during a disturbance in South Africa on June 7, 1996.

In Florida [30] and in South Africa [31] incorrect relay behaviour during power swings has been (and still is) a major concern.

An unwarranted distance relay operation due to a power swing was the immediate reason for the system breakdown in the south-western part of Sweden and Denmark in 1956 [32]. As a result power oscillations and associated protection measures were given significant attention. However, apart from a limited number serving interconnections between Sweden and the other Nordic countries, all Power Swing Detectors were taken out of service in the middle of the seventies. To the author's knowledge no formal investigation was carried out and the decision was most likely based on the following arguments. As the transmission system recently had been reinforced power oscillations were not expected to cause any trouble and PSDs were therefore considered unnecessary. In addition some doubts were addressed towards their operational reliability. The general opinion is that power oscillations were rare in the Swedish transmission system during this period and the removal of the PSDs was never questioned. However, in the late evening of the New Years day, 1997, the Nordic power system was subjected to serious inter-area oscillations. The oscillations resulted from a busbar fault coincident with large power flows in an unusual direction. A few generator units and lines were lost but no load was affected. However, a couple of distance relays were very close to trip due to the impedance swings. In case these relays had ordered tripping a disturbance similar to the 1983 [11] had most likely occurred. In case PSDs had been in service, the risk of incorrect relay operation due to the swings had been eliminated. The number of recorded oscillation events has increased significantly during recent years in the Swedish power system. In 1996 the annual number of

recorded inter-area oscillation events amounted to about 15 while in the year 2000 this number had increased to more than 300 [33]! In fact, in a few cases, operating conditions have occurred where the system was close to its limits and on the brink of a severe disturbance. Note that about 30 % of the events recorded in 2000 were related to one specific maintenance job lasting a period of three weeks.

Chapter 4 Power System Instability and System Protection Schemes

The protection schemes discussed here are intended to counter extreme contingencies and normally involve dispersed system devices for detection, data acquisition and curative measures. These schemes are referred to by different names e.g ”System Protection Scheme”, ”Wide Area Protection Scheme”, ”Special Protection Scheme”, ”Contingency Arming Scheme”, ”Discrete Supplementary Controls” and ”Remedial Action Scheme”. Normally the expression ”Wide Area Protection Scheme” is exclusively used for schemes introduced to counter complex and large phenomena which may jeopardise the integrity of the whole system. Other expressions may range from very local schemes to extensive wide area schemes. In a recent report [3] published by CIGRÉ, TF 38.02.19 the term ”System Protection Scheme” has been selected and will also be used throughout this thesis.

System Protection Schemes are an attractive alternative for increasing the utilisation of electrical power systems. First of all the economical aspects are in favour of System Protection Schemes as control and protection equipment are less expensive than EHV hardware equipment. Furthermore, System Protection Schemes can mitigate wide area disturbances effectively. Finally, the environmental aspects of System Protection Schemes are appealing as no new line corridors are required. The fast progress during recent years within the area of numerical and communication technologies has increased the potential of technically complex and cost-effective System Protection Schemes. The ability to acquire and process wide area data has also improved significantly. The Phasor Measurement Unit [34-36] and inexpensive fibre optics are two attributes which have simplified the realization of these features. Particularly the reliability can be improved if compared to older solutions. Moreover there is a trend today that protection and control functions are merged together in sophisticated substation and control units. This process also facilitates System Protection Schemes.

Extensive surveys over System Protection Schemes have been made by both Cigré and IEEE [3,37-39]. In addition a number of detailed publications over specific System Protection Schemes [40-44] and related subjects [45-56] have been published. The material in this chapter is to a large extent based on these publications. Appendix 1 gives a general overview with respect to the relations between different power system events, type of system, network configurations, curative

measures and the indicators to be used to detect abnormal operating conditions and initiate the curative measures. The appendix can be considered as a summary of the material published in this chapter.

4.1 System Protection Schemes

Conventional power system protection is mainly used to protect power system equipment from damage while the fundamental aim of System Protection Schemes is to protect the power system against partial or total breakdown. To obtain this objective protective measures are taken when abnormal operating conditions are identified. For these occasions no ”traditional fault situation” is present but the system itself may be in transition to a dangerous situation such as a wide area disturbance or a complete system blackout. Accordingly the protective measures are used to counteract this transition and bring the system back to a safe operating condition.

In [3] the following definition is given, ”*A System Protection Scheme is designed to detect abnormal system conditions and take predetermined, corrective action (other than the isolation of faulted elements) to preserve system integrity and provide acceptable system performance*” and in [37] ”*A System Protection Scheme is a protection scheme that is designed to detect a particular system condition that is known to cause unusual stress to the power system, and to take some type of predetermined action to counteract the observed condition in a controlled manner*”. Note that in [37] System Protection Schemes are referred to as Special Protection Schemes.

System Protection Schemes (SPS) are used for different purposes. Below their main objectives are listed:

1. **Operate power systems closer to their limits.**
   Due to deregulation and environmental constraints the operating margins have been reduced in many power systems worldwide. SPS are used to operate power systems closer to their limits without reducing the operating security of the system or impairing overall economic objectives. A typical application may be the reduction of congestion limitations between supply and load areas. Similarly, in the case of limited financial resources SPS may be used to avoid or postpone reinforcements of the transmission system without reducing its operating security.

2. **Increase power system security (particularly for extreme contingencies leading to system collapse).**
   By including SPS and maintaining the original operating limits the power system security can be increased. This type of SPS are often designed to counteract serious disturbances.

3. **Improve power system operation.**
   SPS may be designed to cope with operational difficulties imposed by certain power system characteristics. Examples are operating conditions characterised by a higher rate of exposure to multiple faults than tolerated by the design criteria or large frequency and voltage variations in adjacent sub-systems. Actions are typically taken when a certain ”key element” is lost or a particular operating condition is present.

4. **Compensate for delays in a construction program.**
   SPS may be used as a temporary solution such as before and during the time a new transmission line is constructed.

Normally, SPS are dormant integrated protection systems which operate infrequently. The control actions taken by SPS are usually pre-determined and the SPS can be armed or disarmed depending on the power system conditions. Fig. 4.1[1] shows the general structure of SPS. Generally all SPS include three main functions. First the scheme collects input data from the power system. These input data may be quantities like voltage or frequency. Alternatively, the input data are

1. Originally published in [3].

related to some specific power system event, for example the tripping of a specific transmission line. Next the scheme evaluates the input data and makes decisions for the actions to be taken. This task is performed in the ”DECISION PROCESS” block where the input data are used to represent some kind of *indicator(s)*. Normally the decision process is based on discrete feed forward laws. Finally the actions to be taken by the SPS are launched by the ”ACTION” block. Typical actions may be load- or generator shedding.

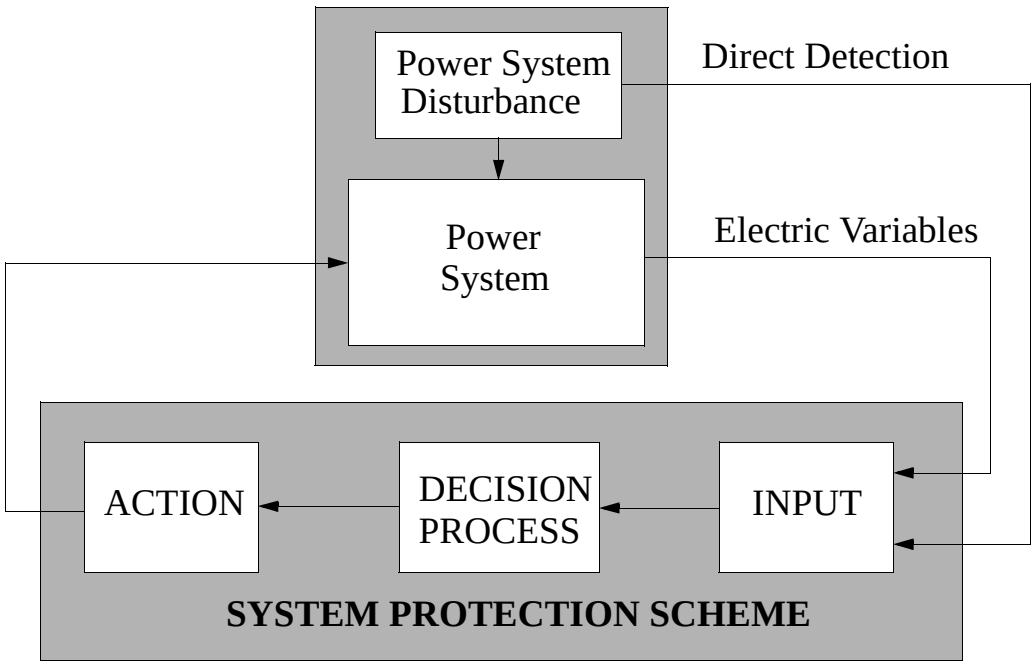

Figure 4.1 General structure of a System Protection Scheme.

4.1.1 Event- and Response based SPS

Dependent on the input variables, SPS are classified as response based or event based. SPS using input signals like voltage and frequency are referred to as ”*response based*”. SPS which use input signals that are based on specific events (or a particular combination of events) like the tripping of a certain line are called ”*event based*”. Event based SPS are of the open loop type whereas response based schemes are of the closed loop type.

Event based SPS are used in the case of critical events which are easy to identify and may lead to consequences which are particularly critical for the system stability and therefore require fast counteraction. The

main benefit of event based SPS are their fast response. The fundamental idea of event based schemes is to initiate curative actions quickly and before overall system behaviour becomes degraded. This type of schemes may be very effective as rapid control actions to limit electromechanical dynamics before system stability is threatened. Event based schemes are based on rules obtained from off-line simulations. Typical examples of applications are generation rejection or remote load shedding initiated by the tripping of a specific transmission line. The major drawback of event based SPS is their reliability, as the performance of the schemes normally relies on a limited number of critical variables.

Response based SPS are inherently slower than event based SPS as they must wait for the system response; e.g the frequency or voltage to drop below a certain threshold. On the other hand response based SPS are more general than event based SPS as they react with respect to critical system quantities whatever the cause of the disturbance. Event based SPS will only take action in the case of specific events. Accordingly, response based SPS are also efficient for events that are not explicitly identified or foreseen. Response based SPS are usually simple and secure schemes and their reliability depend mainly on the variables chosen and their behaviour. Moreover, these schemes are usually insensitive to the failure of a single component as they are often decentralised. Two common examples of response based SPS are underfrequency- and undervoltage load shedding.

4.1.2 Local-, Central-, Remote-, Limited Area and Wide Area Applications

System Protection Schemes can be based on local, central-, remote-, limited area or wide area arrangements.

Local SPS acquire all the information necessary for the decision process at the same location as where the curative actions are performed. Generally local SPS are considered to be very reliable and secure as they are not dependent on long distance communication and their actions are limited. Often such schemes are distributed throughout a region of the network and together they fulfil the requirements. An example is UnderFrequency Load Shedding (UFLS), likely the most common local system protection scheme application. Normally a complete UFLS strategy is based on a number of load blocks at different locations (local UFLS SPS) which all are tripped with respect to local frequency criteria. In case of failure of a single local scheme the other devices will still be able to counteract the disturbance. *Limited area Remote* SPS are here considered to represent applications which affect a limited area but include more than one location, e.g remote load shedding. A typical example of limited area remote load shedding is that in case a unit is lost in a generator station a signal is sent from that station to initiate load shedding in another substation.

Central SPS collect data from remote locations and process these data at a central location. This central location may for example be the utility's main building complex where the control room is located. When the decision process is completed, signals are sent to the remote locations to launch the curative measures. Obviously the central schemes are highly dependent on telecommunication facilities which influence their reliability. Central SPS may have the *Limited area* feature. However, more common is the *Wide area* approach. The difference between a Limited area remote scheme and a Limited area central scheme can be explained as follows. When the contingency has been detected locally the remote scheme directly issues orders to the remote station where the corrective actions should be taken. In the case of a Limited area central scheme, signals are first sent from the station where the contingency is detected to the central location, and after processing, from the central location to the remote station where the corrective actions are carried out.

The decision process of *Wide area* SPS uses input data from a large number of locations throughout a wide area. They can have the central

approach but can also be represented by a number of remote stations interacting with each other. SPS based on a network of remote stations together with central schemes are obviously more complex than local SPS and are strongly dependent on communication tools. For these schemes the security is the main concern as in case of undesirable operation (during normal operation) the consequences will be significant. The different types of SPS arrangements are illustrated in Fig. 4.2.

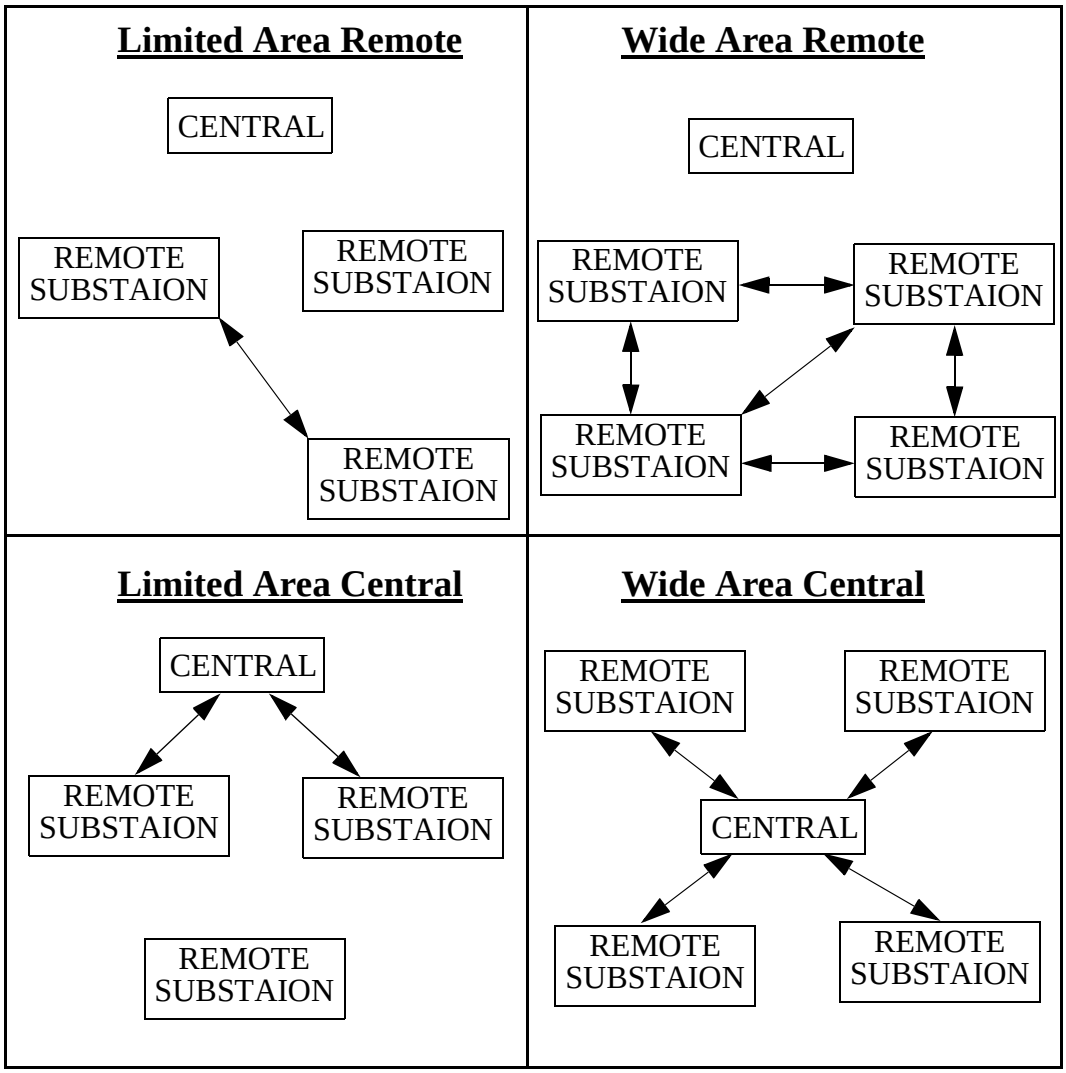

Figure 4.2 Illustration of Limited-/Wide area Central and Remote applications.

4.2 Detection and Control Indicators for System Protection Schemes

In order to obtain appropriate SPS operation, detection and control indicators are required. A large number of indicators based on sophisticated mathematical methods have been proposed for off-line studies applicable during the planning phase. However, real-time applications require indicators which are obtained very fast and thus there are few indicators, apart from measured electrical quantities and direct events, which are applicable. Dimension-less indices are also sometimes useful, for example in case of long term voltage stability events. However, they are more applicable as guidance for operators. Often the main concerns in case of SPS design may not only be the choice of indicators but the way of obtaining appropriate setting values for the indicators. The next sections briefly describe indicators applicable for the determination of power system instability.

4.2.1 Indicators to Determine Voltage Instability

Indicators for voltage instability are often related to the maximum loadability of the system. For event based SPS loss of generation, reactive resources and transmission facilities are typically used as indicators as they represent phenomena which may contribute to voltage instability. In the case of response based SPS the following indicators based on direct measurement represent the most common inputs:

- Bus voltage magnitude. In many systems the bus voltage magnitude is the main indicator available to detect voltage instability. However depending on the location in the system its reliability as an indicator varies significantly. For example, close to generators and at buses with a high level of shunt capacitor compensation the voltage may indicate a too positive system status. For buses located away from generation and with no shunt capacitor compensation the voltage may well be a valuable indicator.
- Reactive and active power output from generators.
- Reactive power reserves within regions.
- Active and reactive power flows on lines (tie-lines).
- Generator (field/armature) current limiter status.
- Active and reactive load demand.

Additional straightforward indicators which can be determined from loadflow solutions or measurements are the active/reactive line losses and sensitivities with respect to changes in active and reactive bus power [57]. A number of Voltage Collapse Indicators have been developed where the distance to voltage collapse can be obtained from a dimension-less index. Mainly two categories exist. First the straightforward type where the index is based on the fraction of the present value and the collapse value of any quantity; e.g the voltage or power flow. The second type is more extensive where the indices typically are given in a general form [58,59] as in (4.1).

$$VCI(z, z^c) = \sum_i w_i \cdot f_i(z, z^c) \tag{4.1}$$

Here $f_i(z,z^c)$ is a real-valued function of z and z^c; z is a vector consisting of measurable variables e.g the load bus voltages, load bus real and reactive power, generator reactive power etc.; z^c is a reference value of z and w_i are positive weighing functions. In order to detect voltage instability the VCI is compared to a threshold (TH) value. Thus system stability is decided with respect to the relations given in (4.2).

$$\begin{aligned} VCI(z, z^c) \le TH &\Rightarrow \text{System is voltage stable} \\ VCI(z, z^c) > TH &\Rightarrow \text{System experience voltage collapse} \end{aligned} \tag{4.2}$$

The indicators given so far are fairly simple (but fast) and are based on the threshold principle i.e when the indicator exceeds or drops below a pre-defined threshold value the corrective measures are carried out. Although the principle is simple the main challenge related to this approach is obviously the choice of appropriate threshold values. Today the setting values are often based on operator experience or numerous simulations. No explicit methods are available to optimize the corrective measures with respect to location, time for activation and extent. However, there are methods to predict voltage instability and thus the normal proceeding is to perform simulations where the point of instability is identified for different contingencies without

corrective measures. The next step is to perform further simulations where corrective actions are included and based on these repeated simulations the setting values for the corrective measures can be decided. A number of methods applicable for the setting process of System Protection Schemes are briefly mentioned below. Most methods are only applicable for the planning phase while a few also can be used as on-line indicators.

Many static methods have been proposed to predict voltage instability. These methods exclude time dependent phenomena but are still considered valuable in the analysis of voltage instability as they are less computational expensive than detailed time-domain simulations. Although time-domain simulations are considered to reflect the most appropriate system behaviour, static and dynamic methods can be used jointly to obtain the most favourable settings of SPS equipment. Methods to identify voltage instability include *PV- and QV curves* [16]. Development of these curves is a fairly extensive work as every network configuration corresponds to a unique curve. In order to reduce the amount of work different curve-fittings methods may be used [60]. There are also methods based on PV curves with some extensions involving load margins, bifurcation points, sensitivity and energy methods [61-66]. Another extension of PV- and QV curves are the *PQV surfaces* [67] which can be developed for the entire system or for individual buses. Generally these curves and surfaces are used for planning, monitoring or post-disturbance investigations but they can also be used to control SPS measures. Different approaches based on the *Jacobian matrix* [68-74] are common tools for voltage instability identification. Generally the Jacobian is too computational demanding to be used as an on-line predictor and thus more suitable for the planning process. However, in [69] areas are merged together and treated as one bus in order to reduce computation data. Another but dubious method, due to its sensitivity to numerical inadequacies, is the *Convergence of the loadflow* [75,76]. There are also numerous *Impedance* based methods proposed for voltage instability identification. The Voltage Instability Predictor (VIP) based on a pair of impedances that coalesce when reaching the critical point [77-80] is the most encouraging as an on-line tool. Other proposals involve a *voltage stability Index for single lines* [81-85]. In [86] a method is proposed where the entire system is reduced to a single line which then is investigated by a single line index. Other methods use *Fourier transforms* [87,88], *Energy functions* [89,90], *Phasors* [91,92],

numerical *Optimization techniques* [93-95] and methods based on *Neural network* [96-100].

Under Voltage Load Shedding represents an important curative measure in the case of voltage instability. Accordingly extensive effort has been given to indicators in order to assure optimal shedding [101,102]. In [103] a method is given to optimize the load shedding for load having a large share of induction motors. Other techniques which have been used to obtain an optimal UVLS scheme are numerical optimization based on an objective function and Fuzzy logic [104-106].

4.2.2 Indicators to Determine Transient Angle Instability

Due to the high speed requirements event based SPS are preferable to prevent transient instability. Typical events used as indicators are related to loss of generation-, transmission- and load facilities. For response based SPS, indicators obtained by direct measurements are normally used, but also indicators based on complex mathematical concepts. Typical quantities that can be monitored (and used as indicators) from both lines and generators include:

- Voltage threshold values exceeded by the voltage within a pre-defined time period.
- Power threshold values exceeded by the active power within a pre-defined time period.
- Apparent power outside pre-defined threshold limits.
- (Frequency).

More extensive methods to investigate, detect and predict transient instability include the *Equal area criterion* [107-112] which probably is the most well known transient stability criterion. This criterion performs best for two machine systems and therefore requires system reduction in the case of large systems. Dependent on the system configuration the reduction may vary in its degree of complexity and accuracy. For practical applications the equal area criterion is most suitable for individual generators feeding large systems through weak interconnections or for weak interconnections connecting large systems. Inherently the *Swing equation* addresses transient instability. However, solving the swing equations for a large system is fairly time

consuming and therefore suitable for the planning stage. In order to obtain on-line tools based on the swing equation decision trees [113], neural networks and pattern recognition have been proposed [114]. *Voltage phasors* are a common tool for transient instability identification where the angle difference between different buses normally is used as a stability measure [115,116]. The voltage phasors to monitor are normally easy to identify in the case of radial system configurations. However, many systems are strongly meshed and have dispersed generation. In order to solve this problem the system is divided into coherent generator groups where one “pilot“ generator is selected for each group. The angle differences between the system regions are obtained by comparing the angles of the “pilot“ generators. A method to merge generators into coherent groups is proposed in [117]. Furthermore, a commissioned scheme based on phase angle validation is described in [118-123]. In [124,125] extra criteria are used in addition to the angle difference criterion to increase the reliability of the protection. These additional criteria must also remain within pre-determined ranges in order to dispense corrective actions. The additional criteria are frequency deviation, load bus voltage magnitude and load bus voltage angle. Another but less common approach to distinguish coherent groups is to study the angle deviation in each bus with respect to the steady state condition [126]. Furthermore, in [127] a method is proposed where the voltage angle is predicted by applying the least square method, and dependent on that prediction the control actions may be carried out. In case of transient instability the different swing modes can be determined from the *Frequency spectrum*. Possible input signals are voltage, frequency, real-/reactive power, rotor angle or rotor speed [128-132]. Other methods proposed for the analysis of transient instability involve *Modal analysis* [133], *Energy functions* [134-139], *Rotor angle* and *Rotor speed deviation* [140], *Time domain* simulations [141], *Taylor/Maclaurin* expansions and *trigonometrical* functions [142-145], *Out-of-Step Relays* [2], *Lyponov stability analysis* [146,147], *Trajectory technique* [148-150] and *Mapping/Pattern recognition* [151,152].

Today the extensive methods mentioned above are often inapplicable as accurate real-time tools for large power systems. In the case of detailed system modelling they often result in mathematical tasks, which the computers are incapable to solve within the required time frame. If simplifications are introduced to facilitate the computational requirements the results may be unreliable. To assure effective curative

actions in the case of transient instability on-line generator coherency determination is often required. Normally reliable generator coherency methods are computational expensive and therefore limited to off-line studies. In ***Paper D*** a simple coherency method is introduced that suits applications based on communication and GPS technology. This new concept results in a more accurate generator coherency than phasor measurements. This is of particular interest as phasor measurements are the most common on-line tool for generator coherency determination. In ***Paper E*** the method is applied on a SPS addressing inter-area oscillations. ***Paper D*** and ***Paper E*** are based on a method briefly introduced in [131].

The extensive methods mentioned above are continuously developed and may become applicable as real-time tools in the future. Present research deals with conventional computer calculation methods but also more modern approaches such as neural networks [113,129,153], decision trees [154], chaos [155], fuzzy logic [156-158] are investigated. Typically neural networks can be used to increase the speed of prediction. Neural networks are trained during off-line simulations; during on-line operation only limited and simple calculations are required.

4.2.3 Indicators to Determine Frequency Instability

Due to the nature of the frequency instability phenomena the following quantities are used as indicators for response based SPS:

- Frequency.
- Rate of change of frequency.

Indicators for event based SPS may be:

- Loss of a power station, a HVDC interconnection or tie-lines.
- Loss of a load centre.
- Pre- and post contingency power flows.

4.3 Curative Measures for System Protection Schemes

Table 4.1 gives an overview of the most common SPS in operation. The table was originally published in [37,38] and is based on a joint survey over SPS performed by IEEE and CIGRÉ. In total 49 utilities from 17 countries responded to a survey describing 111 schemes. Furthermore, Table 4.2 gives a general overview for which categories of power system instability the different types of curative measures are suitable. The table was originally published in [3].

Table 4.1: Mixture of most common SPS types.

Type of SPS	[%]
Generation Rejection	21.6
Load Rejection	10.8
Underfrequency load shedding	8.2
Controlled system separation	6.3
Turbine fast valving	6.3
Load & Generator rejection	4.5
Stabilizers	4.5
HVDC fast power change	3.6
Out-of-step relaying	2.7
Discrete excitation control	1.8
Braking resistor	1.8
Generator run-back	1.8
Var compensation	1.8
Combination of schemes	11.7
Others	12.6
All SPS	100

Table 4.2: Curative measures and their fields of application.

	Generation Rejection	Turbine fast valving	Gas turbine start-up	Actions on the AGC	Underfrequency load shedding	Undervoltage load shedding	Load rejection	HVDC fast power change	Automatic shunt switching	Braking resistor	Controlled system separation	Tap changer blocking
Transient instability	X	X					X	X	X	X	X	
Frequency instability (freq. decay)			X		X			X			X	X
Frequency instability (freq. rise)	X							X				
Voltage instability	X		X	X		X		X	X		X	X
Cascade line outages	X		X	X			X	X				

Fig. 4.3[1] shows the relationship between the duration of major power system phenomena and the approximate time frame of SPS actions used to limit their consequences. The time frames for different control and protection categories are indicated. The time scale is logarithmic and solid lines represent the typical operating range for the curative measures while dotted lines indicate potential operating ranges.

1. Originally published in [3].

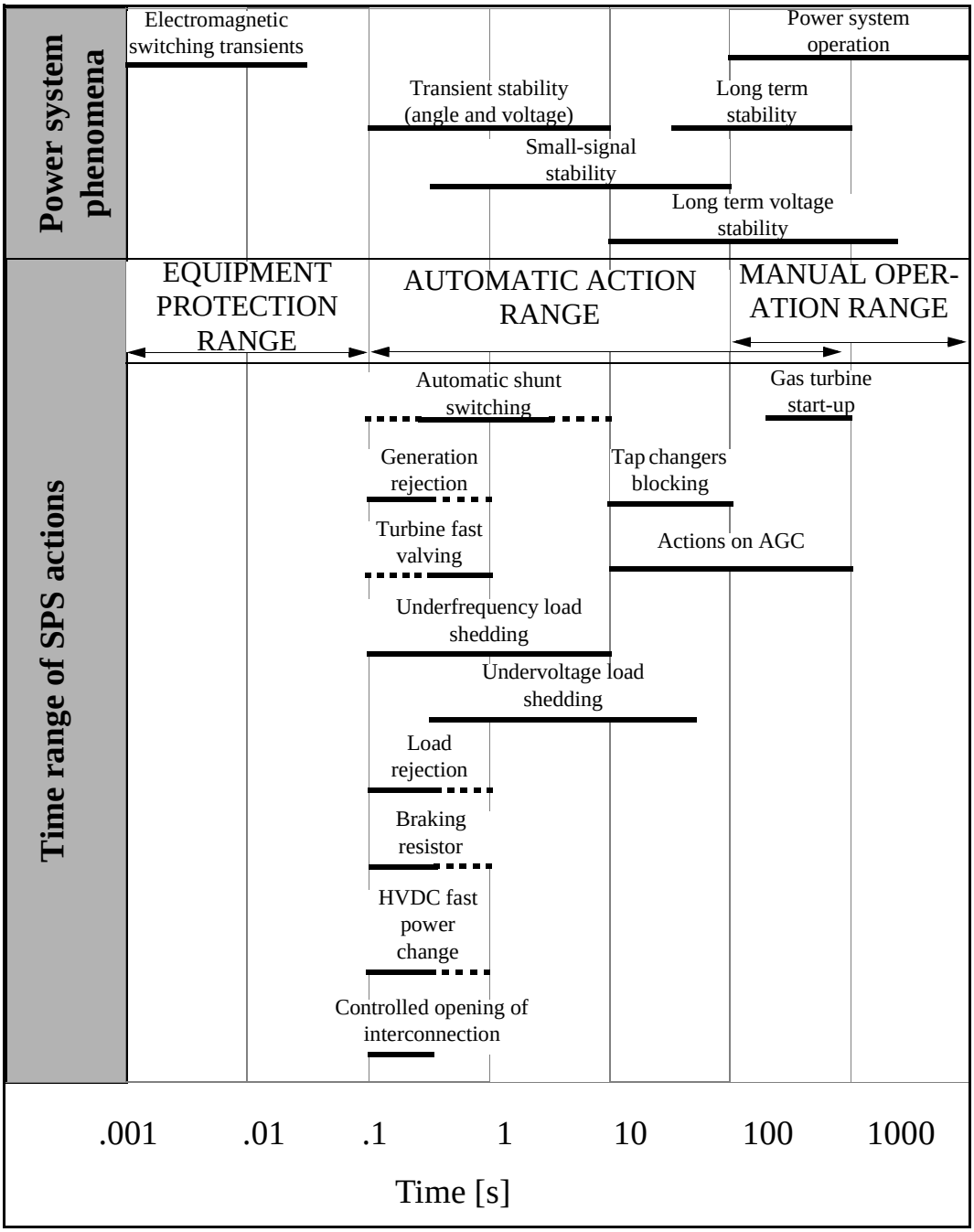

Figure 4.3 Time frame relation between curative measures and power system phenomena.

System separation schemes are normally used as a curative measure for transient instability. However, sometimes separation schemes can also be designed to prevent the penetration of voltage instability from neighbouring systems. These schemes are normally applied on the borderline between different countries or large utilities. ***Paper F*** is

introducing a similar scheme but instead of invoking large system regions the aim of this scheme is to secure voltage stability in at least one part of the system in order to avoid a black start. The scheme is using conventional distance protection and should operate when a complete breakdown cannot be obstructed by any other means.

4.4 System Protection Schemes in the Nordel System

SPS in the Nordel system will be treated here. An extensive survey on SPS and field experience worldwide is given in [159].

The instantaneous emergency reserve in the Nordel system is equivalent to the loss of the largest unit in service; normally about 1200 MW. In addition SPS are used for extreme contingencies such as severe grid weakening or a loss of generation exceeding the largest unit. There are a number of SPS operating in the Nordel system today, addressing all different types of power system instability, involving large and small areas. Examples are active power support from neighbouring regions via HVDC links, automatic conversion from pure reactive generation to active generation for some hydro units, automatic start of gas turbines, load shedding or system separation. To avoid overload or instability in case of reduced transfer capacity in critical intersections generator shedding is applied. The HVDC support is activated in case of low frequency and/or low voltage in the HVDC station or low voltage in a remote station. A number of Emergency Power Control steps are implemented in the control systems of the links. There are different setting possibilities but the most common way to control the power flow is to apply a number of time-delayed step-changes e.g ΔP=50 MW with a 2 s time delay. Automatic frequency controlled start of gas-turbines is used to some extent within the Nordel system. In Sweden these units are started at 49.5 Hz. Non-discriminative UFLS is used as a final curative measure in case of extreme loss of generation. The UFLS is divided into five steps where each step has two different time delays.

Fig. 4.4 gives an overview of the main corrective measures used to counteract the different types of power system instability in the Nordel system. The grey window represents the emergency reserve together with on-line hydro units. The emergency reserve is divided into instantaneous-, fast- and slow reserves. The emergency reserve is intended to counter frequency decays down to 49.5 Hz. In case the

frequency drops below 49.5 Hz a severe contingency has occurred according to the design criteria. Thus additional SPS (e.g UFLS) is used to arrest further frequency decay.

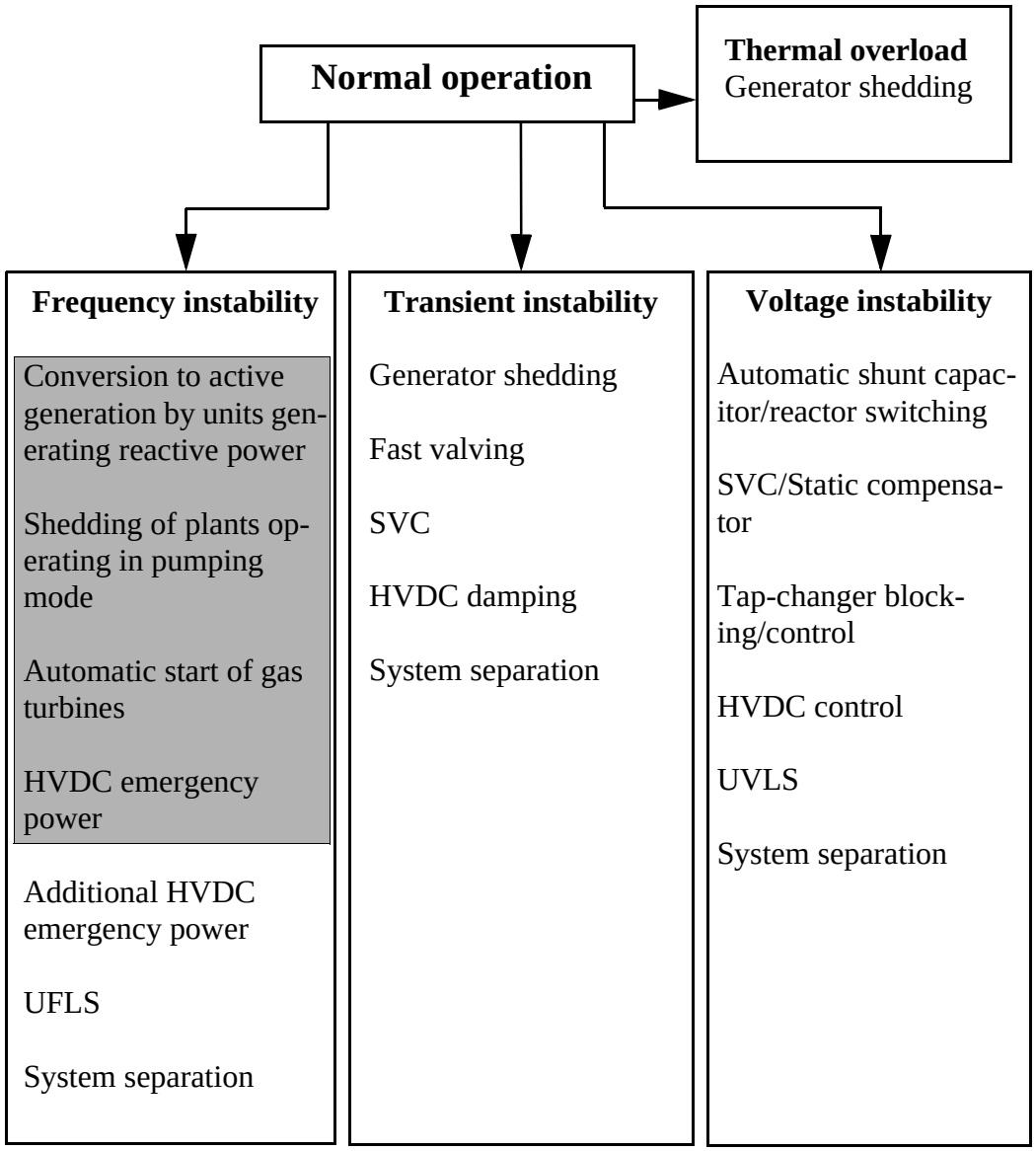

Figure 4.4 Main System Protection Schemes in the Nordel system. The grey window represents corrective measures which are a part of the emergency reserve.

Table 4.1 gives an overview of the extent of installations of corrective measures used for SPS in the Nordel system. Some schemes involve only one type of corrective action while other schemes comprise numerous actions. The extent of installations in 2001 is compared to the situation in 1992 [160,161].

Table 4.1: Overview of SPS in the Nordel system 1992 and 2001.

SPS	Available 1992	Available 2001
Generator shedding	approx. 7000 MW	approx. 7000 MW
Fast valving	max. 350 MW	approx. 480 MW
Conversion to active power generation by hydro units generating reactive power	approx. 1795 MW	approx. 438 MW
Shedding of plant operating in pumping mode	950 MW	550 MW
Automatic start of gas turbines (and a diesel unit)	695 MW (20 MW)	485 MW (20 MW)
Automatic shunt capacitor switching[a]	about 1500 MVAr + 23 capacitors in Finland	about 1750 MVAr + 26 capacitors in Finland
Automatic shunt reactor switching	3700 MVAr + the reactors in Sweden minus the reactors in the Sydkraft area	8500 MVAr
SVC	±930 MVAr +360 MVAr inductive	±1250 MVAr +360 MVAr inductive
Static compensators	-	140 MVAr
Tap-changer blocking	-	In operation in Finland and Norway

SPS	Available 1992	Available 2001
HVDC, Control of Norway - Denmark power flow in case of low voltage in Norway	max. 240 MW	max. 240 MW
		Similar scheme for Baltic cable (max. 200 MW), SwePol Link (max. 300 MW) and Kontek (max. 250 MW) in case of low voltage in local station or in Sege
HVDC emergency power	max. 560 MW to counter frequency decay	max. 890 MW to counter frequency decay
HVDC damping	?	±100 MW
UVLS	max. 200	max. 200
Automatic UFLS[b]	Sweden: 34 % of tot. load Norway: 32 % of tot. load Finland: 20 % of tot. load Denmark: 45 % of tot. load	Sweden: 34 % of tot. load Norway: 32 % of tot. load Finland: 20 % of tot. load Denmark: 45 % of tot. load
System separation	Similar to the 2001 situation	HVDC interconnections are severed in case of severe underfrequency or overvoltage. Finland: Isolated island operation in case of underfrequency. The south part of Norway is separated from the remaining system in case of strained operation of the Hassle bottleneck. Splitting schemes based on power-, voltage levels and loss of circuit also exist.

SPS	Available 1992	Available 2001
Power swing detectors	Similar to the 2001 situation	Generally used to detect power swings but not to avoid undesirable relay operation or control system separation. However, in Norway there is a limited number of detectors which also control corrective actions (generator rejection).

a. Although the numbers are according to [160] and [161] information is missing or presented differently for certain countries which may affect the presented data.
b. The values presented here were slightly updated when the new load shedding policy was introduced on January 1, 2002.

Chapter 5 Summary of Publications

As a part of this Ph.D dissertation the papers presented below are published in their full length. ***Paper A*** - ***Paper C*** address local area protection while ***Paper D*** - ***Paper F*** analyse applications associated with System Protection Schemes.

5.1 *Paper A*: An Adaptive Scheme to Prevent Undesirable Distance Protection Operation During Voltage Instability

The paper introduces an adaptive algorithm to prevent undesirable distance protection operation during voltage instability. The rate of change of voltage is used as an additional relay criterion to improve the distance relay security with respect to voltage instability. The performance of the new algorithm is analysed using two different test systems; a 15 bus system developed by the authors and the NORDIC32 system [162].

This paper has been published in condensed form as [163].

5.2 *Paper B*: A New Protection Scheme to Prevent Mal-trips due to Power Swings

In this paper distance protection algorithms based on mathematical logic blocks are proposed. The algorithms prevent mal-trips due to power oscillations using additional criteria in combination with traditional distance relaying. These additional criteria are based on symmetrical components and the rate of change of the phase angle associated with the current as seen by the relay. Finally, the performance of the algorithms is analysed in a simulation performed in a eighteen bus system developed by the authors.

5.3 *Paper C*: A Distance Protection Scheme to Prevent Mal-trips During Abnormal Power System Conditions

In this paper distance relay algorithms are further developed based on ***Paper A*** and ***Paper B***. The eighteen bus system introduced in ***Paper B*** is used to investigate the performance of the algorithms.

5.4 *Paper D*: A New Method Suitable for Real Time Generator Coherency Determination

Based on three test cases in a 68 bus system the paper illustrates that wide area generator speed measurements combined with Fourier analysis can be used to determine coherent generator groups. To verify its performance the new method is compared to conventional methods based on the generator speed, modal analysis and phasor angle measurements.

5.5 *Paper E*: A System Protection Scheme Concept to Counter Inter-Area Oscillations

This paper introduces a concept of a generator coherency based System Protection Scheme, addressing inter-area oscillation events. The scheme is based on the coherency method introduced in ***Paper D***. A simulated test case in a 68 bus system is used to introduce the operating principle of the scheme. The test case is also used to evaluate the scheme's suitability for different well established DSP methods. Aspects such as evolving-/sliding window functions, window size and frequency resolution are examined.

5.6 *Paper F*: An Emergency Strategy Scheme Based on Conventional Distance Protection to Avoid Complete System Collapse

In order to reduce the restoration time after a voltage collapse affecting a large system an emergency protection scheme based on conventional distance protection is proposed. The performance of the scheme is investigated using the NORDIC32 test system [162].

5.7 Other Publications Reported within the Scope of the Project

In addition to this Ph.D thesis a licentiate thesis [2] and a technical report [159] have been published.

5.7.1 Licentiate thesis - Line Protection and Power System Collapse

In the licentiate thesis the influence of line protection on transient- and voltage instability is investigated. Different types of line protection applications are discussed and their likelihood of contributing to power system instability is analysed. The different types of relay characteristics used in distance protection are analysed and their relative numbers in the Swedish transmission system are given. Statistics of zone 3 distance protection operation in the Swedish transmission system are shown for the period 1985 - 2000. Additionally, a number of disturbances related to distance protection and power system instability is investigated.

Also the significance of co-ordination between distance protection and generator current limiters in case of voltage instability is investigated. Subsequently the interaction between distance protection and other protection devices during power system instability is discussed. Conventional Power Swing Detectors and Out-of-Step Protection have also been examined.

Papers A-C introduced above are all incorporated into the thesis.

5.7.2 Technical Report - Present Status of System Protection Schemes

The report gives an overview of publications and projects within the area of System Protection Schemes. Different theoretical aspects involving power system instability, indicators, system configuration, curative measures and their internal relations are examined. Furthermore, an extensive survey of commissioned System Protection Schemes worldwide is presented.

Chapter 6 Conclusions and Future Work

6.1 Conclusions

This thesis introduces new methods to improve the performance of power system protection in case of system instability. The methods are primarily designed to mitigate power system breakdown.

Distance protection may contribute to power system instability. Measures to improve its performance have been proposed using new relay criteria combined with conventional impedance characteristics. In case of voltage instability the criteria are based on the derivative of the voltage whereas the rate of change of the phase angle of the current is used for transient instability. The measures improve the relay security with respect to voltage instability whereas the reach of the distance protection is unrestricted. Line length, different swing frequencies or faults having a slowly decreasing impedance will not affect the performance and availability of the proposed schemes, which may be the case for conventional Power Swing Detectors. Furthermore, fault clearing will not be blocked as in the case of conventional PSD applications.

A high degree of security is relevant today as the trend implies that utilities are subjected to penalty fees in the case of undelivered energy. Companies therefore want to avoid undesirable relay tripping indeed. The methods proposed here are based on mathematical logic blocks which are easily adapted to numerical relays.

In the Swedish bulk power system the number of power oscillations has increased significantly during recent years. To dampen oscillations a well established generator coherency is often required. In this thesis a method based on wide area generator speed measurements and Fourier analysis is proposed for the purpose of on-line coherency tracking. The performance of the new method has been evaluated by comparing the generator coherency obtained from the new method with coherencies obtained from conventional methods based on generator speed, modal analysis and phasor angle measurements. The new method and the off-line methods based on generator speed and modal analysis give almost identical results, however the results obtained from phasor measurements show deviations. This is particularly interesting as the generator angle probably is the most common on-line indicator for

generator coherency determination. Furthermore, taking the transient distortion immediately after a disturbance into account, this work indicates that the method introduced here generates a reliable coherency considerably quicker than the methods based on pure speed or generator voltage angle measurements.

Using a method based on speed measurement combined with Fourier analysis a concept for a System Protection Scheme addressing inter-area events is proposed. Different Digital Signal Processing issues such as window functions, time-frequency resolution and signal analysis methods have been investigated. Based on these investigations a scheme was designed. For the detection of inter-area modes, parametric methods are the most feasible. Evolving window functions generally detect the main mode somewhat faster than sliding windows. However, evolving windows require a trigger activated by the presence of an inter-area mode. This trigger may complicate the design of the scheme and therefore the design proposed here is based on a sliding window. To shorten the detection time of the main mode, a reduced frequency resolution can be applied. However, a lower frequency resolution contributes to spectral mode shifts and reduces the quality of the estimate of the instantaneous speed deviation. As a result the discrimination of the unstable/stable nature of the modes is of a lower quality. Also the phase estimation deteriorates which in turn leads to a less reliable generator coherency determination. The design proposed here is therefore based on a high frequency resolution, accepting a somewhat slower response.

Finally, an emergency scheme is proposed utilising conventional distance relays to avoid a complete system collapse in case of severe voltage instability. The purpose of the scheme is to co-ordinate all distance relays belonging to a transfer section so they will simultaneously operate due to the voltage instability. As a result a part of the system can be saved from the collapse, black-start can be avoided and the restoration time can be reduced. Furthermore, in case long distance communication is introduced the scheme can be utilized for the supervision of corrective measures such as generator or load shedding.

6.2 Future Work

Future work directly linked to the work in this thesis includes various practical issues related to the realization of the proposed applications. For the distance relay algorithms emphasising security, issues such as data memory, window size and data filtering must be further investigated. To obtain reliable operation well defined setting procedures for the new relay criteria should also be developed.

The System Protection Scheme based on speed measurements and Fourier Analysis is still at an early stage of development. An adaptive frequency resolution for the detection process could be used to further improve the performance of the scheme. Also the main mode tracking systems could be based on a combination of evolving and sliding window functions.

A future approach could be the use of extensive protection systems where equipment protection and System Protection Schemes are closely related to each other. As communicative relays become more widely used a large amount of data is available and the number of possible remedial actions increases significantly. These features are attractive for SPS. At the same time the wide area data acquisition used to control the actions associated with the SPS, can also be used to prevent incorrect equipment protection performance, as their algorithms can be based on wide area data. Possible research topics are the optimal utilization of the extensive data with respect to relay algorithms and the detection and counteraction of different power system phenomena. Also the optimal co-ordination between local and system wide protection applications with respect to dependability and security should be investigated.

Traditionally measures taken by System Protection Schemes have been extensive. The schemes have not been adjusted to each specific disturbance and sometimes the overstated curative measures have resulted in needless social inconvenience and unnecessary large disturbance cost. Another aspect is the relation between operating safety limits and the (real-time) prevailing operating conditions where the remedial measures represent one feature. To utilize the system (at every single moment) to its maximum capacity a continuous optimization must be performed with respect to all parameters where also the remedial actions should be adjusted based on the actual system condition. There are therefore major incentives for more accurate and intelligent (adaptive) applications controlling the corrective measures.

One interesting tool for this purpose is GPS synchronized wide area measurements where the system status is provided in real-time. This feature combined with for example Artificial Intelligence could be a fruitful area.

As computers become faster more sophisticated DSP methods can be used for protection applications. Traditionally the measured relay signals have been processed based on DSP techniques, and then the electrical quantities associated with the signals have been used as relay criteria. However, the present situation makes it interesting to search for new relay criteria based on inherent DSP parameters. Typically the criteria could be an intermediate quantity obtained from the DSP process during the evaluation of the electrical signal.

An observation made during the project is the importance of accurate protection modelling during simulation based studies. Another observation is the influence of numerical defects during simulations close to instability. An ever lasting important task is to further develop simulations tools, both with respect to numerical and modelling aspects.

A result of the more extensive use of communication in power system protection are the increased requirements of data security. Overall this is a very relevant topic involving numerous aspects of power system operation. The topic offers many challenges within a broad range of different research areas.

References

[1] Kundur P, ”Power System Stability and Control”, ISBN 0-07-035958-X, McGraw - Hill, 1994.

[2] Jonsson M, ”Line Protection and Power System Collapse”, Technical Report No. 393L, Chalmers University of Technology, Sweden, 2001.

[3] CIGRÉ, TF 38.02.19, ”System protection schemes in power networks”, June, 2001.

[4] ANSI/IEEE C37.106-1987, ”Guide for abnormal frequency protection for power generating plants”.

[5] Lindahl S, ”Frekvenshållning inom Nordel-systemet”, Nordel 1983, Särtryck ur årsberättelsen, Sydkraft AB, 1983 (In Swedish).

[6] Horowitz S.H, Phadke A.G, ”Power System Relaying”, ISBN 0-86380-185-4, Research Studies Press Ltd, 1995.

[7] ”The blackout in Sweden 27-12-1983”, Vattenfall publication, February 1984.

[8] Larsson S, Kearsly R, ”The blackout in the Swedish Power Supply System, December 1983”, CEPSI Conference, Manilla, Philippines, November 1984.

[9] Kearsly R, ”Restoration in Sweden and Experience Gained from the Blackout of 1983”, IEEE Transactions on Power Systems, Vol. PWRS-2, No. 2, May 1987, pp. 422-428.

[10] Otterberg R, ”Restoration After Disturbances in the Swedish Bulk-Power Network - Instruction System and Automatic Equipment”, CIGRÉ Study Committee 39 Colloquim, Toronto, Canada, September 1985.

[11] ”DRIFTSTÖRNING 83-12-27”, RAPPORT FRÅN ARBETSGRUPP, MARS 1984 (In Swedish).

[12] Western Systems Coordinating Council Disturbance Report For the Power System Outages that Occurred on the Western Interconnection on July 2, 1996, 1424 MAST and July 3, 1996, 1403 MAST, Approved September 19, 1996.

[13] Taylor C.W, Erickson D.C, ”Recording and Analyzing the July 2 Cascading Outage”, IEEE Computer Applications in Power, Vol. 10, No. 1, January 1997, pp. 26 - 30.

[14] Samuelsson O, ”Wide Area Measurements of Power System Dynamics - The North American WAMS Project and its Applicability to the Nordic Countries”, Elfork report 99:50, January 2000.

[15] X. Vieira *et. al*, ”The March 11:th 1999 Blackout: Short-Term Measures to Improve System Security and Overview of the Reports Prepared by the International Experts”, CIGRÉ Session, SC 39 Workshop on Large Disturbances, Paris, August 29, 2000.

[16] Taylor C.W, ”Power System Voltage Stability”, ISBN 0-07-113708-4, McGraw-Hill, 1994, pp. 263.

[17] Mechraoui A, Thomas D.W.P, ”A new distance protection scheme which can operate during fast power swings”, IEE Conference Publication No. 434, Developments in Power System Protection, March 25-27, 1997, pp 206 - 209.

[18] Ilar F, ”Innovations in the Detection of Power Swings in Electrical Networks”, Brown Boveri Review No. 68, 1981.

[19] Machowski J, Nelles D, ”Licentia Patent-Verwaltungs-GmbH AEG-Franfurt, P4100646.1”.

[20] Machowski J, Nelles D, ”New Power Swing Blocking Method”, IEE Developments in Power System Protection, Conference Publication No. 434, March 25-27, 1997, pp 218 - 221.

[21] Rovnyak S *et.al*, ”Decision trees for real-time transient stability prediction”, IEEE Transaction on Power Systems, Vol. 9, No. 3, August 1994, pp. 1417-1426.

[22] Jiali H, Yuqian D, Yongli L, Gang W, Shanshan L, ”Distance Relay Protection Based on Artificial Neural Network”, Proceedings of the 4th International Conference on Advances in Power System Control, Operation and Management, APSCOM-97, Hong Kong, November 1997, pp. 515 - 520.

[23] Centeno V *et. al*, ”An adaptive out-of-step relay”, IEEE Transaction on Power Delivery, Vol. 12, No. 1, January 1997, pp. 61-71.

[24] Centeno V, Phadke A.G, Edris A, ”Adaptive out-of-step relay with phasor measurement”, IEE Conference Publication No. 434, Developments in Power System Protection, March 25-27, 1997, pp 210 - 213.

[25] Redfern M.A, Checksfield M.J, ”A new pole slipping protection algorithm for dispersed storage and generation using the equal area criterion”, IEEE Transaction on Power Delivery, Vol. 10, No. 1, January 1995, pp. 194-202.

[26] Hemmingsson M, “Power System Oscillations - Detection, Estimation & Control“, Ph.D thesis, ISBN 91-88934-27-6, Lund University, 2003.

[27] ”Protective Relays Application Guide”, GEC ALSTHOM, ed. 3, 1987.

[28] IEEE Working Group Report, ”Out of Step Relaying for Generators”, IEEE Transaction, Vol. PAS-96, September /October 1977, pp. 1556-1564.

[29] Elmore W.A, ”Pilot Protective Relaying”, ISBN 0-8247-8195-3, Marcel Dekker Inc, 2000.

[30] Fouad A.A *et.al,* ” Investigation of Loss of Generation Disturbances in the Florida Power and Light Company Network by the Transient Energy Function Method”, IEEE Transaction on Power Systems, PWRS-1, No. 3, 1986, pp. 60-66.

[31] van Eyssen J, ”Introducing a new application philosophy for out-of-step protection”, IEE Conference Publication No. 434, Developments in Power System Protection, March 25-27, 1997, pp 214 - 217.

[32] ”The Swedish 380 kV System”, Kungl. Vattenfallsstyrelsen, Kungl. Boktryckeriet P.A Norstedt & Söner, 1960.

[33] Wide Area Protection seminar, “Real-Time Monitoring of Fast Dynamic in the Swedish National Grid (Fast RTMS)”, Presentation by Svenska Kraftnät, Västerås, Sweden, April 2, 2001.

[34] Phadke A.G, ”Synchronized Phasor Measurements in Power Systems”, IEEE Computer Applications in Power, Vol. 6, No. 2, April 1993, pp. 10 - 15.

[35] Martin K.E *et.al*, ”IEEE Standards for Synchrophasors for Power Systems”, IEEE Transactions on Power Delivery, Vol. 13, No. 1, January 1998, pp. 73 - 77.

[36] Hauer J.F, ”Validation Of Phasor Calculations In The Macrodyne PMU For California-Oregon Transmission Project Tests Of March 1993”, IEEE Transactions on Power Delivery, Vol. 11, No. 3, July 1996, pp. 1224-1231.

[37] Anderson P.M, LeReverend B.K, ”Industry Experience with Special Protection Schemes”, IEEE Transactions on Power Systems, Vol. 11, No. 3, August 1996, pp. 1166- 1179.

[38] CIGRÉ WG 39.05, LeReverend B.K, Anderson P.M, ”Industry Experience with Special Protection Schemes”, Electra, No. 155, August, 1994.

[39] IEEE Power System Relaying Committee C6, ”Wide Area Protection and Emergency Control”, working.

[40] Trudel G *et.al*, ”Hydro-Québec’s defence plan against extreme contingencies”, IEEE Transactions on Power Systems, Vol. 14, No. 3, August 1999, pp. 958 - 966.

[41] Faucon O, Dousset L, ”Coordinated Defence Plan Protects Against Transient Instabilities”, IEEE Computer Applications in Power, Vol. 10, Issue. 3, July 1997, pp. 22 - 26.

[42] Harker K, ”The North Wales supergrid special protection schemes”, Electronics & Power, no. 9, September, 1984, pp. 719 - 724.

[43] Coetzee G.J, Wittwer F, ”Development of a transient stability protection system for Eskom’s Matimba power station”, IEE Conference Publication No. 434, Developments in Power System Protection, March 25 - 27, 1997, pp. 36 - 39.

[44] Ingelsson B, Lindström P-O, Karlsson D, Runvik G, Sjödin J-O, ”Wide-area protection against voltage collapse”, IEEE Computer Applications in Power, Vol. 10, Issue. 4, October 1997, pp. 30 - 35.

[45] CIGRÉ TF 38.01.03, ”Planning against voltage collapse”, 1987.

[46] CIGRÉ TF 38.02.08, ”Long Term Dynamic Simulation Methods”, 1995.

[47] CIGRÉ TF 38.02.10, ”Modelling of Voltage Collapse Including Dynamic Phenomena”, 1993.

[48] CIGRÉ TF 38.02.11, ”Indices Predicting Voltage Collapse Including Dynamic Phenomena”, 1994.

[49] CIGRÉ TF 38.02.12, ”Criteria and Countermeasures for Voltage Collapse”, 1995.

[50] CIGRÉ TF 38.01.07, ”Control of Power System Oscillations”, 1996.

[51] CIGRÉ WG 34.08, ”Protection against Voltage Collapse”, No. 128, August, 1998.

[52] CIGRÉ TF 38.02.14, ”Analysis and Modelling Needs of Power Systems under Major Frequency Disturbances”, 1999.

[53] CIGRÉ TF 38.02.17, ”Advanced Angle Stability Controls”, 1999.

[54] IEEE Power System Relaying Committee K12, ”System Protection and Voltage Stability”, 1993.

[55] IEEE Power System Relaying Committee K12, ”Voltage Collapse Mitigation”, 1997.

[56] IEEE Power System Relaying Committee C6, ”Performance of Generator Protection During Major System Disturbances”, working.

[57] Ajjarapu V, Feng Z, ”A novel approach for voltage collapse analysis and control”, Proceedings of PowerCon, 1998, pp. 1499 - 1503.

[58] Fischl R, Mercede F, ”Can Voltage Security Indices Predict Voltage Collapse Problems in Large-Scale Power Networks”, Proceedings of IEEE International Symposium on Circuit and Systems, 1988, pp.665 - 668.

[59] Fischl R *et.al*, ”A comparison of indices for predicting voltage collapse in power systems”, Proceedings of the 27th Conference on Decision and Control, Austin, Texas, USA, December, 1988.

[60] Ejebe G.C *et.al*, ”On-Line Voltage Stability Assessment: Framework and Implementation”, Proceedings of IEEE PES Winter meeting, Tampa, Florida, USA, 1998.

[61] Dobson I *et.al*, “Voltage Collapse in Power Systems”, IEEE Circuit and Devices Magazine, Vol. 8, Issue. 3, May 1992, pp. 40 - 45.

[62] Evers T.A *et.al*, “Prediction of Voltage Collapse in Power Systems”, Proceedings of the Thirtieth Southeastern Symposium on System Theory, 1998, pp. 354 - 358.

[63] Greene S *et.al*, ”Sensitivity of the load margin to voltage collapse with respect to arbitrary parameters”, IEEE Transactions on Power Systems, Vol. 12, No. 1, February 1997, pp. 262 - 272.

[64] Sam D *et.al*, “Local Severity Indices and Alarm Processing for Small Scale Power Systems”, Proceedings of the American Control Conference, Arlington, USA, June 25 - 27, 2001.

[65] Crow M.L, Lesieutre B.C, “Voltage collapse”, IEEE Potentials, Vol. 13, No.2, April 1994, pp. 18 - 21.

[66] Kulkarni S.S *et.al*, ”New perceptions in integrated power system operation and control”, Proceedings of IEEE Region 10 International Conference on Global Connectivity in Energy, Computer, Communication and Control, 1998, pp. 489 - 496.

[67] Yabe K *et.al*, ”Conceptual Designs of AI-based Systems for Local Prediction of Voltage Collapse”, IEEE Transactions on Power Systems, Vol. 11, No. 1, February 1996, pp. 137 - 145.

[68] Momoh J.A, Zhang Y, ”Voltage Stability Estimation”, Proceedings of IEEE International Conference on Systems, Man and Cybernetics, 1990, pp. 94 - 97.

[69] Begovic M.M, Phadke A.G, ”Voltage stability assessment through measurement of a reduced state vector”, IEEE Transactions on Power Systems, Vol. 5, No. 1, February 1990, pp. 198 - 203.

[70] Chiang H-D, René J-J, ”Toward a Practical Performance Index for Predicting Voltage Collapse in Electric Power Systems”, IEEE Transactions on Power Systems, Vol. 10, No. 2, May 1995, pp. 584- 592.

[71] Canizares C.A *et.al*, ”Comparison of Performance Indices for Detection of Proximity to Voltage Collapse”, IEEE Transactions on Power Systems, Vol. 11, No. 3, August 1996, pp. 1441 - 1450.

[72] Madan S, Bollinger K.E, ”Artificial Intelligence Assisted Voltage Stability Enhancement”, Proceedings of Canadian Conference on Electrical and Computer Engineering, 1996, pp. 392 - 395.

[73] De Angelis G *et.al*, ”Transient voltage stability signature in time domain simulations”, Proceedings of MELECON 8th Mediterranean Electrotechnical Conference, 1996, pp. 859 - 862.

[74] Löf P.A *et.al*, ”Fast calculation of a voltage stability index”, IEEE Transactions on Power Systems, Vol. 7, No. 1, February 1992, pp. 54 - 64.

[75] Tamura Y *et.al*, ”Voltage Instability Proximity Index (VIPI) Based on Multiple Load Flow Solutions in Ill-conditioned Power Systems”, Proceedings of the 27th Conference on Decision and Control, Austin, Texas, USA, December, 1988.

[76] Tamura Y *et.al*, ”Relationship between voltage instability and multiple load flow solutions in electric power systems”, IEEE Transactions on Power Apparatus and Systems, Vol. 102, No. 5, May 1983, pp. 1115 - 1125.

[77] Vu K *et.al*, ”Use of Local Measurement to Estimate Voltage-Stability Margin”, IEEE Transactions on Power Systems, Vol. 14, No. 3, August 1999, pp. 1029- 1035.

[78] Vu K *et.al*, ”Voltage Instability Predictor (VIP) and Its Applications”, Proceedings of PSCC 99 Conference, June, 1999.

[79] Vu K *et.al*, ”Grids Get Smart Protection and Control”, IEEE Computer Applications in Power, October, 1997.

[80] Julian D.E *et.al*, ”Quantifying Proximity To Voltage Collapse Using The Voltage Instability Predictor (VIP)”, Proceedings of IEEE Power Engineering Society Summer Meeting, 2000, pp. 931 - 936.

[81] Moghavvemi M, Omar F.M, ”Technique for contingency monitoring and voltage collapse prediction”, IEE Proceedings on Generation, Transmission and Distribution, Vol. 145, No. 6, November 1998, pp. 634 - 640.

[82] Moghavvemi M, Omar F.M, ”A Line Outage Study for Prediction of Static Voltage Collapse”, IEEE Power Engineering Review, Vol. 18, No. 7, July 1998, pp. 52- 54.

[83] Moghavvemi M, Faruque M.O, ”Estimation of Voltage Collapse from Local Measurement of Line Power Flow and Bus Voltages”, Proceedings of International Conference on Electric Power Engineering (PowerTech). Budapest, 1999, pp. 77.

[84] Chiang H-D *et.al*, ”On voltage collapse in electric power systems”, Proceedings of Power Industry Computer Application Conference (PICA), 1989, pp. 342 - 349.

[85] Chiang H-D *et.al*, ”On voltage collapse in electric power systems”, IEEE Transactions on Power Systems, Vol. 5, No. 2, May 1990, pp. 601 - 611.

[86] Jasmon G.B *et.al*, ”Prediction of voltage collapse in power systems using a reduced system model”, International Conference on Control, 1991, pp. 32 - 36.

[87] Marceau R.J *et.al*, ”Fourier methods for estimating power system stability limits”, Proceedings of the Power Industry Computer Application Conference, 1993, pp. 418 - 425.

[88] Marceau R.J *et.al*, ”Fourier methods for estimating power system stability limits”, IEEE Transactions on Power Systems, Vol. 9, No. 2, May 1994, pp. 764 - 771.

[89] DeMarco C.L, Overbye T.J, ”An energy based security measure for assessing vulnerability to voltage collapse”, IEEE Transactions on Power Systems, Vol. 5, No. 2, May 1990, pp. 419 - 427.

[90] Overbye T.J *et.al*, ”A composite framework for synchronous and voltage stability in power systems”, Proceedings of IEEE International Symposium on Circuit and Systems, 1992, pp. 2541 - 2544.

[91] Gubina F, Strmcnik B, ”Voltage Collapse Proximity Index Determination Using Voltage Phasors Approach”, IEEE Transactions on Power Systems, Vol. 10, No. 2, May 1995, pp. 788 - 794.

[92] Verbic G, Gubina F, ”A new concept of Protection against Voltage Collapse Based on Local Phasors”, Proceedings of PowerCon 2000, 2000, pp. 965 - 970.

[93] Guo R *et.al*, ”Preventive/Corrective Control for Voltage Stability Using Predictor-Corrector Interior Method”, Proceedings of PowerCon 1998, 1998, pp. 1513 - 1517.

[94] Tuglie E.D *et.al*, ”Real-time preventive actions for the enhancement of voltage-degraded trajectories”, IEEE Transactions on Power Systems, Vol. 14, No. 2, May 1999, pp. 561 - 568.

[95] Tuglie E.D *et.al*, ”A Corrective Control for Angle and Voltage Stability Enhancement on the Transient Time-Scale”, IEEE Transactions on Power Systems, Vol. 15, No. 4, November 2000, pp. 1345- 1353.

[96] Hui K.C, Short N.J, ”Voltage security monitoring, prediction and control by neural networks”, Proceedings of IEE International Conference on Advances in Power System Control, Operation and Management, November 1991, Hong Kong.

[97] Momoh J.A *et.al*, ”Investigation of Artificial Neural Networks for Voltage Stability Assessment”, Proceedings of IEEE International Conference on Systems, Man and Cybernetics, 1995, pp. 2188 - 2192.

[98] Chen D, Mohler R, “Load modelling and voltage stability analysis by neural networks”, Proceedings of the American Control Conference, June 1997, Albuquerque, New Mexico, USA.

[99] Belhadj C.A *et.al*, “Voltage stability estimation and prediction using neural network”, Proceedings of PowerCon 1998, 1998, pp. 1464 - 1467.

[100] Dinavahi V.R, Srivastava S.C, “ANN Based Voltage Stability Margin Prediction”, Proceedings of IEEE Power Engineering Society Summer Meeting, 2001, pp.1275 - 1280.

[101] Moors C *et.al*, ”Load Shedding Controllers against Voltage Instability: a comparison of designs”, Proceedings of IEEE Porto Power Tech. Conference, Porto, Portugal, September 10 - 13, 2001.

[102] Arnborg S, ”Emergency Control of Power Systems in Voltage Unstable conditions”, Ph.D thesis, ISSN 1100-1607, Stockholm, Sweden, 1997.

[103] Balanathan R *et.al*, ”Undervoltage load shedding for induction motor dominant loads considering P,Q coupling”, IEE Proceedings on Generation, Transmission and Distribution, Vol. 146, No. 4, July 1999, pp. 337- 342.

[104] Tso S.K *et.al*, ”Evaluation of load shedding to prevent dynamic voltage instability based on extended fuzzy reasoning”, IEE Proceedings on Generation, Transmission and Distribution, Vol. 144, No. 2, March 1997, pp. 81 - 86.

[105] Balanathan R *et.al*, ”Undervoltage load shedding to avoid voltage instability”, IEE Proceedings on Generation, Transmission and Distribution, Vol. 145, No. 2, March 1998, pp. 175 - 181.

[106] Tuan T.Q *et.al*, ”Emergency load shedding to avoid risks of voltage instability using indicators”, IEEE Transactions on Power Systems, Vol. 9, No. 1, February 1994, pp. 341 - 351.

[107] Lemmon W.W *et.al*, ”Transient stability prediction and control in real-time by QUEP”, IEEE Transactions on Power Systems, Vol. 4, No. 2, May 1989, pp. 627 - 642.

[108] Dong Y, Pota H.R, ”Transient stability margin prediction using equal-area criterion”, IEE Proceedings on Generation, Transmission and Distribution, Vol. 140, No. 2, March 1993, pp. 96 - 104.

[109] Redfern M.A, Checksfield M.J, ”A new pole slipping protection algorithm for dispersed storage and generation using the equal area criterion”, IEEE Transactions on Power Systems, Vol. 10, No. 1, January 1995, pp. 194 - 202.

[110] Tso S.K, Cheung S.P, “Fast prediction of transient stability margin in systems with SVC control and HVDC link”, Proceedings of EMPD 95 International Conference on Energy Management and Power Delivery, 1995, pp. 456 - 461.

[111] Wang L *et.al*, “Quantitative search of transient stability limits using EEAC”, Proceedings of IEEE Power Engineering Society Summer Meeting, 1997.

[112] Pavella M *et.al*, “An approach to real-time transient stability assessment and control”, Proceedings of IEEE Power Engineering Society Summer Meeting, 1997.

[113] Ah King R.T.F, Rughooputh H.C.S, “Real-time transient stability prediction using neural tree networks”, Proceedings of the IEEE International Conference on Intelligent Systems for the 21st Century, June 1995, pp. 2182 - 2187.

[114] Yan P, “Pattern recognition techniques applied to the classification of swing curves generated in a power system transient stability study”, Proceedings of the IEEE Southeastcon 2000, 2000, pp. 493 - 496.

[115] Bretas N.G, Phadke A.G, “Real time instability prediction through adaptive time series coefficients”, Proceedings of IEEE Power Engineering Society Winter Meeting, 1999, pp. 731 - 736.

[116] Su M-C *et.al*, ”Neural-network based fuzzy model and its application to transient stability prediction in power systems”, IEEE Transactions on Systems, Man and Cybernetics - Part C: Application and Reviews, Vol. 29, No. 1, February 1999, pp. 149 - 157.

[117] Ota Y *et.al*, “Evaluation of stability and electric power quality in power system by using phasor measurements”, Proceedings of PowerCon 2000, 2000, pp. 1335 - 1340.

[118] Trotignon M *et.al*, ”Plan de défence du réseau THT Francais contre les incidents généralisés: dispositions actuelles et perspectives d´évolution”, CIGRÉ Report 39-306, September, 1992, Paris, France.

[119] Counan C *et.al*, ”Major incidents on the French electric system: potentiality and curative measures studies”, IEEE/PES Summer meeting, Paper 92 SM 432-5 PWRS, July, 1992, Seattle, USA.

[120] Bidet M, ”Contingencies: system against losses of synchronism based on phase angle measurements”, IEEE/PES Winter meeting, Panel session on application and experiences in power system monitoring with phasor measurement, 1993.

[121] Faucon O, Dousset L, Boisseau, Harmand Y, ”Coordinated Defence Plan - an integrated protection system”, CIGRÉ Report 200-07, Symposium, 1995, Helsinki, Finland.

[122] Denys P *et.al*, ”Measurement of voltage phase for the French future defence plan against losses of synchronism”, IEEE Transactions on Power Delivery, Vol. 7, No. 1, January 1992, pp. 62 - 69.

[123] Lemoing H. *et.al*, ”Experiment of a satellite-type transmission network for the defence plan”, SEE meeting, August 10, 1991, Paris.

[124] Liu C-W, Thorp J, ”Application of synchronised phasor measurements to real-time transient stability prediction”, IEE Proceedings on Generation, Transmission and Distribution, Vol. 142, No. 4, July 1995, pp. 355 - 360.

[125] Liu C-W *et.al*, ”New Methods for computing power system dynamic response for real-time transient stability prediction”, IEEE Transactions on Circuit and Systems-I: Fundamental Theory and Applications, Vol. 47, No. 3, March 2000, pp. 324 - 337.

[126] Minakawa T, “The required technological breakthrough in developing universal emergency control systems in terms with transient and dynamic stability”, Proceedings of IEEE Power Engineering Society Winter Meeting, 2000, pp. 66 - 71.

[127] Wang Y-J *et.al*, "A remedial control scheme protects against transient instabilities based on Phasor Measurement Units (PMUs) - A case study" Proceedings of IEEE Power Engineering Society Summer Meeting, 2000, pp. 1191 - 1195.

[128] Chang C-L *et.al*, "Oscillatory stability analysis using real-time measured data", IEEE Transactions on Power Systems, Vol. 8, No. 3, August 1993, pp. 823 - 829.

[129] Sharaf A.M *et.al*, "Transient stability and critical clearing time classification using neural networks", Proceedings of IEE 2nd International Conference on Advances in Power System Control, Operation and Management, December 1993, Hong Kong, pp. 365 - 372.

[130] Sharaf A.M *et.al*, "Neural network pattern classification of transient stability and loss of excitation for synchronous generators", Proceedings of IEEE International Conference on Neural Networks, 1994, pp. 2916 -2921.

[131] Begovic M.M, Milisavljevic M, "Monitoring and Control of Interarea Oscillations Via Real-Time Measurements and TCSC Control", Proceedings of the Bulk Power System Dynamics and Control IV - Restructuring, Santorini, Greece, August 24 - 28, 1997.

[132] Hemmingsson M *et.al*, "Estimation of electro-mechanical mode parameters using frequency measurements", Proceedings of IEEE Power Engineering Society Winter Meeting, 2001.

[133] Demarco C.L, "Identifying swing mode bifurcations and associated limits on available transfer capability", Proceedings of the American Control Conference, Philadelphia, Pennsylvania, USA, June 1998.

[134] Vittal V *et.al*, "Transient stability analysis of stressed power systems using the energy function method", IEEE Transactions on Power Systems, Vol. 3, No. 1, February 1988, pp. 239 - 244.

[135] Chiang H-D *et.al*, "Direct stability analysis of electric power systems using energy functions: theory, applications, and perspectives", Proceedings of the IEEE, Vol. 83, No. 11, November 1995 pp. 1497 - 1529.

[136] Lo K.L *et.al*, "Power system transient stability analysis by using modified Kohonen network", Proceedings of IEEE International Conference on Neural Networks, 1995, pp. 893 - 898.

[137] Marceau R.J *et.al*, "Signal energy search strategies for transient stability transfer limit determination", Proceedings of IEEE Power Engineering Society Summer Meeting, 1997.

[138] Marceau R.J, Soumare S, "A unified approach for estimating transient and long-term stability transfer limits", IEEE Transactions on Power Systems, Vol. 14, No. 2, May 1999, pp. 693 - 701.

[139] Tao W, Liu S, "Stability limits prediction by second order sensitivity based BCU method with structure preserving model", Proceedings of PowerCon 1998, 1998, pp. 1325 - 1330.

[140] Morioka Y *et.al*, "System separation equipment to minimize power system instability using generator's angular-velocity measurement", IEEE Transactions on Power Delivery, Vol. 8, No. 3, July 1993, pp. 941 - 947.

[141] Tang C.K *et.al*, "Transient stability index from conventional time domain simulation", IEEE Transactions on Power Systems, Vol. 9, No. 3, August 1994, pp. 1524 - 1530.

[142] Sun J.H, Lo K.L, "Transient stability real-time prediction for multi-machine power systems by using observation", Proceedings of TENCON '93, IEEE Region 10 Conference on Computer, Communication, Control and Power Engineering, 1993, pp. 217 -221.

[143] Auckland D.W *et.al*, "Artificial neural network-based method for transient response prediction", IEE Proceedings on Generation, Transmission and Distribution, Vol. 142, No. 3, November 1995, pp. 323 - 329.

[144] Qingsheng L *et.al*, "Real-time prediction and control for transient stability of multi-machine power system", Proceedings of PowerCon 1998, 1998, pp. 1361 - 1363.

[145] Daoud A.A *et.al*, "A new fast-learning algorithm for predicting power system stability", Proceedings of IEEE Power Engineering Society Winter Meeting, 2001, pp. 594 - 598.

[146] Lyapunov A.M, "General problem of stability of motion", (English translation) Academic Press, Inc., 1967.

[147] Machowski J *et.al*, "Power system dynamics and stability", ISBN 0-471-95643-0, John Wiley & Sons, 1998.

[148] Ejebe G.C *et.al*, “Transient energy based screening and monitoring for stability limits”, Proceedings of IEEE Power Engineering Society Summer Meeting, 2001.

[149] Wang L, Girgis A.A, ”A new method for power system transient instability detection”, IEEE Transactions on Power Delivery, Vol. 12, No. 3, July 1997, pp. 1082 - 1089.

[150] Hiskens I.A, Akke M, ”Analysis of the Nordel power grid disturbance of January 1, 1997 using trajectory sensitivities”, IEEE Transactions on Power Systems, Vol. 14, No. 3, August 1999, pp. 987- 994.

[151] Mannerback K-J, Rydberg J, ”On line fault identification algorithms on severe fault conditions in weak network supported by HVDC light”, Master-thesis, Department of Electrical Power Engineering, CHALMERS, 2001.

[152] Chang C.S, ”A hybrid model for transient stability evaluation of interconnected longitudinal power systems using neural network/pattern recognition approach”, IEEE Transactions on Power Systems, Vol. 9, No. 1, February 1994, pp. 85- 92.

[153] Huang K *et.al*, ”Neural-net based critical clearing time prediction in power system transient stability analysis”, Proceedings of IEE 2nd International Conference on Advances in Power System Control, Operation and Management, December 1993, Hong Kong, pp. 679 - 683.

[154] Rovnyak S *et.al*, ”Decision trees for real-time transient stability prediction”, IEEE Transactions on Power Systems, Vol. 9, No. 3, August 1994, pp. 1417 - 1426.

[155] Liu C-W *et.al*, ”Detection of transiently chaotic swings in power systems using real-time phasor measurement”, IEEE Transactions on Power Systems, Vol. 9, No. 3, August 1994, pp. 1285 - 1292.

[156] Tso S.K *et.al*, ”Fuzzy assessment of power system transient stability level based on steady-state data”, IEE Proceedings on Generation, Transmission and Distribution, Vol. 144, No. 6, November 1997, pp. 525 - 531.

[157] Xinli S *et.al*, “A fuzzy theory based principle to distinguish stable swings and unstable swings in complicated power systems”, Proceedings of PowerCon 1998, 1998, pp. 1091 - 1095.

[158] Liu C-W *et.al*, ”Application of a novel fuzzy neural network to real-time transient stability swings prediction based on synchronized phasor measurement”, IEEE Transactions on Power Systems, Vol. 14, No. 2, May 1999, pp. 685 - 692.

[159] Jonsson M, “Present Status of System Protection Schemes“, Tech.Report 23R, ISSN 1401-6167, Chalmers University of Technology, Gothenburg, Sweden, 2002.

[160] Fismen S.A, ”Nettvern i Nordel-området”, NOSY-rapport, June 29, 1992, Oslo, Norway, (in Norwegian).

[161] Janset O.P, ”Nettvern i Nordel-området”, NOSY-rapport, status 2000, Oslo, Norway, (in Norwegian).

[162] CIGRÉ TF 38-02-08, ”Long Term Dynamics Phase II”, 1995.

[163] Jonsson M, Daalder J, “Distance Protection and Voltage Stability“, PowerCon 2000, December 4-7, Perth, Australia, Proceedings Vol.2, pp. 971-976.

Appendix I Summary of Important SPS Features

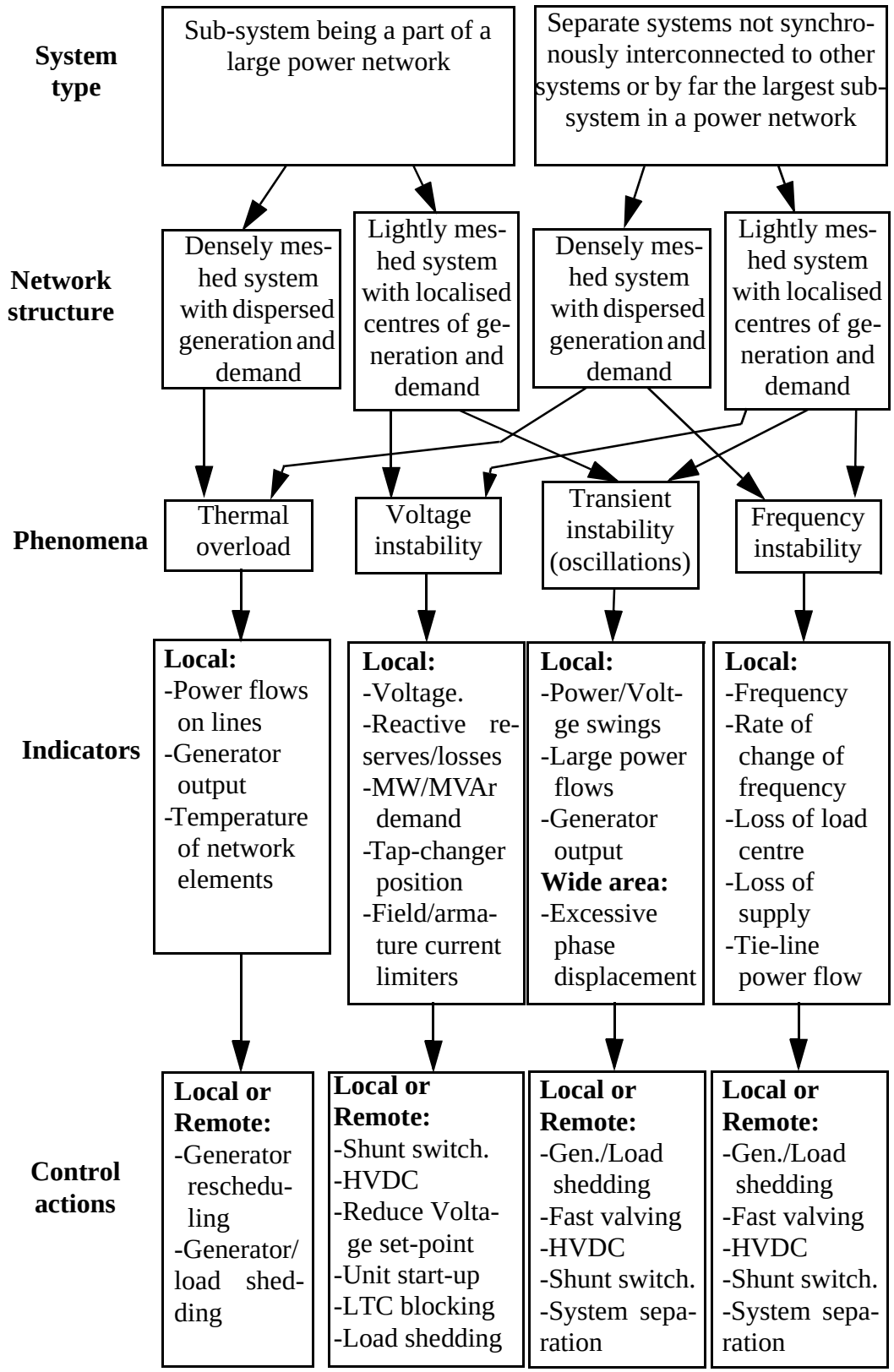

Paper A

An adaptive scheme to prevent undesirable distance protection operation during voltage instability

M. Jonsson, J. Daalder

Accepted for IEEE Transactions on Power Delivery

An Adaptive Scheme to Prevent Undesirable Distance Protection Operation During Voltage Instability

Mattias Jonsson, *Student member, IEEE,* and Jaap Daalder

Abstract: An adaptive algorithm to prevent undesirable distance protection operations during voltage instability is proposed. The algorithm is based on mathematical logic blocks and uses the rate of change of voltage as an additional relay criteria to increase the relay security with respect to voltage instability.

Studies are based on simulations using two different test systems; a fifteen bus system developed by the authors and the Nordic32 system.

The investigation shows that undesirable zone 3 distance relay operations can be the difference between a blackout and a recovering system during voltage instability. However simulations have shown that the adaptive algorithm may save the system from a collapse. Although the algorithm prevents mal-trips due to voltage instability the reach of the distance relay will not be restricted.

Keywords: Adaptive relaying, Distance protection, Remote back-up, Voltage stability.

I. INTRODUCTION

Undesirable (zone 3) distance relay operations have contributed to voltage collapses world wide. The most well known incident is perhaps the July 2, 1996 outage in the WSCC system [1] where zone 3 mal-trips occurred which gave rise to the collapse. Other examples are Brazil 1999 [2] and Sweden 1983 [3].

Zone 3 distance relays are mainly used to provide remote back-up protection for adjacent sections of transmission circuits. In the ideal case the entire length of all adjacent circuits are back-up protected. However long lines, infeed and load encroachment may cause difficulties to obtain that result in a secure manner. It is the opinion of the authors that uncontrolled disconnection of power lines should be avoided during voltage instability. For example distance relays should not trip transmission lines prior to the disconnection of generators by their own protection equipment as this possibly will cause cascading outages when all of the remaining generation capacity is further used. Thus where transmission lines are provided with duplicate main protection and/or where difficulties with settings exist there may be reason for not applying zone 3 distance element at all, as the zone 3 protection will offer little improvement in fault clearance but may form a considerable threat to system security. However many utilities rely on non-duplicated line protection systems using remote back-up as their standard solution. Furthermore, for systems applying duplicated line protection and no remote back-up, maintenance of one of the protection groups will lead to a temporary absence of back-up protection. The algorithm proposed here facilitates these situations as it is a cost-effective and plain way of improving the relay security with respect to voltage instability.

Adaptive relaying is a suitable tool in case of stressed power system conditions. In [4] a scheme is described where dependability is provided during normal system conditions but security is emphasized during abnormal conditions. The same approach is used for the algorithm proposed here to avoid load encroachment during voltage instability.

Modern numerical relays give a wide range of relay inputs to choose between and thus unique protection schemes can easily be developed. The algorithm proposed here utilizes these new possibilities by using the derivative of the voltage as relay input. Additionally the algorithm is based on mathematical logic blocks which makes it easy to realize for numerical relays where the relay scheme is developed in a user friendly computer software.

The type of events addressed in this paper are rare occasions. However, when they occur usually a major part of the system load is affected. Hence these disturbances may be extremely costly and can cause much social inconvenience. It is likely that the frequency of these occasions will increase in the future as power systems are operated closer to their stability limits due to environmental constraints and deregulation.

II. DISTANCE RELAYS MAY CONTRIBUTE TO VOLTAGE INSTABILITY

Voltage instability is a phase symmetrical phenomenon. Hence no zero sequence component is present and the phase voltages and currents are symmetrical. Thus the apparent impedance $\overline{Z}_r$ as seen by a distance relay during voltage insta-

This work was financially supported by Svenska Kraftnät.

Mattias Jonsson and Jaap Daalder are both with Department of Electric Power Engineering, Chalmers University of Technology, 412 96 Gothenburg, Sweden. Their e-mail addresses are mattias.jonsson@elteknik.chalmers.se and jaap.daalder@elteknik.chalmers.se.

bility corresponds to (1). Here $\overline{U}$ is the line to line voltage and P and Q are the injected active and reactive power at the location of the relay.

$$\overline{Z}_r = \frac{|\overline{U}|^2 \cdot (P + jQ)}{P^2 + Q^2} \quad (1)$$

In case $\overline{Z}_r$ remains within the area of one of the pre-defined zones of operation during a time exceeding the setting of the timer associated to the zone, the relay will operate. Low system voltages and high (reactive) power flows are typical features of voltage instability events. It follows from (1) that these events may cause distance relays to mal-trip. This behaviour is undesirable since it will aggravate the status of the power system in an already severe situation.

Undesirable relay operations due to voltage instability will mainly be initiated by the zone with the longest reach. Normally this is the zone used for remote back-up protection which usually is zone 3. Accordingly the algorithm proposed here is presented with respect to zone 3 but can obviously be applied on any zone.

III. AN ADAPTIVE ALGORITHM TO PREVENT MAL-TRIPS DUE TO VOLTAGE INSTABILITY

For numerical relays it is usually possible to choose between different setting groups; i.e choose different settings of the zones of operation depending on the prevailing power system state. This could be done by the relay itself; e.g. based on a voltage criterion or manually by the operator.

The adaptive part of the algorithm proposed here is based on the same principle but instead of solely changing the reach of the zones of operation the whole relay algorithm is changed according to Fig. 1. During normal operation the conventional distance protection algorithm is used but when a stressed operation condition occurs, where security is more of an issue, the relay switches to the algorithm in Fig. 2. The criterion used to decide which algorithm to be applied may be based on the voltage level, the reactive power or the impedance method proposed in [5].

The algorithm in Fig. 2 may also be used as a non-adaptive algorithm where it is applied as the exclusive distance relay algorithm.

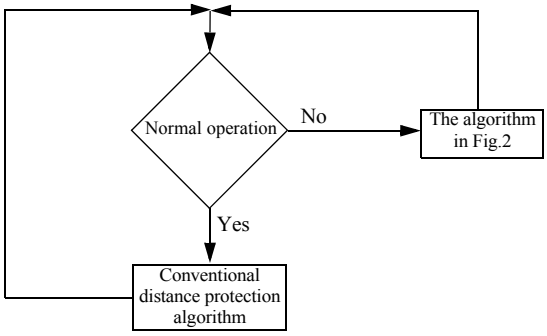

Fig. 1. Adaptive distance relay.

The algorithm proposed in Fig. 2 is based on simple mathematical logic blocks where the dependability is decreased and the security is increased as compared to traditional distance relaying. The idea is not only to consider the relation between the apparent impedance and the zones of operation but also the different events which occur in the system when the zone 3 is entered. These events can be determined from changes in the voltage.

When a short circuit fault occurs the change of the voltage is substantial in the faulted phases in the area close to the location of the fault [6]. In case of voltage instability the voltage changes are mostly low to moderate until close to the final collapse. Hence the derivative of the voltage may be used to distinguish between short circuit faults and voltage changes due to stressed system conditions. In the algorithm of Fig. 2 the voltage is measured continuously and used as an input. The main challenge in the algorithm is to determine the different types of events based only on information from the derivative of voltage, and this with a high degree of reliability. However simulations and measurements have shown that there is a considerable difference between a short circuit fault, a fault clearance and other power system events.

It is important that the relay will operate as planned when a short circuit fault occurs at the same time as voltage instability is present. Therefore when the apparent impedance has entered the zone 3 the derivative of the voltage is continuously analysed and thus used to detect short circuit faults. In Fig. 2 the quantities with a subscript (except t_{start} which is associated to the start of the timer) are given a fixed value by the relay operator. The remaining quantities are continuously updated by the relay during operation. Throughout operation the pre-set values are compared with the real-time updated values to obtain correct relay activity.

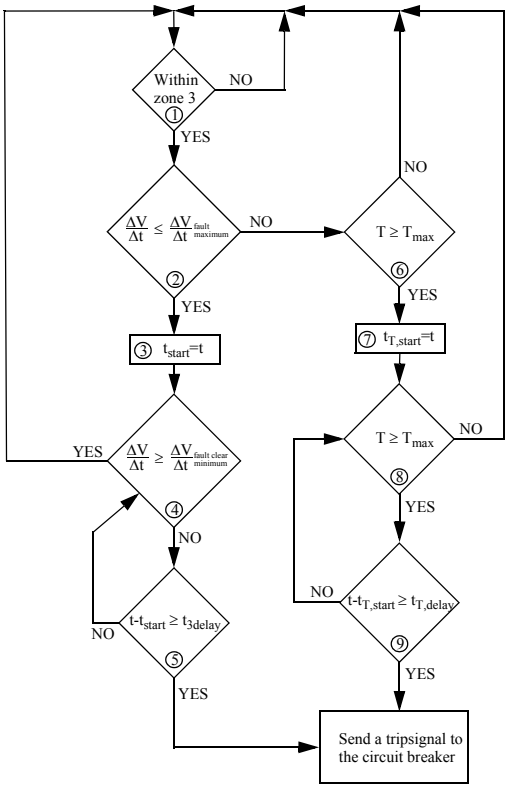

Fig. 2. Relay algorithm used during voltage instability.

The following is a description of the block functions.

Block 1: Checks if the apparent impedance is within zone 3.

Block 2: Decides if a short circuit fault has occurred. When a fault occurs $\Delta V/\Delta t$ will have a negative value with a large magnitude.

$$\frac{\Delta V}{\Delta t} \leq \frac{\Delta V}{\Delta t}_{maximum}^{fault} \qquad \text{A fault has occured.}$$

$$\frac{\Delta V}{\Delta t} > \frac{\Delta V}{\Delta t}_{maximum}^{fault} \qquad \text{No fault has occured.}$$

Block 3: The timer associated to zone 3 is started.
t_{start} = time when zone 3 is entered.

Block 4: Decides if the fault is cleared by primary protection. When the fault is cleared $\Delta V/\Delta t$ will have a positive value with a large magnitude.

$$\frac{\Delta V}{\Delta t} \geq \frac{\Delta V}{\Delta t}_{minimum}^{fault\ clear} \qquad \text{The fault has been cleared.}$$

$$\frac{\Delta V}{\Delta t} < \frac{\Delta V}{\Delta t}_{minimum}^{fault\ clear} \qquad \text{The fault has not been cleared.}$$

Block 5: Waits for the fault to be cleared by primary protection.
t_{3delay} = time delay associated to zone 3.

Blocks 6 to 9 may be implemented in the algorithm when distance protection is used to protect overhead lines due to thermal overload etc.

Block 6 & 8: Checks if the line temperature T exceeds the pre-set maximum limit.
T_{max}= maximum allowed temperature in the circuit.

Block 7: Timer is started for the thermal overload protection.
$t_{T,\ start}$ = time when the maximum allowed temperature is reached.

Block 9: Regulates temporary overload.
$t_{T,delay}$ = time delay associated to the thermal overload protection.

Most cases are handled well by the algorithm. However a few cases may cause the algorithm difficulties to operate as planned. The reason for this is that unexpected values of the derivative of the voltage may occur for some events in combination with tight or wrong settings of the parameters. The most dangerous case is when a voltage step increasing action occurs between a short circuit fault and a fault clearance. Block 4 may apprehend the positive voltage step as fault clearance by primary protection. Thus the algorithm will not clear the fault. During voltage instability scenarios load shedding and manually or automatic capacitor switching may be the source of this type of problem. Shunt capacitor switching will not have a significant impact during the time when a fault is present as the voltage will be extremely low and therefore a capacitor will not increase the voltage much when it is connected. When load shedding is performed some communication device can be used in combination with logic blocks to set the output from block 4 to NO during the moment of action. In this way the security will be increased.

Most likely current limiters will be activated and generators tripped during a severe voltage instability. This will cause voltage decays of a more or less outspoken nature. Close to a collapse the negative derivative of the voltage may be difficult to distinguish from the one caused by a short circuit fault. Still it is undesirable that these negative derivatives are treated as faults. These inadequacies can be avoided by using communication devices. When a generator is tripped or a current limiter activated a notifying signal can be sent to the relays within the affected region. Hence the output from block 2 can be set to NO for a few cycles and the event will not be treated as a fault.

To find suitable values of the settings, events such as shunt capacitor switching, line tripping, load shedding and short circuit faults must be considered for each relay bus at different operation modes. Modern communication technology has created the possibility for centralised calculation of settings and local in-service adjustment and therefore suits the purpose well. A computer based network model may be used for on-line calculations. Hence the relay settings can continuously be updated to the prevailing power system condition. Today these type of calculations are usually done manually.

One may ask oneself, why not use the derivative of the measured impedance as a criterion in the algorithm? Simulations have shown that the derivative of the impedance does not act logically stringent for similar power system occurrences; especially when long and heavily loaded lines are considered. Also the fault location versus relay bus location has a strong influence on the apparent impedance in the R-X diagram; e.g if a fault occurs on an adjacent or a parallel line. The derivative of the resistance and reactance has similar disadvantages compared to the derivative of the impedance. Another disadvantage is that the derivative of the impedance is more complicated to obtain as compared to the derivative of the voltage.

The discussion in this paper is to demonstrate the principles of a new adaptive algorithm. In case of actual implementation attention has to be paid to practical issues such as communication devices, data memory, window size, noise in measurements etc. Also when the algorithm is programmed some functions have to be added. For instance in case of a short circuit fault occurring at the same time as the line is overloaded, block 2 has to be activated in parallel with the alternating blocks 8 and 9. Depending on how $t_{T,delay}$ is chosen in relation with t_{3delay} a timer coordination may be necessary to determine whether the trip signal will be sent due to the short circuit fault or due to the overload.

IV. TEST SYSTEMS

Two different test systems have been used for simulations. The first one is a 15 bus system representative for the Swedish transmission grid; the second is the more extensive Nordic32 system [7]. The 15 bus system is mainly used to illustrate the performance of the adaptive algorithm while the Nordic32 system is used to compare results of the 15 bus system with results of a more comprehensive grid.

Fig. 3 shows the 15 bus system. Two voltage levels are used, where the main part of the equipment is connected to the 400 kV level. However, the loads and a few shunt devices are connected to the 130 kV level.

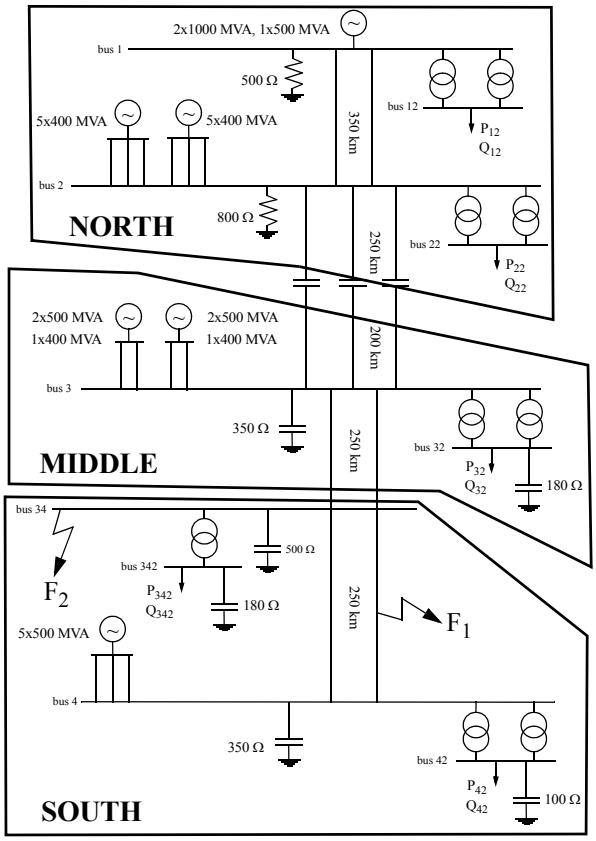

Fig. 3. The fifteen bus system representative for the Swedish system.

The generation in the system is a mixture of hydro- and nuclear power. All generator units are equipped with field current limiters, in addition the nuclear units have stator current limiters. In the NORTH area, all generators are hydro units which are responsible for the frequency control; in the MIDDLE and SOUTH areas the nuclear power units have a fixed active output. The loads in the MIDDLE and SOUTH areas dominate the total consumption in the system. Thus a large amount of power will be transported from NORTH to MIDDLE and also from MIDDLE towards SOUTH. The transmission lines between bus 2 and bus 3 are equipped with serie capacitors giving a line compensation of 50 %. Observe that the electrical parallel circuits in the system are not considered to be geographically parallel. The load models used in the system are based on the experimental work of le Dous *et al*. [8] and all the other models are identical to the ones applied in the Nordic32 system [7].

When the reach of the zone 3 element is determined infeed is considered and the idea is that the whole length of all adjacent lines should be protected.

V. SIMULATIONS IN THE 15 BUS SYSTEM

The simulations have been performed in SIMPOW [9] and the improvement due to the adaptive algorithm is demonstrated. For

illustration both the mho and quadrilateral relay characteristics are used.

At the pre-fault state the system is heavily loaded in the SOUTH area. The power transfer from bus 3 towards bus 34 is about 2200 MW and from bus 34 to bus 4 around 1200 MW. The initial disturbance F_1 is a permanent three phase short circuit fault having zero fault resistance and located in the middle of one of the transmission lines between bus 34 and bus 4. The fault is cleared by the primary protection. To further demonstrate the performance of the algorithm in Fig. 2 an additional fault F_2 is applied. This fault is a busbar fault at bus 342 and occurs when the apparent impedance already has entered the zone 3.

Fig. 4 shows the voltages at bus 3 and bus 34 before and after the faults. When conventional zone 3 distance relaying is applied with settings based on the criteria mentioned earlier the system will collapse approximately 83 seconds after the initial fault independent of the shape of the operating zone used. In the case of mho relays the collapse will be initiated by the zone 3 elements at bus 3 protecting the lines between bus 3 and bus 34; Fig. 5. When quadrilateral relays are used the collapse will be initiated by the zone 3 element located at bus 34 protecting the remaining line between bus 34 and bus 4. This should be compared with the situation that either the reach of the conventional relays is decreased or the algorithm in Fig. 2 is applied. In these cases the system will recover to a stable operating point. Without the adaptive algorithm the reach of the mho relays at bus 3 protecting the lines between bus 3 and bus 34 must be decreased to avoid a voltage collapse. If this approach is applied only 60 % or less of the adjacent lines will be remote back-up protected. When quadrilateral relays are in operation their reach at bus 34 must be decreased in resistive direction from 105 Ω to about 85 Ω to avoid a collapse. The collapse plotted in Fig. 4 is valid for the case of mho relays.

1: Pre fault state.

1-2: At t=5 s a permanent three phase fault (F_1) occurs on one of the lines between bus 34 and bus 4.

2-3: At t=5.09 s the fault is cleared.

3-4: At t=5.5 s the shunt capacitor at bus 32 is connected and the reactors at bus 1 and bus 2 are disconnected.

4-5: At t=5.8 s auto reclosing.

5-6: At t=5.89 s the faulted line is permanently disconnected.

6-8: The impedance as seen by the relays is slowly decreasing due to decreasing voltages and increasing (reactive) power flows.

7: At t=87.2 s the zone 3 of the mho relays located at bus 3 protecting the lines between bus 3 and bus 34 are entered. About the same time zone 3 of the quadrilateral relay located at bus 34 protecting the remaining line between bus 34 and bus 4 is also entered.

8-9: At t=250 s a bus fault (F_2) occurs at bus 342.

9-10: At t=250.09 s the bus fault is cleared.

11: The system starts to recover and will attain a stable operating mode.

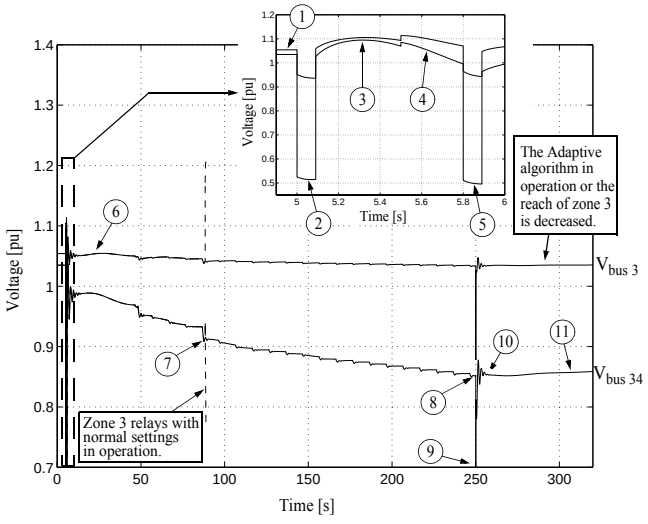

Fig. 4. Voltages at bus 3 and bus 34. In case of normal zone 3 settings collapse occurs at indication 7 whereas using the adaptive algorithm or a decrease in element reach the system survives.

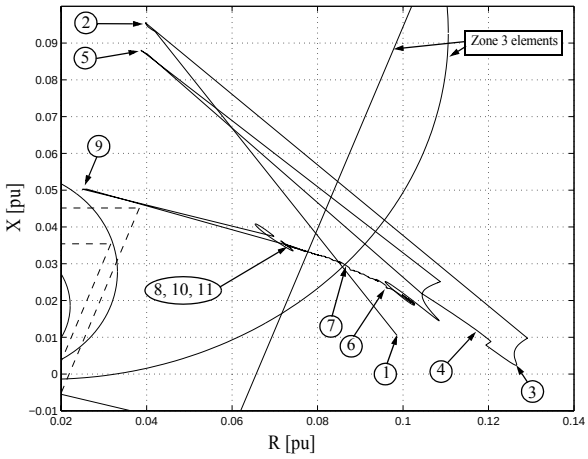

Fig. 5. The impedance as seen by a mho and quadrilateral relay located at bus 3 protecting one of the transmission line between bus 3 and bus 34.

In this simulation the injected reactive power at bus 3 towards bus 34 increases about 100 % during the first 83 seconds after

the initial three phase fault. The other power flows in the system are approximately the same. When mho relays are used it is not the relay located at the bus with the lowest voltage level which operates first but the relays that meet the largest increase in power flows. This shows that it is not only low voltage levels which are important to consider in order to avoid mal-trips due to voltage instability but also reactive power flows which may increase considerably.

The criterion used to choose between the conventional and the proposed relay algorithm is based on the reactive power. Basically the criterion applies the conventional distance relay algorithm when the protected line generates reactive power. When the line consumes reactive power the proposed algorithm is activated emphasizing security. This criterion is suitable in systems where the lines generally are operated below the surge impedance load. For example, in the Swedish transmission system. However in systems where the lines normally are loaded above the surge impedance load the algorithm in Fig. 2 can be activated when the reactive power consumed by the protected line exceeds a certain level.

One reason why the reactive power and not the voltage is used to decide which algorithm should be used is that the voltage sometimes is a bad indicator of the system conditions. For example, bus 3 is located close to generator buses. Consequently and as illustrated in Fig. 4, the voltage at bus 3 will be held at a fairly high voltage level by the voltage control of the generators until very close to a collapse. Hence if the relay would base its adaptivity on the voltage level, then the probability for a too late change of algorithms would be significant. In this case the lines between bus 3 and bus 34 are heavily loaded, i.e they consume reactive power prior to the initial fault. As a consequence the relays located at bus 3 have already adjusted their relay algorithm to the one proposed in Fig. 2 before the three phase fault occurs. The lines between bus 34 and bus 4 generate reactive power before the initial three phase fault and thus the relays located at bus 34 are applying the conventional distance relay algorithm. However as the faulted line is disconnected the remaining line between bus 34 and bus 4 start to consume reactive power and thus the associated relay adjusts its relay algorithm.

Since the derivative of the voltage due to the disturbance is the same at bus 3 and bus 34 apart from the magnitude the fundamental method of operation will be the same at these two buses. Hence only the derivative of the voltage as seen by the relays located at bus 3 is investigated.

In Fig. 6 we see that there is a considerable difference in the magnitude of the negative peaks of the derivative of the voltage (which fall in between indications 6 and 8) caused by tap-changer operations and current limiter actions as compared with the peaks caused by the short circuit faults. As described earlier, this is the phenomenon used by the algorithm to distinguish short circuit faults from other events in the system.

.

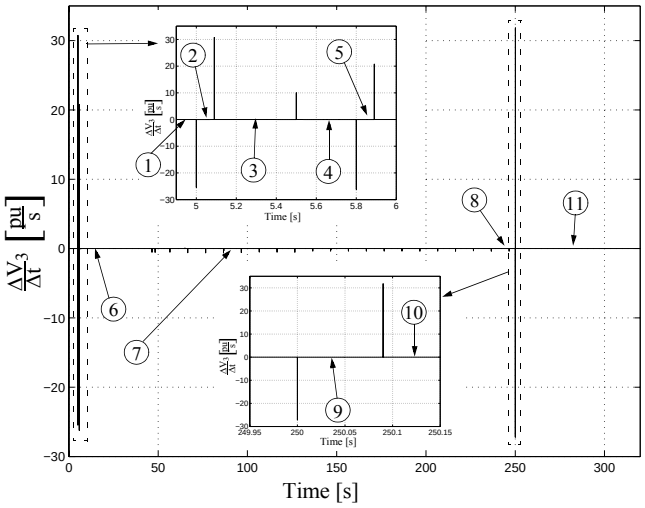

Fig. 6. The derivative of the voltage at bus 3.

The negative and positive peaks of the voltage derivative which are generated when the initial fault occurs and is cleared (between indications 1 to 6), make that the proposed algorithm achieves the same result as conventional remote back-up distance relaying. When the initial three phase fault occurs the apparent impedance enters the zone 3; Fig. 5. At the same time the relays see a high peak of the derivative of the voltage with a negative sign. Hence the criteria in blocks 1 and 2 are fulfilled and the timer in block 3 is started. The algorithm starts to alternate between blocks 4 and 5 waiting for the fault to be cleared by the main protection. This happens 90 ms after the initial fault. Consequently the relays located at bus 3 see a positive peak of the derivative of the voltage and the apparent impedance leaves the zone 3 of operation. Hence the algorithm again starts to wait for the criterion in block 1 to be fulfilled. The criterion in block 1 is once again fulfilled when the auto-reclosing is performed. As the auto-reclosing is not successful the operating sequence described is repeated for the algorithm.

When the zone 3 elements are entered at 87.2 s due to the decreasing voltages and increasing power flows, block 2 in Fig. 2 will not treat this as a fault as no large negative peak of the derivative of the voltage is present. Thus when the apparent impedance as seen by the relay further moves into zone 3 the algorithm will make the relay to continue to wait for a true short circuit fault as the algorithm will alternate between blocks 1,2 and 6. This will continue until the impedance leaves zone 3, the line is thermally overloaded or a high negative peak of the derivative of the voltage occurs.

When the bus fault at indication 8 occurs the impedance as

seen by the relay will be located within zone 3 at the same time as the relay will sense a high negative peak of the derivative of the voltage. Hence the algorithm will start to alternate between blocks 4 and 5 waiting for a high positive peak to arise; i.e the fault to be cleared. This process may continue until the time delay of zone 3 expires and a trip signal will be sent to the circuit breaker. However in this case the fault is cleared by the primary protection. Thus the algorithm will be reset and continue to alternate between blocks 1,2 and 6. The line will not be tripped and the system starts to recover.

Bus 3 is a typical bus where the algorithm may be expected to work inadequately. When the initial fault is cleared the algorithm may meet a proportionally low positive peak of the derivative of the voltage since the relay is located quite far from the fault. At the same time the capacity of shunt capacitors close to the bus is high. This may cause trouble when the values of the parameters in the algorithm are selected. In Fig. 6 we see that the shunt switching between indication 3 and 4 causes a positive peak which is about 50 % of the derivative of the voltage caused by the final fault clearing. If the capacitor switching occurs during the time when the fault is present the algorithm may interpret this as a fault clearance. This set of events has been simulated where the result shows that the positive peak of the derivative of the voltage due to the shunt switching in this case will only be about 15 % of the peak caused by the fault clearance. This is due to the low voltage in the system when the fault is present.

Simulations have also shown that different fault resistances have little impact on the magnitude of the derivative of the voltage.

VI. SIMULATION IN THE NORDIC32 TEST SYSTEM

The Nordic32 system has been simulated in ARISTO [10]. The initial disturbance for this case is a permanent three phase short circuit fault located in the middle of the transmission line indicated as Line 2 in Fig. 7. Thirty seconds before the fault occurs the system is weakened as Line 1 is manually taken out of operation. Still the power flows from the North to the Central region are fairly normal and the voltage is close to the nominal 400 kV at all system buses. In Fig. 8 the fault occurs at 150 seconds and is immediately cleared by primary protection. The voltage level starts to decrease and the reactive power demand starts to increase, especially in the framed area. Automatic shunt switching is performed to halt the voltage reduction and to restore the voltage level. In case the adaptive algorithm is used or when the reach of the zone 3 element is decreased this proceeding will succeed as Relay A will not operate when zone 3 is entered due to the voltage instability. In Fig. 7 the system is displayed in the stable operation mode which is reached approximately 9 minutes after the short circuit fault when one or both of these actions are taken. However if neither the algorithm is applied nor the reach of the zone 3 element is decreased Relay A will operate about 8 minutes after the fault and initiate a total blackout in the framed region.

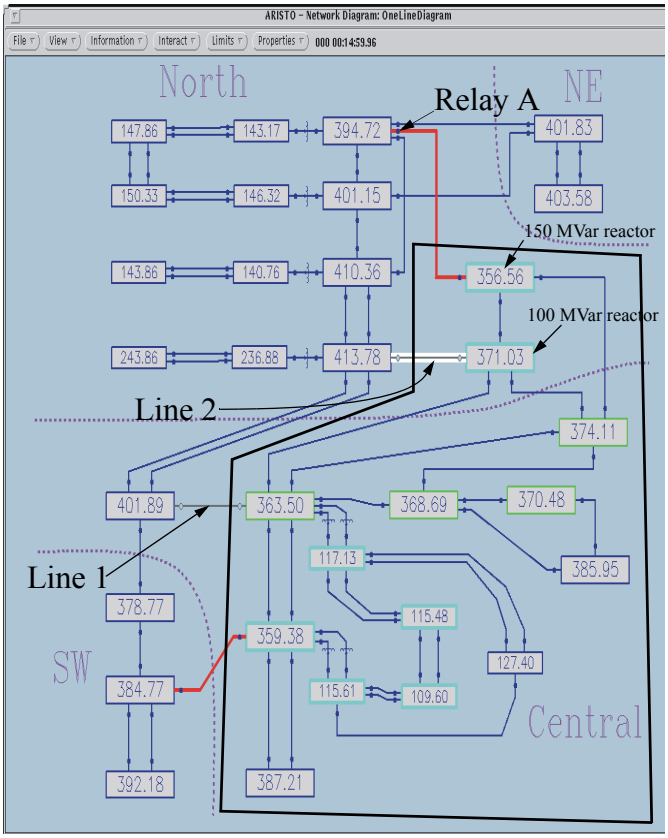

Fig. 7. Final system condition after a permanent three phase fault on line 2 when the adaptive algorithm is applied for Relay A. The voltage at each bus is displayed.

The impedance relay characteristic of the distance element applied is of the quadrilateral type operated in combination with no devices such as load blinders, start relays or general start criteria. All zone 3 elements in the system are set to cover all adjacent lines in reactive direction. In resistive direction the sensitivity among the relays varies but Relay A is set to operate for fault resistances of 115.2 Ω or less.

From Fig. 8 we see that the peaks of the derivative of the voltage for the three phase fault and fault clearing is totally dominating compared to the peaks caused by the automatic shunt switching and the disconnection of Line 1. Notice that the peaks of the derivative with origin in the disconnection of Line 1 and the reactor switching are less then 2% of the magnitude of the derivative for the fault and fault clearing.

The input voltage used for the calculation of the derivative of the voltage is in this simulation sampled with a lower fre-

quency then used for the 15 bus system. Therefore the peaks of the derivative in Fig. 8 are not as distinct as in Fig. 6.

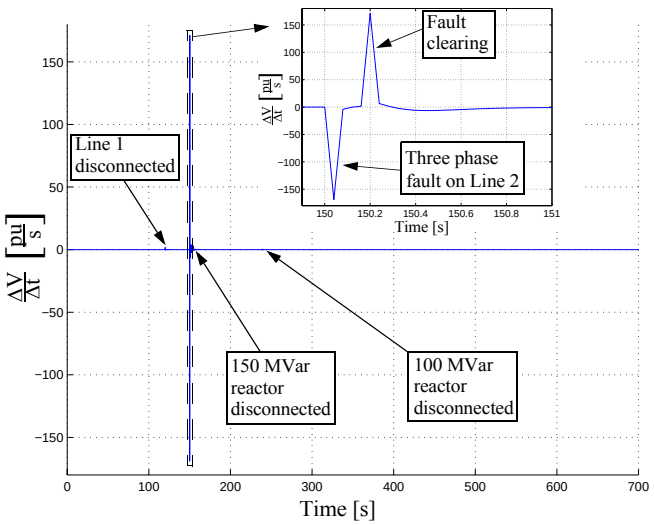

Fig. 8. The derivative of the voltage at the location of Relay A.

VII. CONCLUSIONS

Simulations in two different test systems have shown that undesirable zone 3 distance relay operations during voltage instability can be the difference between a total blackout and a recovering system. The reasons for these mal-trips are often a combination of decreasing system voltages and increasing reactive power flows.

In order to avoid these unwanted relay operations an adaptive algorithm which prevents mal-tripping due to voltage instability has been proposed. The algorithm not only considers the relation between the apparent impedance and the zone of operation but also uses the derivative of the voltage to distinguish short circuit faults from other events in the system. Although the algorithm prevents mal-trips due to load encroachment associated with voltage instability the reach of the distance relay will not be restricted.

VIII. ACKNOWLEDGEMENTS

The authors would like to thank Svenska Kraftnät for their interest in this research area and for their financial support. The authors also would like to thank ABB Power Systems for providing Simpow.

IX. REFERENCES

[1] Western Systems Coordinating Council Disturbance Report For the Power System Outages that Occurred on the Western Interconnection on July 2, 1996, 1424 MAST and July 3, 1996, 1403 MAST, Approved September 19, 1996, Internet URL http://www.wscc.com/distnews.htm.

[2] X. Vieira *et al.*, "The March 11:th 1999 Blackout: Short-Term Measures to Improve System Security and Overview of the Reports Prepared by the International Experts", CIGRÉ Session, SC 39 Workshop on Large Disturbances, Paris, August 29, 2000.

[3] "The blackout in Sweden 27-12-1983", Vattenfall publication, February 1984.

[4] Horowitz S.H, Phadke A.G, Thorp J.S, "Adaptive Transmission System Relaying", IEEE Transaction on Power Delivery, Vol. 3, No. 4, October 1988, pp. 1436 - 1445.

[5] Vu K, Begovic M.M, Novosel D, Saha M.M, "Use of Local Measurements to Estimate Voltage-Stability Margin", IEEE Transaction on Power Systems, Vol. 14, No. 3, August 1999, pp. 1029 - 1035.

[6] Rockefeller G.D et al. "Adaptive transmission relaying concepts for improved performance", IEEE Transaction on Power Delivery, Vol. 3, No. 4, October 1988, pp. 1446 - 1457.

[7] CIGRÉ TF 38-02-08, "Long Term Dynamics Phase II", 1995.

[8] le Dous G, Daalder J, Karlsson D, "Dynamical Load Measurement in a 2000 MW System in order to Operate Power Systems Closer to their Limits", CIGRÈ Report 39-107, Paris, August 1998.

[9] Fankhauser H.R, Aneros K, A-A Edris. and Torseng S, "Advanced Simulation Techniques for the Analysis of Power System Dynamics", IEEE Computer Applications in Power, Vol. 3, No. 4, October 1990, pp. 31 - 36.

[10] Edström A, Walve K, "A Highly Interactive Fast Simulator Covering Transients Stability and Long Term Dynamics in Large Power Systems", CIGRÉ Report 38-204, Paris, august 28-September 3, 1994.

X. BIOGRAPHIES

Mattias Jonsson received his M. Sc. from Chalmers University of Technology in 1998. His interest lies in power system stability and power system protection. At present he works towards a Ph.D. thesis.

Jaap E. Daalder obtained his Ph.D in power engineering from the Eindhoven University of Technology, The Netherlands. He worked there as an Associate Professor until 1984 when he left for Norway to become a Director of Technology and Member of the Board of a subsidiary of the Brown Boveri Company, nowadays ABB. In 1993 he was appointed as full Professor at Chalmers University of Technology. Since 1997 he is heading the Department of Electric Power Engineering. His areas of interest are power systems and environmental issues related to power engineering.

Paper B

A new protection scheme to prevent mal-trips due to power swings

M. Jonsson, J. Daalder

Presented at
IEEE/PES Transmission and Distribution Conference and Exposition,
October 28 - November 2, 2001, Atlanta, USA.

A new protection scheme to prevent mal-trips due to power swings

Mattias Jonsson
mattias.jonsson@elteknik.chalmers.se

Jaap Daalder
jaap.daalder@elteknik.chalmers.se

Department of Electric Power Engineering
Chalmers University of Technology
Gothenburg, S-41296 Sweden,
www.elteknik.chalmers.se

Abstract: New distance protection algorithms based on mathematical logic blocks are introduced in this paper. The algorithms prevent mal-trips due to power oscillations using additional criteria in combination with traditional distance relaying. These additional criteria are based on symmetrical components and the derivative of the phase angle associated with the current as seen by the relay.

A simulation is performed in a eighteen bus system developed by the authors where the performance of the algorithms is analysed.

No timer settings as is necessary for conventional Power Swing Detectors are needed. Thus different cycle times of the power oscillations will not affect the performance of the algorithms. Neither an area in the RX-diagram has to be pre-defined which may cause extraordinary difficulties for applications serving long distance transmission lines.

Keywords: Distance protection, Transient stability, Power swings, Numerical relays, Power Swing Detector.

I. INTRODUCTION

Transient instability in power systems generate power oscillations. These oscillations may cause unwanted tripping of distance relays. To prevent these mal-trips the distance relay is often combined with a Power Swing Detector (PSD). Conventional PSD's usually measure the time it takes for the apparent impedance to travel through a pre-defined impedance area in the RX-diagram which is located outside the area of the zones of operation. Due to the varying cycle times of the power oscillations a satisfactory setting of the timer associated with the PSD may be difficult to obtain. In an yet unpublished CIGRÉ WG34.09 investigation several cases of incorrect PSD behaviour due to this phenomenon are reported. For long transmission lines difficulties may occur when the location of the pre-defined PSD impedance area is chosen. As the operation point at peak load may be close to the boundary of the fault detector zone there may not be enough place for the impedance area of the PSD [1]. Hence a PSD which is not sensitive to the cycle time of power swings or the line length would be desirable. In particular the limitations of the PSD associated with the line length are undesirable as power oscillations mainly occur on tie-lines and long transmission lines.

From a technical point of view correct operating relays have obviously been an important issue throughout the years. However the issue grow even more important in a deregulated market. An incorrect outage of a transmission line may lead to advantages for competitors, penalty fees and an (unnecessary) absence of income. Unreliable relays may lead to situations where grid owners give their protection equipment narrow settings to avoid unwanted relay operations due to power swings. In some cases the settings may be too narrow and the relays will not operate for all possible fault conditions. In a broader perspective this behaviour may be a threat to system security.

Many relay solutions applied today have their origin in former technical hardware limitations and thus the possibilities given by new numerical and communication technologies are not always utilized to their maximum capacity. An example is the PSD based on the transition time through a blocking impedance area. As already mentioned the solution have not operated as desired several times throughout the years. Nevertheless it is still the main method used in numerical distance relays to prevent mal-trips due to power oscillations. As numerical and signal processing technologies develop, new electrical quantities may become attractive as relay inputs. For example, as the sampling frequency increases the derivative of electrical quantities may become a widely used relay criterion. Additionally the fast development of information technology in power system applications may lead to the launch of economically and reliable protection strategies based to a great extent on communication devices.

In modern numerical relays a computer software is used to create the operation scheme of the relay based on mathematical logic blocks. Hence unique solutions suitable for each user can easily be obtained. The PSD suggested here is based on this new user friendly relay approach and is incorporated in the relay algorithm. The algorithm is based on traditional distance relaying in combination with additional criteria. To initiate relay operation not only the apparent impedance has to be within the zone of operation during a pre-defined time but at least one additional criterion has also to be fulfilled.

II. ADDITIONAL CRITERIA FOR A DISTANCE RELAY ALGORITHM

The criteria which may be combined with the conventional distance relay methods vary for different types of distance elements. For phase to ground elements the residual current may be used. During unsymmetrical phase to phase faults a negative-sequence current will arise in the system and may therefore be a suitable criterion. However phase to phase elements must also be able to distinguish symmetrical three phase faults. A criterion associated with a negative- or zero-sequence current will not achieve this demand and therefore another method is introduced below.

The fundamental behaviour of the phase angles of the voltage and current at the sending end of a transmission line immediately before and after a three phase short circuit fault is briefly studied using the small power system in figure 1. During normal operation the voltage $\overline{V}$ and current $\overline{I}$ are given as in (1) and (2).

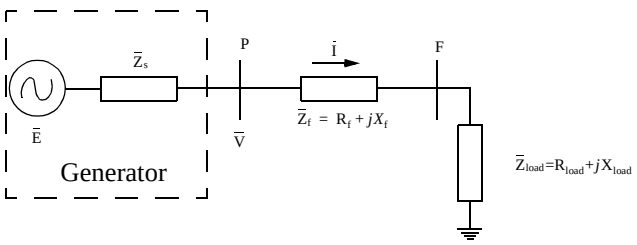

Fig. 1. A small transmission system during normal operation.

$$\overline{V} = \frac{\overline{Z}_f + \overline{Z}_{load}}{\overline{Z}_s + \overline{Z}_f + \overline{Z}_{load}} \cdot \overline{E} \approx \overline{E} \qquad \forall \begin{Bmatrix} \overline{Z}_{load} \gg \overline{Z}_f \\ \overline{Z}_{load} \gg \overline{Z}_s \end{Bmatrix} \tag{1}$$

$$\overline{I} = \frac{\overline{V}}{\overline{Z}_f + \overline{Z}_{load}} \approx \frac{\overline{V}}{R_{load}} \qquad \forall \begin{Bmatrix} R_{load} \gg X_{load} \\ R_{load} \gg X_f \gg R_f \end{Bmatrix} \tag{2}$$

When a three phase fault occurs at node F the voltage and current can be written as in (3) and (4). The voltage at the fault location is assumed to be zero when the fault is present.

$$\overline{V} = \frac{\overline{Z}_f}{\overline{Z}_s + \overline{Z}_f} \cdot \overline{E} \sim \overline{E} \qquad \forall \begin{Bmatrix} X_f \gg R_f \\ X_s \gg R_s \end{Bmatrix} \tag{3}$$

$$\overline{I} = \frac{\overline{V}}{\overline{Z}_f} \approx \frac{\overline{V}}{jX_f} \qquad \forall \{X_f \gg R_f\} \tag{4}$$

Immediately before and after the fault the phase angle of the internal generator voltage may considered to be the same. Accordingly (1) and (3) show that the phase angle associated with the voltage $\overline{V}$ will not change significantly. When the fault occurs the system impedance as seen at P instantaneously changes from a primarily resistive to a primarily reactive impedance. Hence the phase angle associated with the current will make a substantial change as can be seen from (2) and (4).

Observe, that these assumptions are not always applicable. The fault impedance will never be zero for a real short circuit fault although the approximation is often applied in EHV studies. Additionally the assumptions made in (1) and (2) are not true for all line configurations and load conditions.

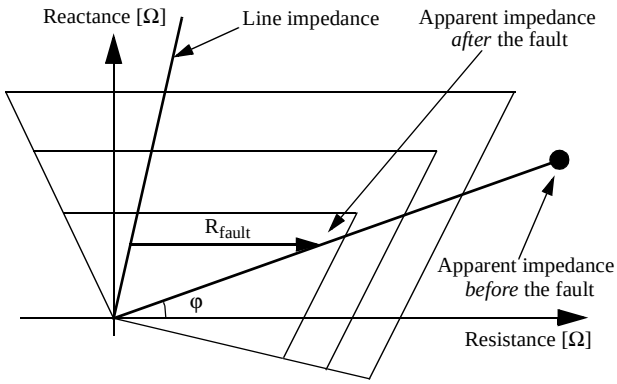

Fig. 2. Possible behaviour of the characteristic angle φ of the apparent impedance as seen by a distance relay during a three phase short circuit fault.

In case of some specific relations between the pre-fault operating point, the fault location and the fault impedance the characteristic angle φ of the apparent impedance as seen by a distance relay may not change during a fault; see figure 2. Hence the phase angle associated with the current will neither change. However as the fault impedance is usually formed by a resistance of a few ohms this behaviour will mainly occur for fault locations close to the relay. Fortunately the closer the fault occurs to the line terminal the greater fault current will be arising from nearby generators. Hence the fault impedance will also for this application be negligible in many cases and thus the phase angle associated with the current will change substantially for nearby faults as well.

For relays located at the receiving end of a transmission line the current usually will switch direction when the fault occurs and thus the phase angle will change approximately 180 degrees.

Power swings are phase symmetrical events with fairly long cycle times. Accordingly the *derivative of the phase angle of the current* can be used as an additional criterion in a

distance relay algorithm to distinguish symmetrical three phase faults from power swings. However, as shown in figure 2 the criterion performs better the greater the fault distance. Hence the criterion is particularly suitable for zones 2 and 3 distance protection. To cope with nearby faults in zone 1, when the fault impedance is not negligible, the criterion may be used in combination with pilot relaying. Alternatively the criterion is only applied for the time delayed zones as power swings are rarely a major concern for zone 1 elements. In fact if power swings are so severe that the zone 1 is entered it may be advisable to trip the circuit breaker and thus split the system.

When a three phase fault occurs in case of an open line situation or a pure reactive load, the phase angle of the current will not change significantly. However for these operating conditions power oscillations are not a major concern. Therefore the conventional distance relay method can be applied to these cases whereas a method based on the derivative of the phase angle of the current is used for operating conditions associated to power oscillations. The appropriate choice of the correct method can easily be determined by adaptive relaying.

III. A MOMENTARY DISTANCE RELAY ALGORITHM

In figure 3 an algorithm for a zone 1 phase to phase relay is proposed. To initiate a trip signal not only the apparent impedance has to be within the zone 1 of operation of the traditional distance element, but at least one of two additional criteria have to be fulfilled.

The quantities marked with the subscript *set* are assigned a fixed value by the relay operator. The remaining quantities are continuously updated by the relay during operation.

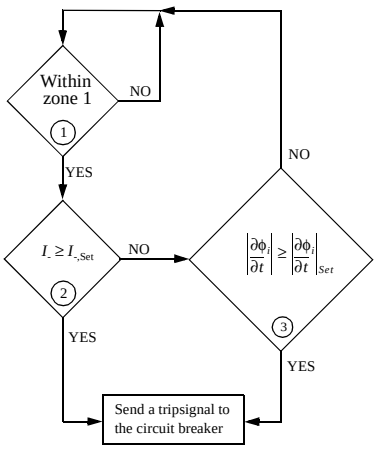

Fig. 3. Zone 1 algorithm for a phase to phase distance relay.

Block 1 consists of the traditional zone 1 distance protection function. When block 1 signals a fault blocks 2 and 3 are applied to verify that a short circuit fault and not a power swing is the reason for the YES signal out from block 1. Verification is carried out by comparing the fixed values of the quantities with the values continuously updated. When the updated value in a block exceeds the fixed value the trip signal is initiated. By studying the negative-sequence current block 2 examines if an unsymmetrical fault is the reason for the activation of block 1. If not, a final check is made in block 3 to validate if a symmetrical three phase fault has occurred using the criterion based on the derivative of the phase angle of the current.

In the case of a phase to ground element the criterion in block 2 is replaced by one based on the residual current and block 3 may be eliminated.

IV. TIME DELAYED DISTANCE RELAY ALGORITHMS FOR SINGLE AND PARALLEL LINES

For the introduction of the time delayed algorithms zone 3 is studied where the traditional zone 3 blocks are considered to cover the whole length of all adjacent sections. However the operation characteristics are similar for the zone 2 algorithms, except for the reach of the traditional distance elements and the timer settings.

First consider a case where the circuit between relay C and relay D in figure 4 is removed. Thus a system consisting of two subsequent single transmission lines is studied where the algorithm in figure 5 is applied on relay A.

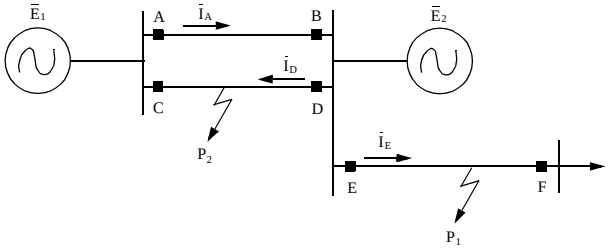

Fig. 4. A system including remote back-up protection.

When a phase to phase fault occurs at P_1 the traditional distance element of both the main protection at E and the remote back-up protection at A will be entered. Additionally the relays will experience at least one of the following events: a high peak of the derivative of the current or a negative-sequence current. Hence the timer in block 4 will be started and the algorithm will begin to alternate between blocks 5 and 6, waiting for the main protection E to clear the fault. However if the main protection fails the algorithm will send a trip signal when the criterion in block 6 is fulfilled.

In case the fault is cleared by the main protection the apparent impedance will leave zone 3 for relay A. Assume that a power swing occurs as a consequence of the grid weakening and the apparent impedance again enters zone 3. This

time no high peak of the derivative associated with the current or negative-sequence current will arise and accordingly the out signal from blocks 2 and 3 will be NO. Thus the timer in block 4 is not started and the algorithm will continue to wait for a true short circuit fault.

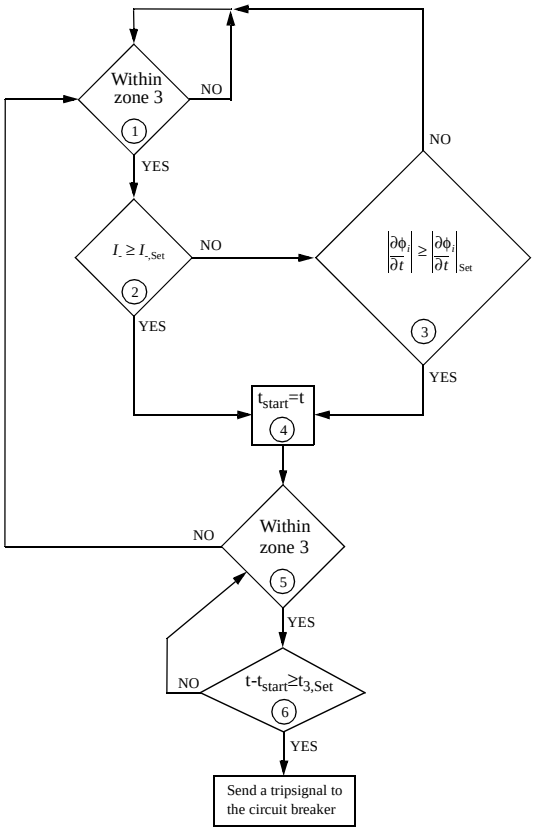

Fig. 5. Zone 3 algorithm for a phase to phase distance relay protecting two subsequent single lines.

In the case of parallel lines the algorithm in figure 5 needs some modification in order to operate properly. The main reason for this is that the derivative of the phase angle of the current as seen by relay A is strongly dependent on the location of the fault P_2.

Simulations were performed for the grid configuration of figure 4, varying the fault location along the line between the relays C and D. It appeared that for a fault close to relay C the relay A experienced a positive derivative of the phase angle, whereas the derivative was negative in case of a fault close to relay D. A mathematical analysis confirmed that both the value and the sign of the derivative of the phase angle of the current as seen by relay A varies along the line. This means that for a particular fault location no change in the phase angle of the current will be observed. To overcome this problem an extra logic block is added to the algorithm of figure 5.

The suggested algorithm in figure 6 relies to a certain degree on communication devices. However conventional ”tripping” or ”blocking” communication techniques fulfil all necessary requirements, also the area of communication will be restricted to the substation.

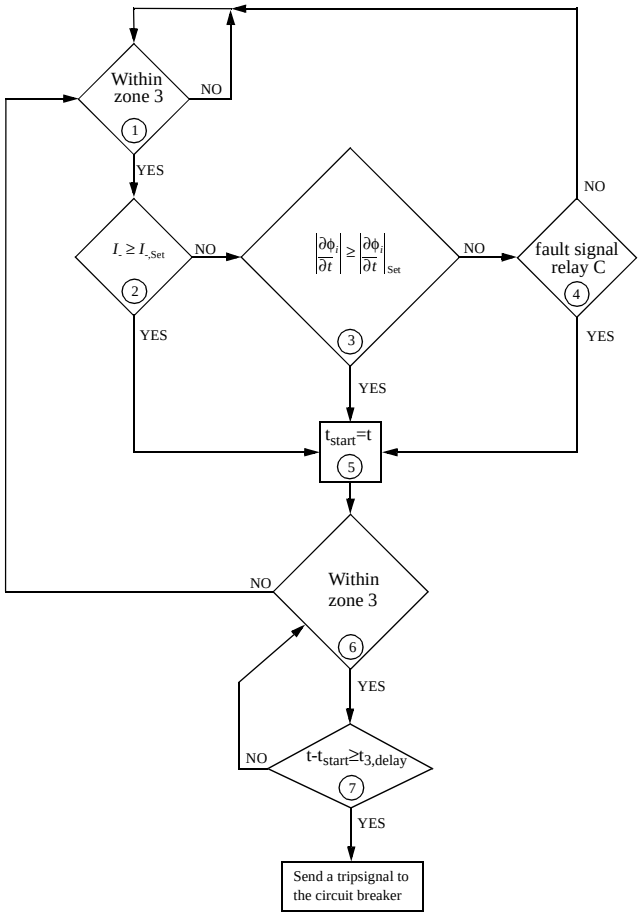

Fig. 6. Zone 3 algorithm for a phase to phase distance relay serving parallel lines.

For faults located on the line between relay E and relay F the operation principle is identical for the algorithm in figure 6 as for the algorithm in figure 5. However as discussed above a high peak of the derivative associated with the current will necessarily not be present when a fault occurs on the line between relay C and relay D. Therefore a signal used as an input in block 4 goes active when the timer in the zone 2 algorithm at relay C is started. Additionally for cases where the fault impedance for nearby faults can not be neglected the signal may also be activated when the zone 1 protection at relay C sees a fault. Hence a symmetrical three phase fault on the line between relay C and relay D where no high peak of the derivative is observed by relay A, will instead be distinguished in block 4.

When directional forward reaching distance elements are used the fault P_2 is not always instantaneously seen by relay A as the apparent impedance is dependent on the location of P_2 and the system configuration around the faulted line. In cases when the fault current is injected at relay A this phenomenon

will not arise. However if the initial fault current is extracted at relay A its traditional zone 3 element may not be entered until relay C has operated. As the current switches direction and consequently the phase angle shifts approximately 180 degrees both the traditional zone 3 will be entered and a high peak of the derivative of the phase angle associated with the current will occur. Thus the algorithm in figure 6 will cope with this phenomenon.

V. SIMULATION

Simulations have been performed using SIMPOW and the test system used is based on the grid introduced in [2]. To this grid a small system consisting of a large hydro generator and a small load is connected via two transmission lines. The algorithms introduced above are implemented in Relays A and C where the traditional zone 3 elements are of the offset mho type, set to cover 185% of the line length.

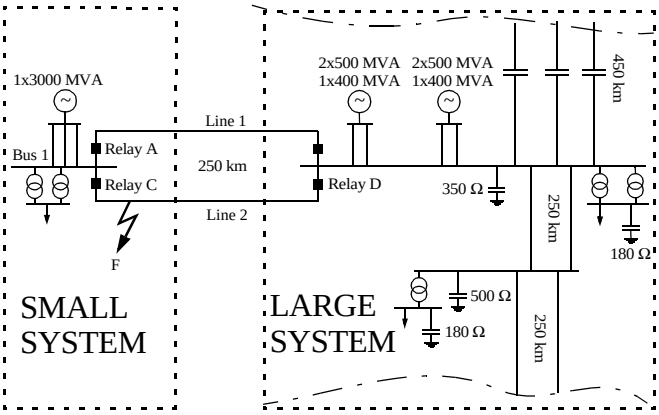

Fig. 7. Test system.

Initially about 1800 MW is transported from the small system towards the large system. Five seconds after the simulation is started a symmetrical three phase fault with zero fault resistance is applied on Line 2, 50 km from Bus 1. The faulted line is disconnected by the main protection. Figure 8 shows the damped power oscillations occurring after the disconnection where the system eventually will return to a stable operating state. However if traditional distance relays without PSD's are used Line 1 will incorrectly be tripped by Relay A as the apparent impedance will stay within zone 3 for more than 1.2 seconds during the first swing after the fault clearance; see figure 10. Consequently the whole system will collapse approximately five seconds after the fault has occurred.

First we examine the operation of Relay C by studying the algorithm shown in figure 3. Immediately after the fault has occurred the apparent impedance will enter the traditional zone 1 element. At the same time the relay will see a high peak of the derivative associated with the current injected into Line 2; see figure 9. Hence the output signal from blocks 1 and 3 will be YES and a trip signal will be sent to the circuit breaker. The fault is cleared in 90 ms which is the total operation time for the relay and the circuit breaker.

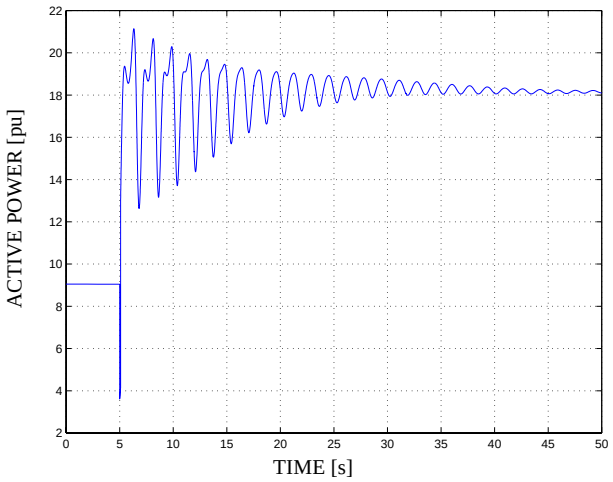

Fig. 8. Active power injected at Relay A.

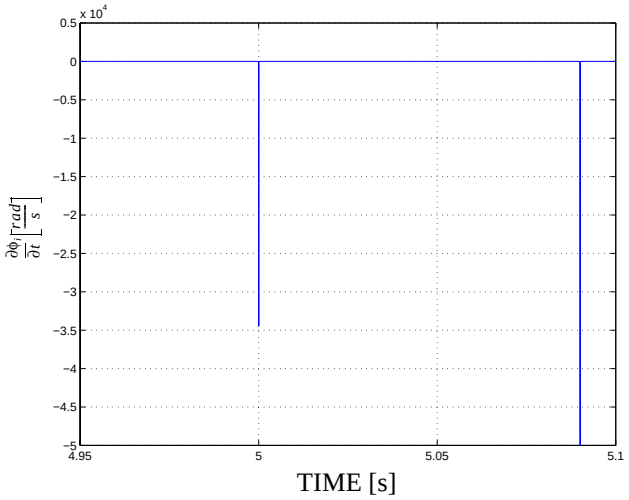

Fig. 9. The derivative of the phase angle associated with the current injected into Line 2 at Relay C.

In figure 10 the apparent impedance as seen by Relay A is displayed. During the short circuit fault the traditional zone 3 mho element will not be entered. However some time after the disconnection of Line 2, zone 3 will be entered by the first power swing. Hence the output from Block 1 in figure 6 will be YES. The power swing is a phase symmetrical event, no high peak of the derivative associated with the current injected into Line 1 is present at 5.26 s in figure 11 and no fault signal is received from Relay C. Therefore the output signals from blocks 2,3 and 4 will be NO. Thus the algorithm will not start the timer and no trip signal will be sent to the circuit breaker. Line 1 will not be tripped and thus the system recovers to a stable state.

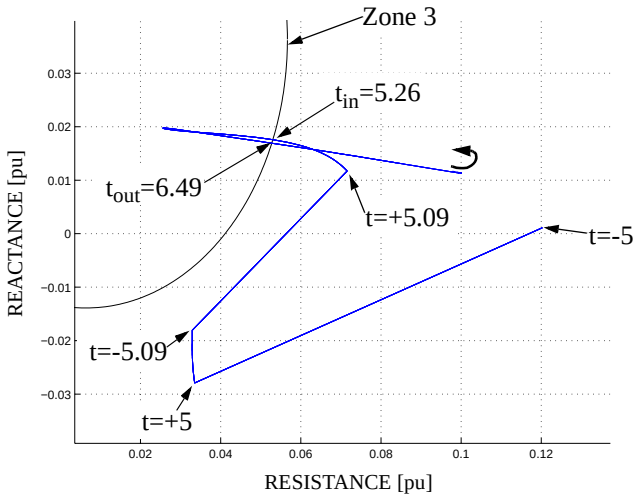

Fig. 10. RX- diagram for traditional zone 3 element at Relay A.

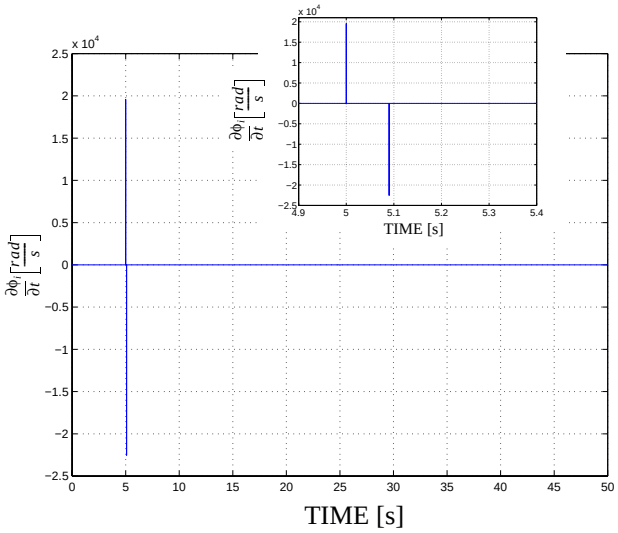

Fig. 11. The derivative of the phase angle associated with the current injected into Line 1 at Relay A.

VI. DISCUSSION

A question which may arise is: why not only use the criterion based on the derivative of the phase angle of the current in the algorithms? Simulations have shown that the peak of the derivative associated with the phase angle of the current is considerably larger for a three phase fault as compared to faults involving two phases or one phase to ground. In order to obtain a high security the settings in the blocks associated with the criterion are made with respect to three phase faults. Apart from short circuit faults, there exist a few additional power system events associated with power oscillations that may have some influence on the phase angle of the current. For example if the settings are done with respect to other faults involving less than three phases there might be a few cases where the algorithms have difficulties to distinguish a power swing caused by load shedding or generator tripping from a long distance fault. The reasons why these events affect the phase angle of the current are as follows: during load shedding or generator tripping the phase angle of the current will not be so much affected by the actual load or generation tripped as about the same relative amount of active and reactive power is removed. However as a new load condition may occur the phase angle of the current as seen by the relay may be altered due to the change in reactive power generated or consumed by the transmission line and/or adjacent shunt devices.

Events such as shunt and transformer switching may also affect the phase angle of the current. However such changes are usually less then in case of a short circuit fault and will most likely not occur in combination with an entrance of zone 3 due to a power swing.

VII. CONCLUSIONS

New distance protection algorithms which prevent mal-trips due to power oscillations have been proposed. Both momentary and time delayed algorithms are introduced where the dependability is decreased and security is increased with respect to traditional distance relaying. This is achieved by requiring additional criteria to be fulfilled at the same time as the apparent impedance enters the traditional distance element to initiate a relay operation. These additional criteria are based on symmetrical components and the derivative of the phase angle associated with the current.

The line length or the cycle time of the power swing will not affect the performance and availability of the algorithms as may be the case with conventional Power Swing Detectors.

Applications for single and parallel lines have been presented. The solution for parallel line require some internal communication between the relays at the terminal.

The algorithms are based on mathematical logics blocks. Thus numerical relays applying a user friendly computer software to create the operation scheme of the relay make it easy for relay engineers to develop the algorithms.

VIII. ACKNOWLEDGEMENTS

The authors would like to thank Svenska Kraftnät for their interest in this research area and for their financial support. The authors also would like to thank ABB Power Systems for providing Simpow.

IX. REFERENCES

[1] Machowski J, Nelles D, "New Power Swing Blocking Method", IEE Developments in Power System Protection, Conference Publication No. 434, March 25-27 1997, pp 218 - 221.

[2] Jonsson M, Daalder J, "Distance Protection and Voltage Stability", PowerCon 2000, December 4-7, 2000, Perth, Australia. Proceeding Vol. 2, pp. 971-976.

Paper C

A distance protection scheme to prevent mal-trips during abnormal power system conditions

M. Jonsson, J. Daalder

Presented at
Cigré Study Committee 34 Colloquium and Meeting,
September 10 - 14, 2001, Sibiu, Romania.

A distance protection scheme to prevent mal-trips during abnormal power system conditions

Mattias Jonsson
mattias.jonsson@elteknik.chalmers.se

Jaap Daalder
jaap.daalder@elteknik.chalmers.se

Department of Electric Power Engineering
Chalmers University of Technology
Gothenburg, S-41296 Sweden
www.elteknik.chalmers.se

Abstract: A new distance protection scheme is proposed to avoid mal-trips due to voltage instability and power oscillations. The scheme is based on mathematical logic blocks and uses traditional distance relaying in combination with certain additional criteria. These additional criteria are based on symmetrical components, the derivative of the phase angle of the current and the derivative of the voltage.

The performance of the scheme is analysed by simulations in a eighteen bus system developed by the authors.

The performance and availability of the scheme is not affected by the line length, different cycle times of the power oscillations and/or faults with a slowly decreasing impedance, which may be the case with conventional Power Swing Detectors. Although the scheme prevent mal-trips due to load encroachment associated with voltage instability the reach of the distance relay will not be restricted.

Keywords: Distance protection, Power oscillations, Voltage stability, Transient stability, Zone 3 element, Numerical relays.

I. INTRODUCTION

Undesirable distance relay operation during abnormal power system conditions have contributed to blackouts worldwide [1,2,3]. If such mal-operations had been avoided these blackouts could have been mitigated and in a few cases most likely completely avoided.

Throughout the years much effort has been used to design relays which function properly and have a high level of security. Nowadays when power systems are deregulated an incorrect outage of a transmission line may lead to advantages for competitors, penalty fees and an (unnecessary) absence of income. Unreliable relays may lead to situations where grid owners choose narrow settings for their protection equipment to avoid unwanted relay operations due to abnormal power system conditions. In some cases the settings may be such that relays will not operate for all possible fault conditions. In a broader perspective this behaviour may be a threat to system security.

Important events which may be initiated or aggravated by mal-operating distance relays are voltage instability and power oscillations. Typical of these abnormal operating conditions is that until the very ultimate phase of collapse the electrical quantities in the system will change moderately and rather slow as compared to a short circuit fault. Another feature is that voltage instability and power oscillations are phase symmetrical events.

In [4] and [5] new distance relay operation schemes have been proposed based on these characteristic features. The schemes use traditional distance relaying in combination with additional criteria. These criteria are used to distinguish encroachments of the fault detector zone caused by voltage instability and power oscillations from encroachment caused by short circuit faults.

Many relay solutions applied today have their origin in former technical hardware limitations and thus the possibilities given by new numerical and communication technologies are not always utilized to their maximum capacity. An example is the Power Swing Detector (PSD) based on the transition time through a blocking impedance area. Often it may be difficult to give the PSD proper settings because of long line lengths, the varying cycle time of the power oscillations and slowly decreasing fault impedances. Consequently this solution has caused several mal-trips throughout the years [5]. Nevertheless it is still the main method used in numerical distance relays to prevent mal-trips due to power oscillations. As numerical and signal processing technologies develop, new electrical quantities may become relevant as relay inputs. For example, as the sampling frequency increases the *derivative* of electrical quantities may become an attractive relay criterion.

In modern numerical relays a computer software is used to create the operation scheme of the relay based on mathematical logic blocks. Additionally the relay operator can choose between a wide range of relay inputs. Accordingly unique protection schemes suitable for each user can be obtained. The distance protection scheme proposed here utilizes the possibilities given by this new user friendly relay approach and is a further development of the algorithms introduced in [4] and [5].

II. NEW CRITERIA FOR A DISTANCE RELAY SCHEME

The criteria which may be combined with conventional distance relay methods vary for different types of distance elements. For phase to ground elements the residual current may be used. During unsymmetrical phase to phase faults a negative-sequence current will arise in the system and may therefore be a suitable criterion. However phase to phase elements must also be able to distinguish symmetrical three phase faults. A criterion associated with a negative- or zero-sequence current will not achieve this demand and therefore another method is introduced below.

The fundamental behaviour of the phase angles of the voltage and current [6] at the sending end of a transmission line immediately before and after a three phase short circuit fault is here briefly studied using the small power system in figure 1. During normal operation the voltage $\overline{V}$ and current $\overline{I}$ are given as in (1) and (2).

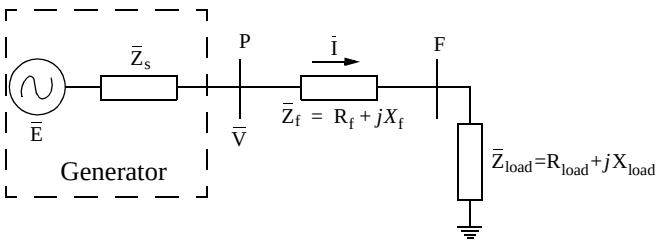

Fig. 1. A small transmission system during normal operation.

$$\bar{V} = \frac{\bar{Z}_f + \bar{Z}_{load}}{\bar{Z}_s + \bar{Z}_f + \bar{Z}_{load}} \cdot \bar{E} \approx \bar{E} \qquad \forall \begin{Bmatrix} \bar{Z}_{load} \gg \bar{Z}_f \\ \bar{Z}_{load} \gg \bar{Z}_s \end{Bmatrix} \tag{1}$$

$$\bar{I} = \frac{\bar{V}}{\bar{Z}_f + \bar{Z}_{load}} \approx \frac{\bar{V}}{R_{load}} \qquad \forall \begin{Bmatrix} R_{load} \gg X_{load} \\ R_{load} \gg X_f \gg R_f \end{Bmatrix} \tag{2}$$

When a three phase fault occurs at node F the voltage and current can be written as in (3) and (4). The voltage at the fault location is assumed to be zero when the fault is present.

$$\bar{V} = \frac{\bar{Z}_f}{\bar{Z}_s + \bar{Z}_f} \cdot \bar{E} \sim \bar{E} \qquad \forall \begin{Bmatrix} X_f \gg R_f \\ X_s \gg R_s \end{Bmatrix} \tag{3}$$

$$\bar{I} = \frac{\bar{V}}{\bar{Z}_f} \approx \frac{\bar{V}}{jX_f} \qquad \forall \{X_f \gg R_f\} \tag{4}$$

Immediately before and after the fault the phase angle of the internal generator voltage may considered to be the same. Accordingly (1) and (3) show that the phase angle associated with the voltage $\overline{V}$ will not change significantly. When the fault occurs the system impedance as seen at P changes instantaneously from a primarily resistive to a primarily reactive impedance. Hence the phase angle associated with the current will make a substantial change as can be seen from (2) and (4).

Observe, that these assumptions are not always applicable. The fault impedance will never be zero for a real short circuit fault although the approximation is often applied in EHV studies. Additionally the assumptions made in (1) and (2) are not true for all line configurations and load conditions.

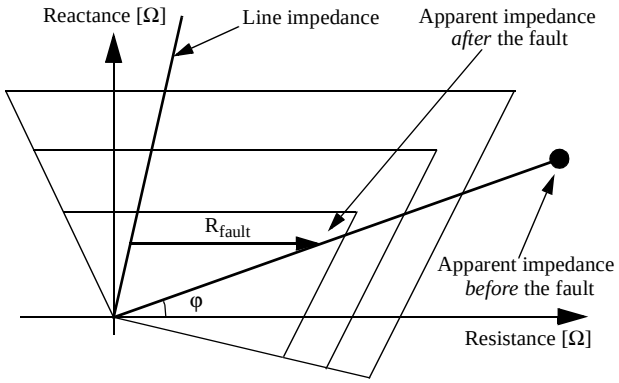

Fig. 2. Possible behaviour of the characteristic angle φ of the apparent impedance as seen by a distance relay during a three phase short circuit fault.

In case of some specific relations between the pre-fault operating point, the fault location and the fault impedance the characteristic angle φ of the apparent impedance as seen by a distance relay may not change during a fault; see figure 2. Hence the phase angle associated with the current will neither change. However as the fault impedance usually is formed by a resistance of a few ohms this behaviour will mainly occur for fault locations close to the relay. Fortunately the closer the fault occurs to the line terminal the greater fault current will be arising from nearby generators. As a result the fault impedance will also in this case be negligible in many instances [7] and thus the phase angle associated with the current will change substantially for nearby faults as well.

For relays located at the receiving end of a transmission line the current usually will switch direction when the fault occurs and thus the phase angle will change approximately 180 degrees.

Power oscillations and voltage instability are phase symmetrical events with fairly long time constants. Accordingly the *derivative of the phase angle of the current* can be used as an additional criterion in a distance relay algorithm to distinguish symmetrical three phase faults from these abnormal operation conditions. However, as shown in figure 2 the criterion performs better for increasing fault distances. This means that the criterion is particularly suitable for zones 2 and 3 distance protection. To cope with nearby faults in zone 1 when the fault impedance is not negligible, the criterion may be used in com-

bination with pilot relaying. Alternatively the criterion may be applied for the time delayed zones only as power swings and voltage instability are rarely a major concern for zone 1 elements. In fact if power swings are so severe that the zone 1 is entered it may be advisable to trip the circuit breaker and thus split up the system.

When a three phase fault occurs in case of an open line situation or a pure reactive load, the phase angle of the current will not change significantly. However for these operating conditions power oscillations or voltage instability are not a major concern. Therefore the conventional distance relay method can be applied to these cases whereas a method based on the derivative of the phase angle of the current is used for operating conditions associated to power oscillations and voltage instability. The appropriate choice of the correct method can easily be determined by adaptive relaying.

Apart from short circuit faults there are other events which may lead to sudden changes of the phase angle of the current [5]. Examples of events which may be associated to voltage instability and power oscillations are load shedding and generator tripping. Usually the peak value of the derivative of the phase angle of the current caused by generator tripping and load shedding are not as large as for three phase faults. However in order to obtain a high relay security and to assure that the relay will not mal-operate due to such events some additional criteria may be used as a supplement to the derivative of the phase angle of the current. For example, to distinguish load shedding from three phase short circuit faults the derivative of the voltage is a good indicator. Whereas a three phase short circuit fault will decrease the voltage the opposite is true in case of load shedding. To avoid any mal-operation due to generator tripping some communication device may be used to inform the relay that generator tripping has been performed. Hence when the operation scheme of the relay is programmed the signal received from the generator may be used to block undesirable relay operation. For example; for the scheme in figure 3 which is introduced in the next section the output from block 3 can be set to NO for a short time when the relay receives the signal announcing generator tripping.

Our intention is to introduce a new method to distinguish symmetrical three phase faults from abnormal operation conditions and explain its fundamental behaviour. Therefore we will assume zero or negligible fault impedance from now on.

III. A ZONE 3 DISTANCE PROTECTION SCHEME

In figure 3 a scheme for a zone 3 phase to phase relay is proposed. To initiate a trip signal not only the apparent impedance has to be within the zone 3 of the traditional distance element, but at least one of three additional criteria has to be fulfilled.

The quantities marked with the subscript *Set* are assigned a fixed value by the relay operator. The remaining quantities are continuously updated by the relay during operation.

Block 1 consists of the conventional zone 3 distance protection function. When block 1 signals a fault blocks 2, 3 and 4 are applied to verify that a short circuit fault and not power oscillations or voltage instability is the reason for the YES signal out from block 1. Verification is carried out by comparing the fixed values of the quantities with the values continuously updated.

By studying the negative-sequence current block 2 examines if an unsymmetrical fault is the reason for the activation of block 1. If not, final checks are made in blocks 3 and 4 to validate if a symmetrical three phase fault has occurred using the criteria based on the derivative of the phase angle of the current and the derivative of the voltage. When the real time value in block 2 exceeds the fixed value or the real time value in block 3 exceeds the fixed value at the same time as the real time value in block 4 falls below the fixed value the timer in block 5 is started.

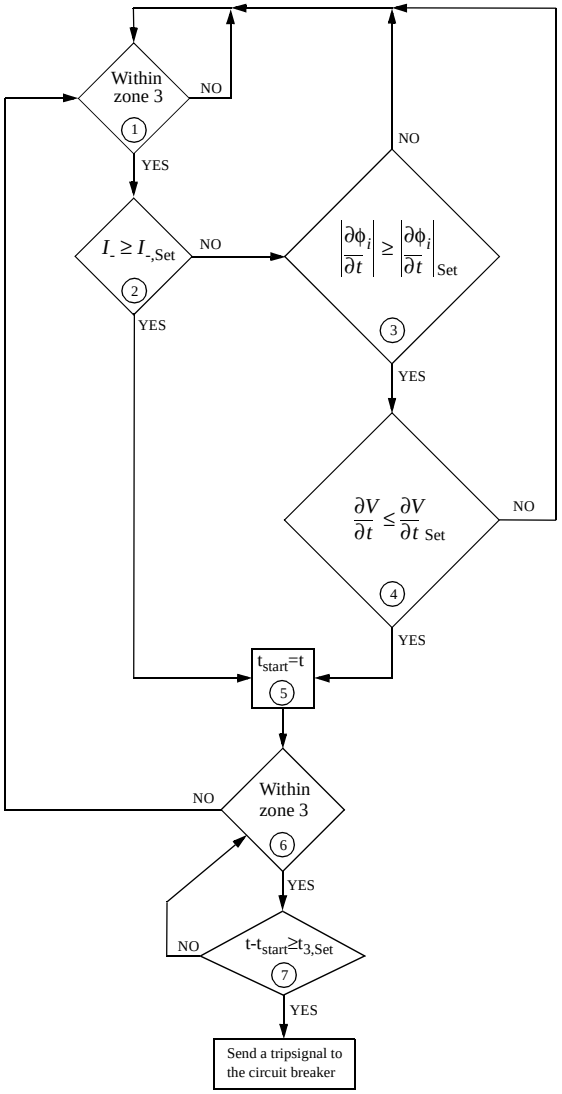

Fig. 3. Zone 3 scheme for a phase to phase distance element.

When a phase to phase fault occurs in the protected area the traditional distance element will be entered. Additionally the relay will experience at least one of the following events: a negative-sequence current or a high peak of the derivative of the current combined with a substantial voltage reduction. Hence the timer in block 5 will be started and the scheme will begin to alternate between blocks 6 and 7, waiting for the main protection to clear the fault. However if the main protection fails the scheme will send a trip signal when the criterion in block 7 is fulfilled.

In case the fault is cleared by the main protection the apparent impedance will leave zone 3. Assume that a power swing occurs as a consequence of the grid weakening and the apparent impedance again enters zone 3. This time no high peak of the derivative associated with the current or negative-sequence current will arise and accordingly the out signal from blocks 2 and 3 will be NO. Thus the timer in block 5 is not started and the scheme will continue to wait for a true short circuit fault.

When zone 3 is entered by a slowly decreasing apparent impedance due to voltage instability the criterion in block 1 will be fulfilled. However the criteria in blocks 2 and 3 will not be fulfilled as there is no negative sequence current present in the system. Neither will the derivative of the phase angle associated with the current possess a value which exceeds the pre-set value in block 3. The apparent impedance stays within zone 3 as the scheme continues to wait for a true short circuit fault. If the voltage instability aggravates load shedding might be performed as a remedial action. Suppose that the load shedding generates an unexpected high absolute peak value of the derivative of the phase angle of the current so that the criterion in block 3 is fulfilled. Consequently the out signal from block 3 is YES. However block 4 will prevent an incorrect start of the timer in block 5 as the peak value of the derivative caused by the load shedding will have a positive sign and thus the criterion in block 5 is not fulfilled. As a result also for this sequence of events the relay scheme will maintain a high security.

Conventional Power Swing Detectors usually interpret a fault with a slowly decreasing impedance as a power oscillation and thus the fault is not cleared. The scheme proposed in figure 3 will only clear all unsymmetrical faults of this type. However pure symmetrical faults with a slowly decreasing impedance are very unlikely to occur.

For applications serving parallel lines further improvements are required for the scheme in figure 3 in order to guarantee reliable operation. The main reason for this is that the derivative of the phase angle of the current as seen by the relay is strongly dependent on the fault location when a fault occurs on the parallel line. This phenomenon and its solution is described in detail in [5].

In the case of a phase to ground element the criterion in block 2 is replaced by one based on the residual current and blocks 3 and 4 may be eliminated.

IV. SIMULATION

Simulations have been performed using SIMPOW [8] and a test system introduced in [5]. The protection scheme in figure 3 is implemented in relays A and B where the traditional distance elements are of the conventional mho type and zone 3 is set to cover 230% of the line length. A global low voltage load shedding scheme is in operation. When the voltage at a bus in the EHV system decreases to 0.7 pu approximately 50% of the load at the closest load bus is disconnected. The performance of the scheme in figure 3 is examined with respect to voltage instability.

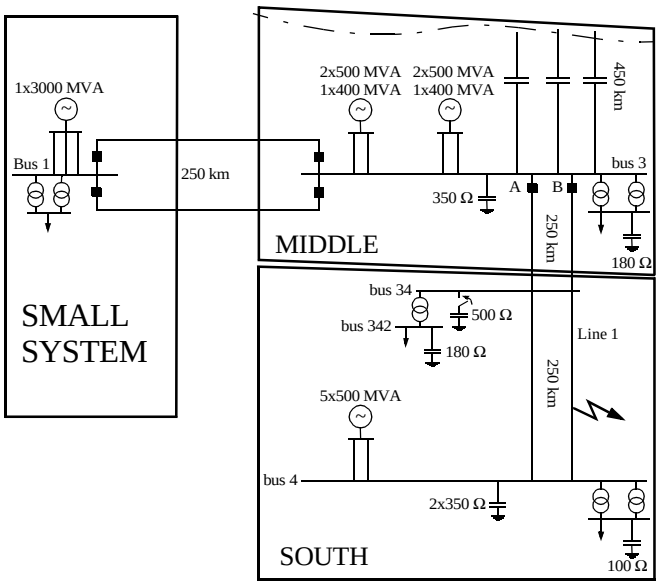

Fig. 4. Test system.

Initially the MIDDLE and SOUTH areas are heavily loaded with large power transports from the MIDDLE area towards the SOUTH area. In the pre-fault state the power transfer from bus 3 towards bus 34 is about 2200 MW and from bus 34 to bus 4 1200 MW. Five seconds after the simulation has started a permanent symmetrical three phase fault with zero fault resistance occurs 150 km from bus 34 on Line 1. After 90 ms the main protection disconnects the faulted line. Consequently the voltage starts to decrease at bus 3 and bus 34 although the shunt capacitor at bus 34 is taken into operation 500 ms after the initiation of the fault; figure 5. About 81 seconds after the fault occurrence the apparent impedance enters the zone 3 of the relays A and B; figure 6. In case of traditional distance relays undesirable operation will occur and consequently the

whole system will collapse almost instantaneously. However when the scheme in figure 3 is used the relays will not mal-operate but the voltage at bus 3 and bus 34 will continue to decrease. At 95.5 seconds the voltage at bus 34 has reached 0.7 pu and thus 50% of the load at bus 342 is disconnected. Instantaneously the voltages in the system increase and the system recovers to a stable operating point.

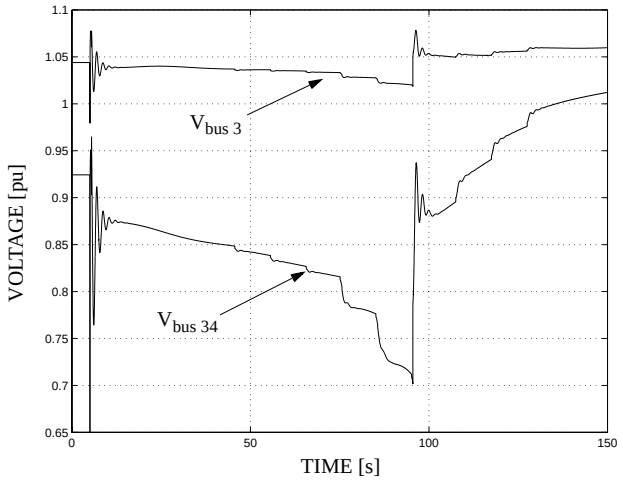

Fig. 5. The voltages at bus 3 and bus 34.

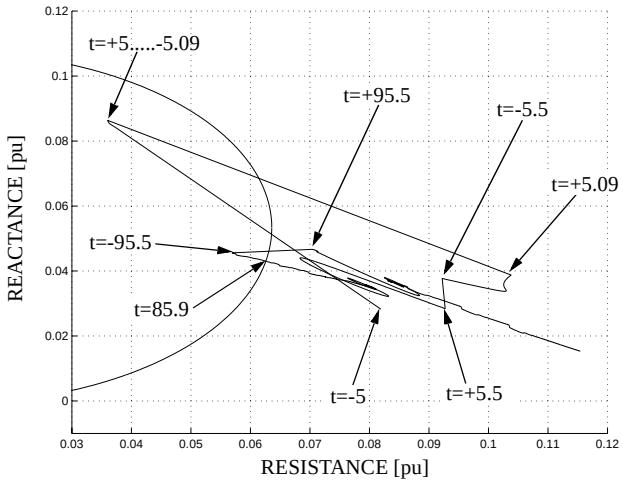

Fig. 6. RX-diagram for relays A and B.

If the performance of the scheme is further analysed we can see that when the initial 3 phase fault occurs the zone 3 of relays A and B is entered; figure 6. At the same time figure 7 shows that the derivative of the phase angle of the current has a negative peak with a large magnitude. In addition the derivative of the voltage shows a negative peak; figure 8. Thus the criteria in blocks 1, 3 and 4 are fulfilled and the timer in block 5 is started. The scheme starts to alternate between blocks 6 and 7, waiting for the main protection to clear the fault. When the main protection clears the fault the apparent impedance leaves zone 3. However as the voltages decrease and the reactive power demand increases the zone 3 is again entered at 85.9 seconds. The criterion in block 1 is again fulfilled but this is not the case for blocks 2 and 3. Hence the relays will not start their timers but continue to wait for a true short circuit fault.

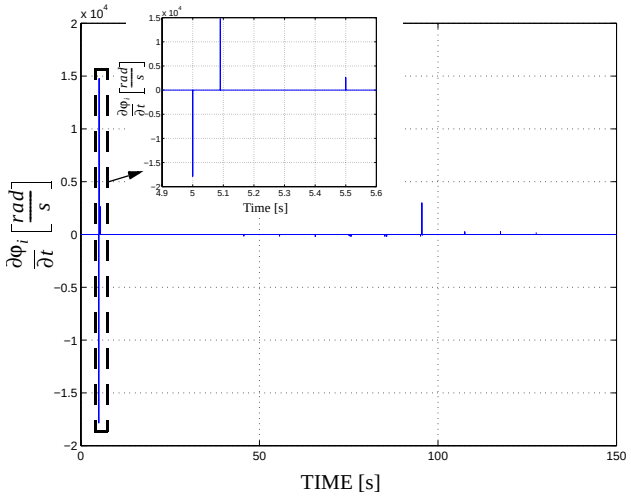

Fig. 7. The derivative of the phase angle of the current as seen by relays A and B.

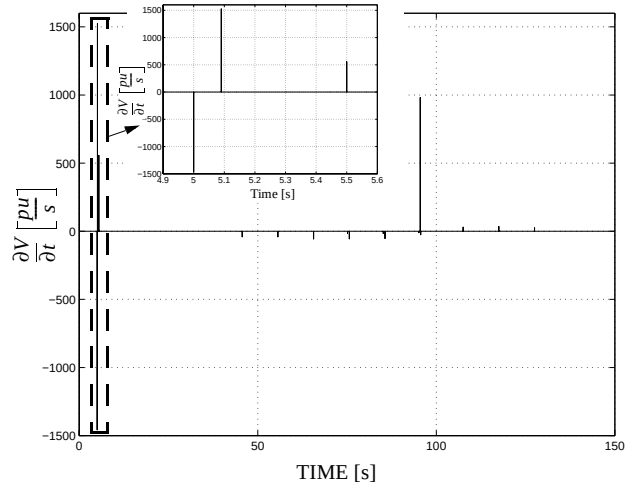

Fig. 8. The derivative of the voltage at bus 3.

An increased relay security is achieved by adding block 4. Assume that a too narrow setting is given to the fixed parameter in block 3. Consequently the peak of the derivative in figure 7 caused by the load shedding may be treated as a short circuit fault (output YES from block 3). However block 4 will prevent a mal-operation as the peak of the derivative of the

voltage at the time for the load shedding has a positive value; figure 8.

The load shedding in this case is performed at a very low voltage level leading to particularly large changes of the electrical quantities. However there is still a significant difference between the absolute value of the peaks of the derivative of the phase angle of the current caused by the three phase fault and by the load shedding respectively. This should be kept in mind when the reliability aspect of the derivative of the phase angle of the current as a relay criterion is discussed.

V. CONCLUSIONS

A new distance protection scheme is proposed where the relay security is increased with respect to traditional distance relaying. The prime reason for increasing the security is to avoid mal-trips due to voltage instability and power oscillations. This is achieved by applying certain criteria in combination with the conventional distance protection function. Unsymmetrical faults are discriminated from other system disturbances by criteria based on symmetrical components. Symmetrical three phase faults are detected by a combination of criteria based on the derivative of the phase angle of the current and the derivative of the voltage. The derivative of the voltage is used as an extra safety measure to secure correct relay operation in case of load shedding as a remedial action during voltage instability.

The line length, different cycle times of the power oscillations and faults having a slowly decreasing impedance will not affect the performance and availability of the scheme as may be the case with conventional Power Swing Detectors. The scheme also prevents mal-trips due to load encroachment associated with voltage instability whereas the reach of the distance relay is not restricted.

The distance protection scheme is based on mathematical logics blocks. Thus numerical relays applying a user friendly computer software to create the relay algorithm make it easy for relay engineers to develop the scheme.

VI. ACKNOWLEDGEMENTS

The authors would like to thank Svenska Kraftnät for their interest in this research area and for their financial and intellectual support. The authors also would like to thank ABB Power Systems for providing Simpow.

VII. REFERENCES

[1] Western Systems Coordinating Council Disturbance Report For the Power System Outages that Occurred on the Western Interconnection on July 2, 1996, 1424 MAST and July 3, 1996, 1403 MAST, Approved September 19, 1996, Internet URL http://www.wscc.com/distnews.htm.

[2] X. Vieira *et. al*, ”The March 11:th 1999 Blackout: Short-Term Measures to Improve System Security and Overview of the Reports Prepared by the International Experts” , 1999, Brazil.

[3] Taylor C.W, ”Power System Voltage Stability”, ISBN 0-07-113708-4, McGraw-Hill, 1994, pp. 263.

[4] Jonsson M, Daalder J, ”Distance Protection and Voltage Stability”, PowerCon 2000, December 4-7, 2000, Perth, Australia. Proceeding Vol. 2, pp. 971-976.

[5] Jonsson M, Daalder J, ”A new protection scheme to prevent mal-trips due to power swings”, Submitted to IEEE/PES Transmission and Distribution Conference and Exposition, October 28 - November 2, 2001, Atlanta, Georgia Usa.

[6] Elmore W.A, ”Protective Relaying Theory and Applications”, ISBN 0-8247-9152-5, Marcel Dekker Inc, 1994, pp. 16.

[7] Warrington A.R, Van C, ”Reactance Relays Negligibly Affected by Arc Impedance”, Electrical World, Vol. 98, No. 12, September 1931, pp. 502 - 505.

[8] Fankhauser H.R, Aneros K, A-A Edris. and Torseng S, ”Advanced Simulation Techniques for the Analysis of Power System Dynamics”, IEEE Computer Applications in Power, Vol. 3, No. 4, October 1990, pp. 31 - 36.

Paper D

A new method suitable for real time generator coherency determination

M. Jonsson, M. Begovic, J. Daalder

Submitted to IEEE Transactions on Power Systems

A NEW METHOD SUITABLE FOR REAL TIME GENERATOR COHERENCY DETERMINATION

Mattias Jonsson, *Student member, IEEE*, Miroslav Begovic, *Senior member, IEEE* and Jaap Daalder

Abstract— **The aim of this paper is to illustrate that wide area generator speed measurements combined with Fourier analysis can be used to determine coherent generator groups.**

Studies are based on simulations in a 68 bus test system. Three test cases are investigated where the new method is compared to conventional methods based on the generator speed, modal analysis and phasor angle measurement.

The method introduced in this paper has proven to be an interesting alternative for generator coherency determination. It gives almost identical results to the off-line methods based on the generator speed or modal analysis. Based on their trustworthiness the test cases indicate that the method reflects a more accurate coherency than the conventional on-line method based on phasor angle measurement. Moreover, compared with on-line applications using modal analysis the method supports real time applications better according to its less extensive computational requirements.

Keywords— **Fourier analysis, Inter-area oscillations, Power system oscillations, Transient instability, Wide area protection.**

I. Introduction

IT is well established that unstable or lightly damped inter-area oscillations in the power system are highly undesirable as it will give additional stress to equipment and reduce the power quality. In the Swedish transmission system the number of inter-area oscillation events has increased significantly during recent years. One reason may be the deregulation which was initiated in 1996. In a deregulated system, power flows are decided by the complex market arrangements between suppliers and demand and the system may operate under conditions for which the system was not originally designed. Consequently the system may become more sensitive to power oscillations. This is especially true for deregulated systems which consist of a few originally regulated sub-systems. In the Scandinavian power system larger power flow variations have been observed after deregulation. In 1996 the annual number of recorded inter-area oscillation events amounted to about 15 while in 2000 this number had increased to more than 300 [1]! In fact, in a few cases, operating conditions have occurred where the system was close to its limits and on the brink of a severe disturbance. Note that about 30 % of the events recorded in 2000 were related to a specific maintenance job during a limited period of three weeks. This trend represents a strong incentive for precise and reliable on-line methods to ensure fast detection and effective counteraction of events involving inter-area modes. Furthermore, the fundamental presumption to assure the most effective corrective actions in case of inter-area events most often involves a well established generator coherency.

This work was financially supported by Svenska Kraftnät. M. Jonsson and J. Daalder are both with Chalmers University of Technology, Gothenburg, Sweden. E-mail: mattias.jonsson@elteknik.chalmers.se, jaap.daalder@elteknik.chalmers.se. M. Begovic is with Georgia Institute of Technology, Atlanta, USA. E-mail: miroslav.begovic@ece.gatech.edu

To detect inter-area modes, many different indicators have been proposed and realized. The most common are probably the active power and frequency [2] but also the voltage has been used quite frequently. Moreover different approaches to determine generator coherency have been proposed [3] and [4], although most of them address off-line studies. In [5], [6] and [7] Fourier analysis of the generator angle and kinetic energy respectively has been used for off-line studies of power system dynamics. Here a similar approach is adopted, although we use the *speed deviation* of the generators for inter-area detection and generator grouping. The speed deviation reflects the energy absorbed or delivered by the generator and can be used to distinguish power oscillations, as their fundamental nature is associated with the energy interaction in the system.

Usually generator coherency methods require fairly extensive calculations. The method introduced here is simple and suits applications based on communication and GPS technology very well. Furthermore the method is exclusively based on the generator speed variation which is straightforward and has a well established accessibility at the generator shaft. The method can be used directly as the main tool to determine generator coherency and for example control system separation. Alternatively, it can be used as a more extensive tool to provide control parameters for system stabilization equipment such as FACTS or PSS devices.

In this paper, network simulations which represent illustrative examples of inter-area events, are used to demonstrate and verify the proposed coherency method. To restrict the size of the paper three representative cases were selected. These cases illustrate well all observations from multiple simulation run. In the paper, the coherency established by the proposed method is obtained from time evolution of the generator speed spectral phase responses, which reveal grouping patterns by visual inspection. The method has good potential for quantitative application in computerized System Protection Schemes.

The work is a continuation of the method briefly introduced in [8].

II. GROUPING OF GENERATORS BY SPEED MEASUREMENT AND FOURIER ANALYSIS

In (1) δ_l corresponds to the angle between the generator stator and rotor flux. Apart from negligible deflections resulting from small load variations the speed deviation ω_l

will be zero during normal operation. In case of a disturbance the present value of δ_l will be altered in order to meet the new system conditions. The transition from the pre- to the post-disturbance operating point appears as more or less developed oscillations resulting from the electrical and mechanical torque deviation. Hence ω_l is obviously an authentic reflection of the oscillations present in the system.

$$\dot{\delta}_l = \omega_l \tag{1}$$

By monitoring the generator speed and applying Fourier analysis the fundamental speed will be reflected by the zero frequency spectral component while the speed deviation can be obtained from the non-zero frequency components. Moreover by determining the phase of the dominant non-zero frequency component in time (i.e the dominant oscillation mode present in the system) the swing characteristic for the machine can be obtained. Furthermore, by comparing the phase of the dominant component for all machines the generator coherency can then be acquired. The procedure is given by (2) to (7).

The Discrete Fourier Transform (DFT) of the generator speed in time C is obtained according to (2) [9] where k and i are integers such that $-\infty \leq k \leq \infty$ and $0 \leq i \leq n-1$. The parameter ω represents the sampled generator speed signal and h the window function, where h controls the extension of the part of the speed signal used to calculate the frequency spectrum associated with the current time of interest k. In this paper, a rectangular window function is defined as $h[m] = 1$ for $0 \leq m \leq l-1$ and otherwise $h[m] = 0$. The rectangular window shape was selected because the equal weighting preserves the phase information of the sustained oscillation modes consistent with inter-area oscillations. Furthermore, n are the number of equally spaced spectral components.

$$C[k,i] = \sum_{m=0}^{l-1} \omega[k+m]h[m]e^{-j\frac{2\pi im}{n}} \tag{2}$$

The oscillation modes present in the system are reflected by the peaks given by the spectra including all non-zero frequency components. Based on (2) we can determine a vector $\mathbf{c_k}$ for each time value k (3) which contains the Fourier coefficients $c_{k,1} \ldots c_{k,i} \ldots c_{k,n-1}$ separated by the spectral frequency resolution decided by n. These coefficients are complex and denote both the magnitude and phase of each oscillation mode. Note that the zero frequency component is excluded in (3) as it corresponds to the fundamental speed. Theoretically the spectra are limited to a domain given by the Nyquist criterium [9]. However, in case of short sampling intervals the investigated frequency range should be further restricted to the domain relevant to inter-area modes.

$$\mathbf{c_k} = (c_{k,1}, \ldots, c_{k,i}, \ldots, c_{k,n-1}) \tag{3}$$

In order to determine the dominant inter-area mode the Fourier coefficient with the largest amplitude $A_{k,dom}$ is identified as given in (4). The index *dom* denotes the position in $\mathbf{c_k}$ for the coefficient representing the largest magnitude. As indicated above the theoretical pick-up value for an inter-area mode is immediately above zero. However, to exclude measurement distortion and frequency deviations due to load variations a minimum value for an acceptable (dominant) Fourier coefficient is required. Thus the final establishment of a dominant inter-area mode is carried out according to (5) where $A_{pick-up}$ is a pre-defined pick-up value outside the range of these phenomena. Note that the dominant mode may change its frequency as a function of time and can therefore be of a temporary nature.

$$A_{k,dom} = max\{\mid c_{k,1} \mid, \ldots, \mid c_{k,i} \mid, \ldots, \mid c_{k,n-1} \mid\} \tag{4}$$

$$c_{k,dom} = \mathbf{c_k}[dom] \leftrightarrow A_{k,dom} \geq A_{pick-up} \tag{5}$$

Once a dominant inter-area mode has been identified the phase of that mode $arg\{c_{k,dom}\}$ is determined for the involved system generators $1 \ldots l \ldots p$ and a vector is organized including all these phases (6).

$$\begin{aligned} \varphi_{\mathbf{k,dom}} \quad = \quad & (arg\{c_{k,dom,1}\}, \ldots, \\ & arg\{c_{k,dom,l}\}, \ldots, arg\{c_{k,dom,p}\}) \end{aligned} \tag{6}$$

Finally, a phase comparison is performed (7) where one of the generators' phase angle is used as the reference angle φ_{ref}. The generator coherency is then defined by $\mathbf{\Delta}\varphi_{\mathbf{k,dom}}$ where generators having (approximately) the same phase difference with respect to φ_{ref} represent a coherent group. Here $\mathbf{E}$ is a unit vector of length p.

$$\mathbf{\Delta}\varphi_{\mathbf{k,dom}} = \varphi_{\text{ref}} \cdot \mathbf{E} - \varphi_{\mathbf{k,dom}} \tag{7}$$

For the case studies in Section IV, parameters l and n were given values corresponding to a window length of 100 s and a spectral frequency resolution of 0.01 Hz. Furthermore, the sampling frequency 20 Hz was used. Note that before the simulations were started the complete data window for each machine was initiated with values corresponding to the initial speed value.

III. TEST SYSTEM

The test system used in this paper is the 68 bus NPCC system which is a reduced order model of the New England/New York interconnection about 30 years ago. The system involves 16 generators where generators G13 to G16 represent large generator group equivalents. The frequency control is maintained by G1 to G9 while G10 to G16 are operated at a constant mechanical torque. In Fig. 1 the dashed lines indicate the coherent groups as given by Rogers [10] and the thick lines indicate the weak tie-lines interconnecting the different regions. System parameters used for the simulations are based on data given in [10]. Machine data are provided in Appendix I. Furthermore, a detailed modal analysis for the base case when all system components are in service, is given in Appendix 2 (Table V, Base case).

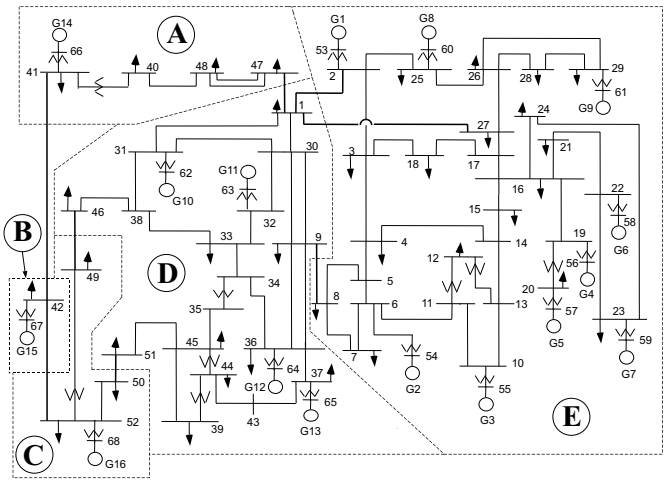

Fig. 1. Test system.

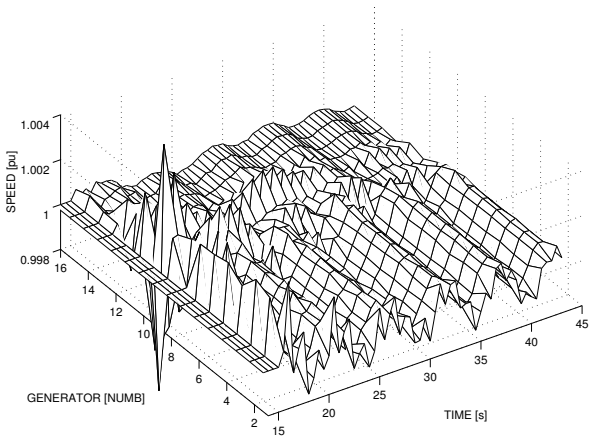

Fig. 2. The speed of all machines.

IV. TEST CASES

Below three test cases are given. The new method based on Fourier analysis is applied on each case and in addition each case is investigated by three conventional methods based on generator speed comparison, generator terminal voltage angle and modal analysis. Furthermore, modal analysis including all relevant inter-machine and inter-area modes for the pre- and post-disturbance systems is given in Appendix 2. All simulations were performed using the power system simulation software SIMPOW [11], [12].

A. CASE I

This case is probably the most obvious scenario. Before the disturbance the system is weakened as the electrical distance between region E and the remaining system is increased due to the removal of line 8-9. The disturbance consists of a permanent three phase fault located immediately outside bus 1 on the line between bus 1 and bus 2 which leads to a permanent disconnection of the faulted line. The fault occurs after 15 seconds and is cleared within 90 ms. As the faulted line is tripped region E becomes weakly interconnected to the remaining regions via the line between buses 1 and 27. As this is by far the longest line present in the system permanent inter-area oscillations result involving all generators in the system; Fig. 2.

For this case the behavior of G1 to G9 is quite similar. The same is true for G10 to G16 although the oscillations are small for G13-G16 as they are extremely large machines representing generator equivalents.

Fig. 3 shows that the dominant swing frequency arising in the system is located in the range of 0.19 Hz. Furthermore, Fig. 4 gives an overview of how the generators separate into groups based on the phase angle of the dominant Fourier coefficient. By grouping of the angle graphs, the figure illustrates that G1-G9 swing against G10-G16. In case of protection applications the generator separation must be determined fast and reliable. Fig. 4 confirms that the separation can be seen within about 3 seconds even though the case involves relatively slow oscillations (0.19 Hz). Both generators G10 and G11 stabilize at a phase angle of around -2π (Fig. 4, lower graph). The generator group G12 to G16 stabilize at phase angle 0 (Fig. 4, uppermost graph). As the difference is 2π (360°) these generators will swing together as a coherent group. For G2 to G9 the behavior of the time-frequency spectrum is similar to the one given for G1 in Fig. 3 and for G11 to G16 the behavior is similar to Fig. 5.

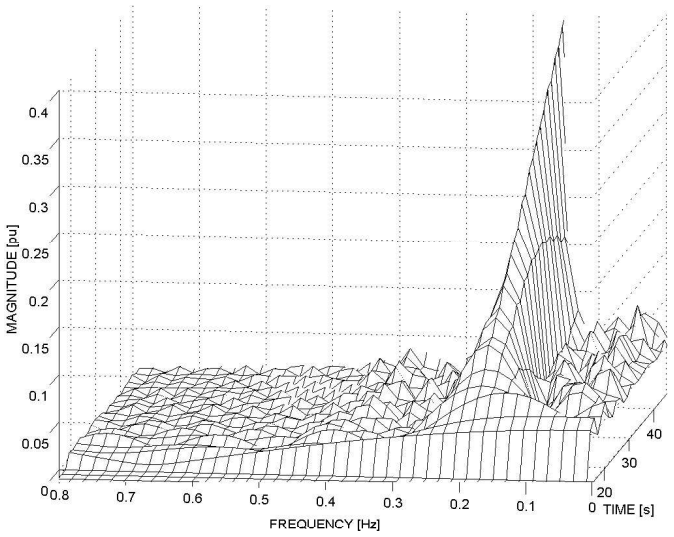

Fig. 3. The magnitude of the Fourier coefficients for G1 within the frequency range of inter-area oscillations.

For G1 to G9 the dominant swing frequency can clearly be distinguished shortly after the initial disturbance. However, a low magnitude of the speed deviation of the dominant inter-area mode, in combination with damped transient swings may complicate the discrimination. An example is given in Fig. 5 where more time is needed in order to make a reliable discrimination as compared to Fig. 3. The magnitude of the damped frequency component in the

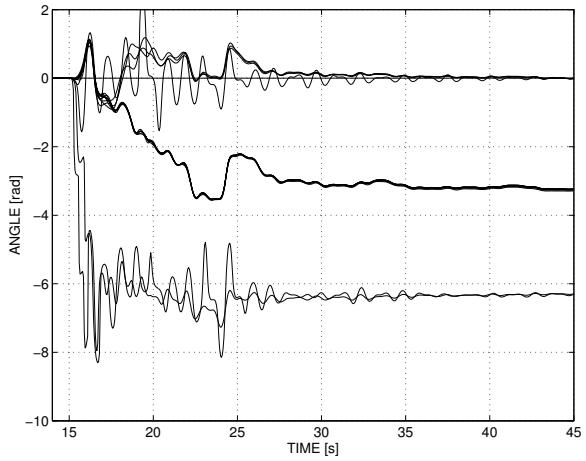

Fig. 4. The phase angles of the 0.19 Hz Fourier coefficients for all generators. The topmost group involves G12 to G16, the middle group G1 to G9 and the lowest group G10 and G11.

vicinity of 0.45 Hz is in the same range as the magnitude of the unstable 0.19 Hz mode for some time after the initial disturbance (note, the complete attenuation of the 0.45 Hz mode takes place outside the time range of Fig. 5). In addition a more or less pronounced damped 0.06 Hz component is present (outside the frequency range of Fig. 5) for G10 to G16 for some time after the three phase fault. As the 0.06 Hz and 0.45 Hz components have damped characteristics, we exclude them in the coherency analysis. However, for determination of the corrective measures these modes should also be considered as they may aggravate if inappropriate control actions are deployed. The low frequency mode (0.06 Hz) may be associated with frequency control. There are also some inter-machine modes present immediately after the short circuit fault.

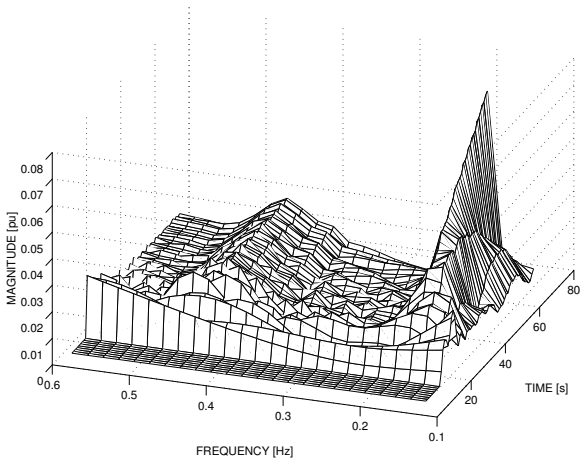

Fig. 5. The magnitude of the Fourier coefficients for G10 within the frequency range of inter-area oscillations.

Fig. 6 illustrates the speed of the generators after the line has been removed. For clarity the machine speeds are shown when the inter-machine modes are completely damped out. Grouping of the generators' speed trajectories confirms the generator separation as given in Fig. 4.

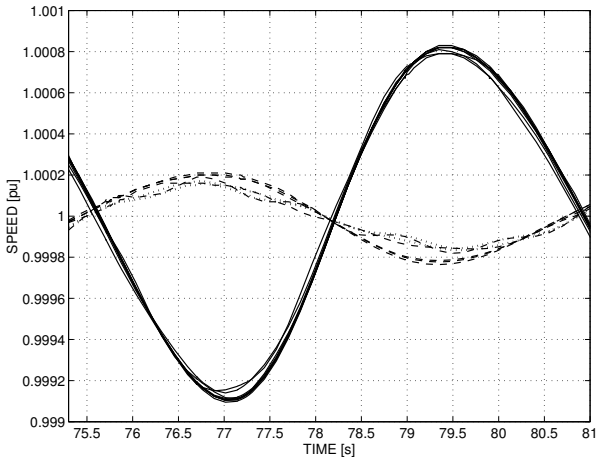

Fig. 6. The speed of G1-G16. G1 to G9 are represented by solid lines, G10 and G11 by dotted lines and G12 to G16 by dashed lines.

The detailed modal analysis for the post-disturbance network configuration is given in Appendix 2, Table VI. There is one unstable eigenvalue corresponding to the frequency 0.162 Hz. Based on modal analysis Table I shows the contribution to the eigenvector related to the machine speed normalized with respect to the inertia constant and the nominal power for this eigenvalue. Referring to the angle values, Table I indicates the same coherency as Fig. 4.

The results of Fourier analysis on generator speed deviation agree well with the generator coherency methods based on modal analysis or speed comparison. The speed comparison approach is a simple off-line method involving data trend examination. For on-line wide area measurements the instantaneous value of the bus angles is normally used for coherency determination [14]. Coherency is established for generators occurring in a given angle interval. Fig. 7 indicates that generators 1-9 swing together if an angle interval of (approximately) 10 degrees is accepted as a criterion for coherency. However, for generator 10-16 an angle difference of almost 35-40 degrees is present during the time interval presented in the figure. In fact, according to Fig. 7, a few among the machines G10 to G16 seem to be in close relation to G1-G9 at approximately 78.5 s. Consequently, the generator coherency based on the instantaneous generator voltage angles gives an inferior result as compared to the results obtained from Fourier analysis on generator speed deviation (which we propose), modal analysis and speed comparison.

TABLE I

The contribution to the eigenvector related to the machine speed and normalized with respect to the inertia constant and the nominal power for the 0.162 Hz mode.

Generator	Magnitude [pu]	Angle [DEGREES]
G1	3.24	158
G2	3.30	158
G3	3.26	158
G4	3.28	158
G5	3.22	158
G6	3.26	158
G7	3.26	158
G8	3.12	161
G9	3.12	159
G10	0.784	-1.47
G11	0.865	-3.10
G12	0.844	-0,822
G13	0.861	1.00
G14	1.00	0.401
G15	1.04	-0.126
G16	1.00	0.00

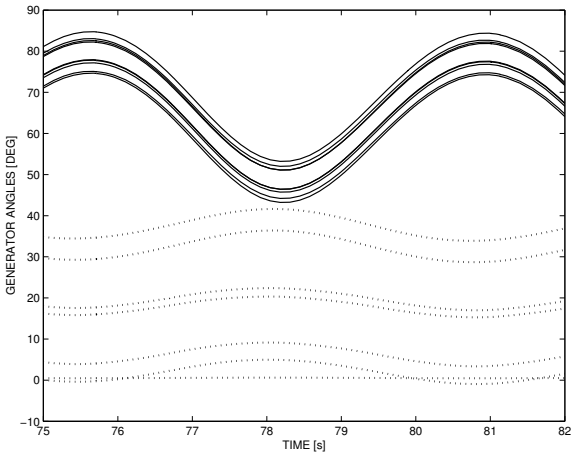

Fig. 7. The angles of the terminal voltages for G1-G16. G1 to G9 are represented by solid lines and G10 to G16 by dotted lines.

B. CASE II

In this case G2 and G3 becomes weakly connected to the surrounding system which in turn leads to inter-area oscillations. Before the time-domain simulation is started, the line between bus 5 and bus 6 is taken out of service. Although a stable loadflow solution is found the system is unstable already at this point according to the modal analysis in Appendix 2, Table V. However, to push the system away from its steady-state solution the system is subjected to an additional disturbance. The disturbance occurs after 15 seconds and consists of a permanent three phase fault located immediately outside bus 14 on the line between bus 13 and bus 14. The three phase fault is cleared within 90 ms as the faulted line is permanently removed by the line protection. Consequently, inter-area oscillations arise involving all generators in the system. The dominant inter-area mode present in this case is in the range of 0.61 Hz; Fig. 8. The frequency-time spectra for G1-G9, G12 and G13 are almost identical.

Similar to the previous case multiple inter-machine and inter-area modes are present immediately after the disturbance. Fig. 9 shows the magnitude of the Fourier coefficients for G15. The figure indicates that there is a mode in the range of 0.42 Hz present with a magnitude similar to the undamped 0.61 Hz mode. Although the 0.42 Hz component will attenuate the magnitude of that mode is in fact larger than the magnitude of the 0.61 Hz mode immediately after the disturbance. This may delay a discrimination of the most important mode based on local data exclusively. The frequency-time spectra look similar for G10, G11, G14, G15 and G16. However, the influence from the 0.42 Hz mode is by far most significant for G15. Thus by comparing the magnitudes in Fig. 8 and Fig. 9 the observation can again be made that the discrimination of the dominant mode is dependent on the extent of the generator involvement in the dominant inter-area mode.

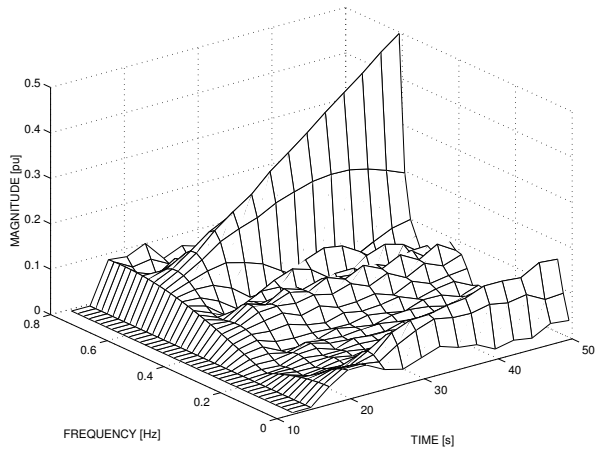

Fig. 8. The magnitude of the Fourier coefficients for G2 within the frequency range of inter-area oscillations.

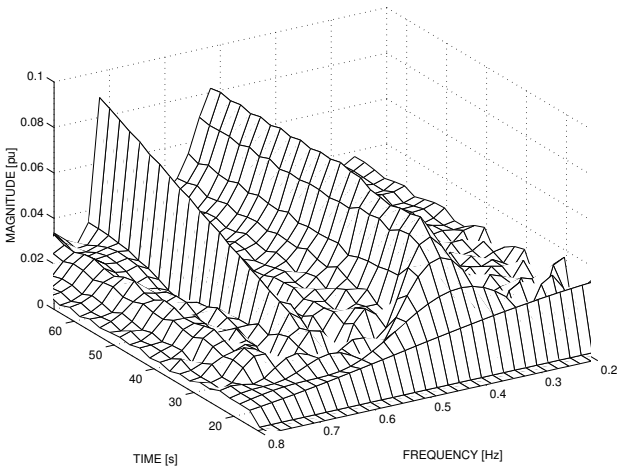

Fig. 9. The magnitude of the Fourier coefficients for G15 within the frequency range of inter-area oscillations.

By grouping the phase angles of the 0.61 Hz Fourier coefficients associated with the generators' speed signals, Fig. 10 indicates that G1-G9 and G11-G14 represent two generator groups while G10, G15-G16 follow separate swing trajectories. Referring to the grouping pattern of the speed trajectories and the angles associated with the modal analysis, respectively, the coherency in Fig. 10 is confirmed by the speed plot in Fig. 11 and the modal analysis in Table II. Table II is given for the unstable eigenvalue corresponding to the 0.607 Hz mode. Note that the angle associated with G14 stabilizes close to 2π in Fig. 10. Thus G14 should be grouped together with G11 to G13 as they stabilize close to the corresponding angle 0.

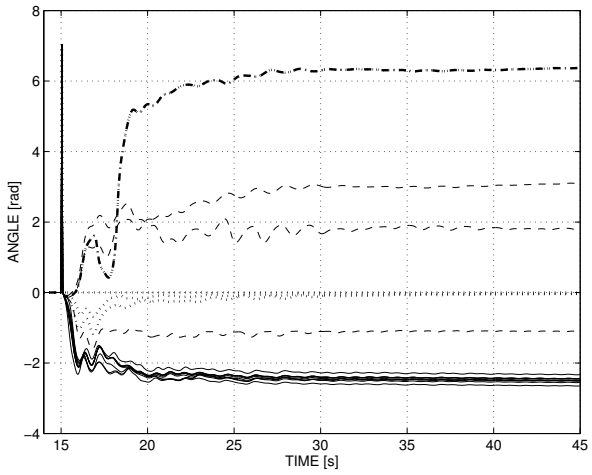

Fig. 10. The phase angles of the 0.61 Hz Fourier coefficients for all generators. Solid lines are used for G1-G9, dashed lines for G10, G15-G16, dotted lines for G11-G13 and the dashed dotted line for G14.

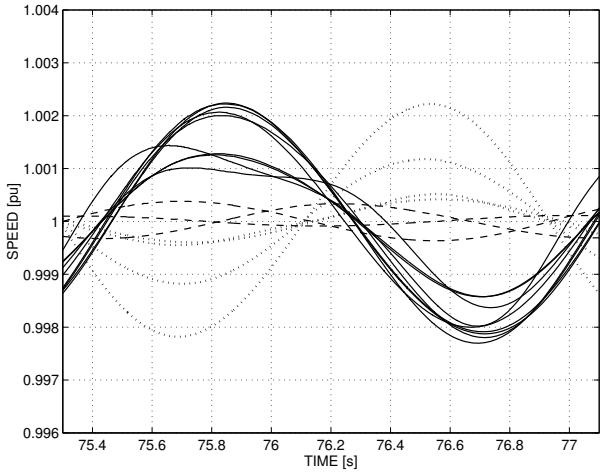

Fig. 11. The speed of G1-G16. Solid lines corresponds to G1-G9, dashed lines to G10, G15-G16 and dotted lines to G11-G14.

In this case too, the generator voltage angle seems to be a dubious indicator of coherency. Herein, the other methods clearly indicate that G11-G14 swing together. However, in Fig. 12 the internal angle differences for some of machines G11-G14 are actually larger than their angle differences with respect to machines G1-G9 and G15-G16.

TABLE II

The contribution to the eigenvector related to the machine speed and normalized with respect to the inertia constant and the nominal power for the 0.607 Hz mode.

Generator	Magnitude [pu]	Angle [DEGREES]
G1	0.57	132
G2	0.58	138
G3	0.59	142
G4	0.93	139
G5	1.01	142
G6	0.97	139
G7	0.94	139
G8	0.71	154
G9	0.89	146
G10	0.174	56.9
G11	0.22	1.31
G12	0.54	1.85
G13	1.00	0.00
G14	0.19	-3.26
G15	0.05	-114
G16	0.18	-175

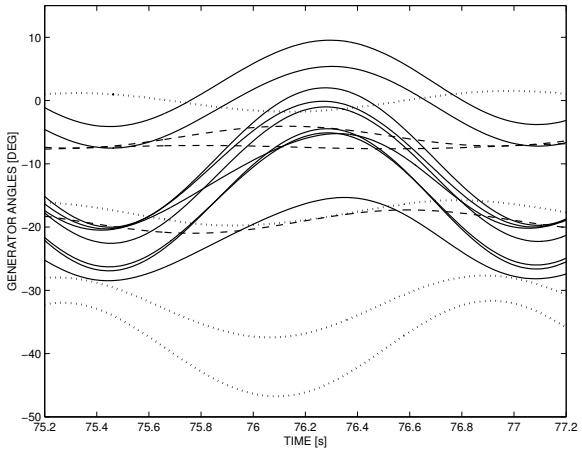

Fig. 12. The angles of the terminal voltages for G1-G16. Solid lines correspond to G1-G9, dashed lines to G10, G15-G16 and dotted lines to G11-G14.

C. CASE III

Before the disturbance region B is separated from the rest of the system as the lines bus 42 - bus 41 and bus 42 - bus 52 are taken out of service. Thus G16 becomes weakly interconnected to the remaining system. For this case the disturbance which occurs after 15 seconds corresponds to a step load reduction at bus 52 amounting to about 4.5% of the total bus load. As a result power oscillations occur where G16 swings against the remaining system.

The most significant mode is located in the vicinity of 0.31 Hz. This is illustrated in Fig. 13. Outside the range of the figure there are some decaying inter-machine modes and a damped mode within the range of 0.05 Hz present

immediately after the load reduction. The 0.31 Hz mode is poorly damped and in fact leads to the loss of synchronism for G16 after about 300 seconds. Cascading outages result leading to a total system blackout.

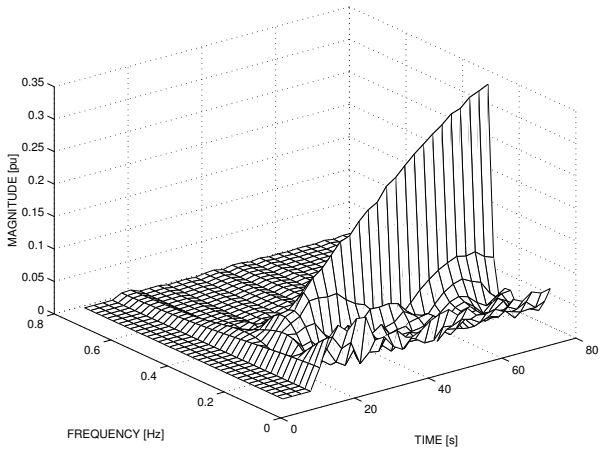

Fig. 13. The magnitude of the Fourier coefficients for G14 within the frequency range of inter area oscillations.

The angle values in Table III suggest a coherency where G1-G14 oscillate against G16. Such a grouping pattern is further disclosed by the phase angles of the 0.31 Hz coefficients illustrated in Fig. 14. Note that G14 with an angle close to -6 rad should be grouped with the generators having the corresponding angles 0. The generator separation revealed by the grouping pattern of speed trajectories in Fig. 15 also agrees well with the separation indicated by the previous methods. The terminal voltage angle for the generators are illustrated in Fig. 16. Disregarded parts of G14s trajectory also the generator angles indicate a similar generator coherency as the other methods for this case. Observe that since G15 is separated from the main system the generator is not represented in Fig. 14, Fig. 15 and Fig. 16.

TABLE III

THE CONTRIBUTION TO THE EIGENVECTOR RELATED TO THE MACHINE SPEED AND NORMALIZED WITH RESPECT TO THE INERTIA CONSTANT AND THE NOMINAL POWER FOR THE 0.330 HZ MODE.

Generator	Magnitude [pu]	Angle [DEGRESS]
G1	0.11	19.3
G2	0.10	20.9
G3	0.10	18.7
G4	0.11	17.0
G5	0.11	15.1
G6	0.11	15.9
G7	0.11	16.4
G8	0.11	9.63
G9	0.12	14.5
G10	0.09	21.7
G11	0.07	21.3
G12	0.06	51.3
G13	0.07	58.1
G14	1.00	0.00
G15	-	-
G16	0.35	166

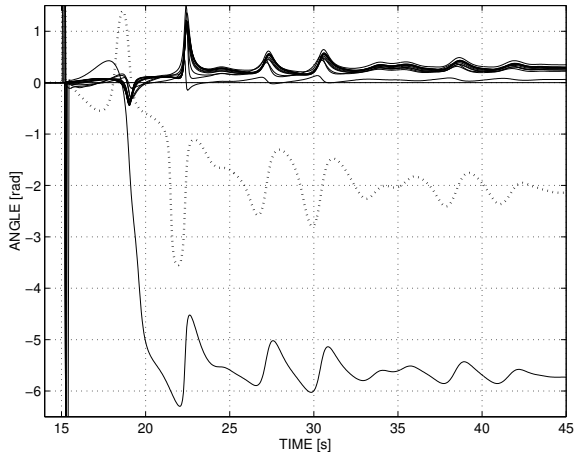

Fig. 14. The phase angles of the 0.31 Hz Fourier coefficients for all generators. Solid lines are used for G1-G14 and G16 is represented by the dotted line.

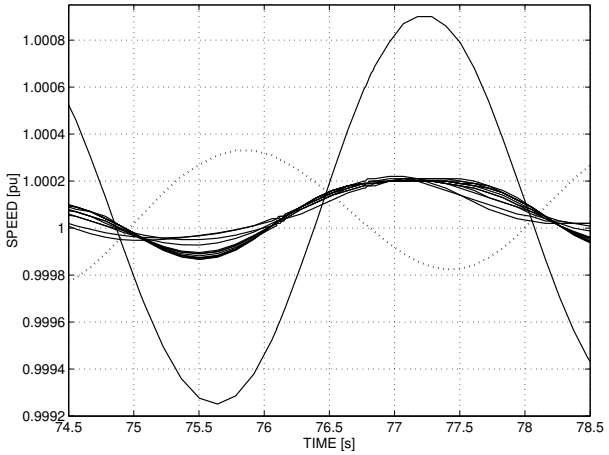

Fig. 15. The speed of G1-G16. Solid lines corresponds to G1-G14 and the dotted line to G16.

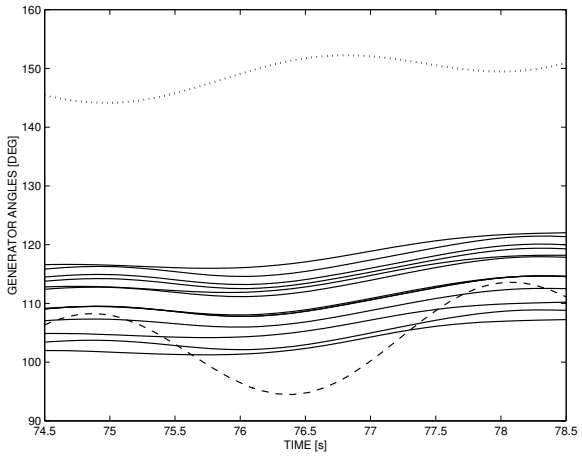

Fig. 16. The angles of the terminal voltages for G1-G14 and G16. G1-G13 are represented by solid lines, G14 by the dashed line and G16 by the dotted line.

In addition to the 0.330 Hz mode used for the modal analysis in Table III, Appendix 2 gives the rest of the relevant modes. For example, in the vicinity of 0.05 Hz is the low frequency 0.042 Hz mode represented.

V. DISCUSSION

Obviously many challenges must be conquered in order to realize a System Protection Scheme (SPS) based on the method introduced in this paper. A few of these challenges are briefly discussed below. At this early stage issues related to the practical implementation are disregarded and thus the focus aims at topics associated with the concept exclusively.

The Digital Signal Processing (DSP) issue is probably the most crucial part to solve in order to obtain a satisfactory operating scheme. Other important issues involve the geographical structure of the system, wide area data processing and the counteractive measures. However, these issues can be solved by fairly conventional solutions, where for example, GPS based Phasor Measurement Units (PMUs) represent powerful tools as they can provide time synchronized wide area speed measurements.

The Digital Signal Processing (DSP) requirements for a SPS based on the method introduced in this paper can be divided into three parts; first the detection and verification of the dominant inter-area mode, then the phase estimation associated with that mode and finally the stable/unstable nature of the mode(s). An accurate and fast distinguishing between unstable and stable modes is of particular importance in order to obtain successful corrective actions. Referring to Fig. 5 and Fig. 9, in some cases and for certain generators more than one mode may initially be present. Obviously this behavior complicates the detection process, nevertheless it is also important to successfully resolve these cases and distinguish the dominant mode as quick as possible.

For optimal performance the Fourier coefficients should be continuously determined with a high frequency resolution at the same time as they are based on data samples corresponding to a very short time segment i.e high time resolution. The nature of these high requirements for the frequency-time resolution is related to the necessity of an accurate monitoring of the instant system status as it is essential for the detection and curative processes. This is especially true if more than one contingency occurs in a short time or in the case of emergency situations involving cascading outages. However, according to the uncertainty principle [13] a trade-off between frequency and time accuracy must always be accepted where the most appropriate frequency-time relation for the given application should be selected. Parameters that will influence the selection involve the possibility of inter-area modes close in frequency and the likelihood for fast subsequent events. As in the case of lower frequency resolution the ability to identify adjacent modes will be reduced while the monitoring of the instantaneous nature of the signal will be deteriorated when the window length is increased. The frequency-time relation applied in Section IV denotes a high frequency accuracy at the expense of the time resolution. According to test simulations a reduced frequency accuracy may lead to enhanced phase fluctuations and therefore the given frequency-time relation was selected in order to clearly illustrate the method. However, for practical events involving changing system configurations the time resolution in Section IV is most likely insufficient.

The most natural choice of a geographical structure for the scheme is either the Wide Area Remote or the Wide Area Central as defined in [14]. Obviously combinations of these two structures are also applicable. Furthermore, the corrective measures controlled by the scheme may involve any conventional curative SPS actions.

The issues discussed above are all addressed in ongoing work.

In the test cases above, direct comparison of the generators' speed was used to visually investigate the generator coherency. The direct speed comparison is acceptable for simulation based coherency analysis, where the complete swing trajectories of the machines covering the entire event are accessible. However, in case of real (time) applications, coherency methods based on instantaneous grouping of the pure speed signals or the rate of change of speed are less reliable. As the measured speed signal normally involves significant transient distortion immediately after the disturbance, which may be difficult to reliably remove by real time filtering. This is also indicated by the three test cases where the speed plots had to be given a substantial time after the initial contingency when the (inter-machine) transients have attenuated in order to obtain a useful illustration. The generator voltage angle also suffers from the same inadequacy. Consequently, according to the investigation a reliable coherency can be established quicker by the method introduced here as compared to methods based on pure speed, rate of change of speed or generator voltage phasor comparison.

In some test cases there are small variations between the inter-area modes obtained from the Fourier based method and the modal analysis. For example, in Case I the Fourier based method indicates that the dominant mode corresponds to 0.19 Hz while the dominant mode obtained from the modal analysis is 0.162 Hz. These small deviations are mainly an effect of the difference between the non-linear simulation model and the linearized modal analysis model.

VI. CONCLUSIONS

A method suitable for on-line determination of generator coherency has been introduced. The method is based on wide area generator speed measurements and Fourier analysis. Three test cases have been used to illustrate the performance, where the new concept is compared to conventional methods based on generator speed comparison, modal analysis and phasor angle measurements. In a broader perspective, the method may be regarded as a tool to interpret the nature of power system oscillations following events for which the system was not planned.

For the test cases the method shows promising results as a tool for generator coherency determination. It gives al-

most identical results if compared with the off-line methods based on the generator speed and modal analysis. Based on the confidence in those methods the test cases indicate that the new concept reflects a more accurate coherency than the conventional method using the generator voltage angle. This is especially interesting as the generator angle probably is todays most common on-line indicator for generator coherency determination. Taking the transient distortion immediately after a disturbance into account, the investigation indicates that the method introduced here, generates a reliable coherency considerably quicker than the methods based on pure speed or generator voltage angle measurements. Finally, compared to on-line methods based on modal analysis the method supports real time applications better according to its less extensive computational requirements.

Acknowledgments

The authors would like to thank Svenska Kraftnät for their interest in this research area and for their financial support. The authors also would like to thank ABB Power Systems for providing Simpow. Graham Rogers is acknowledged for his help related to the test system.

Mattias Jonsson would like to express his sincere gratitude to Professor Miroslav Begovic for accepting him as a visiting scholar in his group during the spring and summer of the year 2002.

References

[1] Wide Area Protection seminar, *Real-Time Monitoring of Fast Dynamic in the Swedish National Grid (Fast RTMS)*, Presentation by Svenska Kraftnät, Västerås, Sweden, April 2, 2001.

[2] Murphy R.J, *Disturbance Recorders Trigger Detection and Protection*, IEEE Computer Applications in Power, Vol. 9, Issue. 1, January 1996, pp. 24 -28.

[3] Ramaswamy G.N *et al.*, *Multi-dimensional synchrony and dynamic equivalencing*, Proceedings of the 4th IEEE Conference on Control Applications, Albany, NY, USA, September 28 - 29, 1995, pp.605 - 610.

[4] Ramaswamy G.N *et al.*, *Synchrony, Aggregation, and Multi-Area Eigenanalysis*, IEEE Transactions on Power Systems, Vol. 10, No. 4, November 1995, pp. 1986 - 1993.

[5] Ostojic D.R, Heydt G.T, *Transient Stability Assessment by Pattern Recognition in the Frequency Domain*, IEEE Transactions on Power Systems, Vol. 6, No. 1, February 1991, pp. 231 - 237.

[6] Ostojic D.R, *Spectral Monitoring of Power System Dynamic Perormances*, IEEE Transactions on Power Systems, Vol. 8, No. 2, May 1993, pp. 445 - 451.

[7] Kamwa I, Grondin R, Loud L, *Time-Varying Contingency Screening for Dynamic Security Assessment Using Intelligent-Systems Techniques*, IEEE Transactions on Power Systems, Vol. 16, No. 3, August 2001, pp. 526 - 536.

[8] Begovic M.M, Milisavljevic M, *Monitoring and Control of Inter-area Oscillations Via Real-Time Measurements and TCSC Control*, Proceedings of the Bulk Power System Dynamics and Control IV - Restructuring, Santorini, Greece, August 24 - 28, 1997.

[9] Oppenheim A.V, Schafer R.W, *Discrete-Time Signal Processing*, 2nd ed, ISBN: 0-13-216292-X, Prentice Hall, 1989.

[10] Rogers G, *Power System Oscillations*, ISBN: 0-7923-7712-5, Kluwer Academic Publisher, 2000.

[11] Fankhauser H.R, Aneros K, A-A Edris. and Torseng S, *Advanced Simulation Techniques for the Analysis of Power System Dynamics*, IEEE Computer Applications in Power, Vol. 3, No. 4, October 1990, pp. 31 - 36.

[12] Internet Address, *www.abb.com/simpow*, 2003.

[13] Qian S, Chen D, *Joint time-frequency analysis - methods and applications*, ISBN: 0-13-254384-2, Prentice-Hall, 1996.

[14] Jonsson M, *Present Status of System Protection Schemes*, Tech. Report 23R, Chalmers University of Technology, Gothenburg, Sweden, 2002. pp. 30.

Mattias Jonsson received his M. Sc. and Lic.Eng from Chalmers University of Technology in 1998 and 2001, respectively. His interest lies in power system stability and power system protection. At present he works towards a Ph.D. thesis.

Miroslav Begovic (S'87, M'89, SM'92) is Associate Professor in the School of ECE, Georgia Institute of Technology in Atlanta, Georgia. His interests are in the general area of computer applications in power system monitoring, protection and control, and design and analysis of renewable energy sources. Dr. Begovic chairs the Working Group "Wide Area Protection and Emergency Control" in the Power Systems Relaying Committee of the IEEE Power Engineering Society. Dr. Begovic's work on distributed generation and photovoltaic (PV) systems has resulted in design of the 340 kW PV system on the roof of the Georgia Tech Aquatic Center, which was the largest of its kind at the time of initial deployment. Dr. Begovic is a Senior Member of IEEE's Power Engineering, Circuits and Systems, and Computer Societies, and a member of Sigma Xi, Tau Beta Pi, Eta Kappa Nu, and Phi Kappa Phi.

Jaap Daalder obtained his Ph.D in power engineering from the Eindhoven University of Technology, The Netherlands. He worked there as an Associate Professor until 1984 when he left for Norway to become a Director of Technology and Member of the Board of a subsidiary of the Brown Boveri Company, nowadays ABB. In 1993 he was appointed as full Professor at Chalmers University of Technology. Since 1997 he is heading the Department of Electric Power Engineering. His areas of interest are power systems and environmental issues related to power engineering.

Appendix I

TABLE IV

Nominal power and inertia constant for the generators in the test system.

Generator	Nominal power [MVA]	H [MWs/MVA]
G1	1800	2.33
G2	610	4.95
G3	721	4.96
G4	687	4.16
G5	545	4.77
G6	709	4.91
G7	610	4.33
G8	621	3.92
G9	855	4.04
G10	1065	2.91
G11	1406	2.00
G12	1782	5.18
G13	12162	4.08
G14	10000	3.00
G15	10000	3.00
G16	10112	4.45

Appendix II

TABLE V

Oscillation frequency f, real part of the eigenvalue σ and damping ratio ζ extracted from the relevant eigenvalues for the base case and the pre-fault systems. The total number of states is 82.

Base case			Case I			Case II			Case III		
f [Hz]	σ [s^{-1}]	ζ [pu]	f [Hz]	σ [s^{-1}]	ζ [pu]	f [Hz]	σ [s^{-1}]	ζ [pu]	f [Hz]	σ [s^{-1}]	ζ [pu]
0.050	-0.0486	0.1535	0.050	-0.0482	0.1528	0.051	-0.0533	0.1655	0.053	-0.0519	0.1550
0.418	-0.1792	0.0681	0.405	-0.1370	0.0538	0.415	-0.1471	0.0564	0.332	-0.0116	0.0056
0.555	-0.0923	0.265	0.522	-0.1269	0.0386	0.554	-0.0787	0.0226	0.441	-0.1193	0.0430
0.627	-0.0311	0.0079	0.573	-0.1100	0.0305	0.603	0.0584	-0.0154	0.636	-0.0695	0.0174
0.716	-0.0972	0.0216	0.715	-0.0967	0.0215	0.715	-0.0965	0.0215	0.972	-0.1083	0.0177
0.972	-0.1083	0.0177	0.962	-0.0795	0.0131	0.971	-0.1041	0.0170	0.982	-0.0799	0.0130
0.978	-0.0731	0.0119	0.976	-0.0673	0.0110	0.974	-0.0661	0.0108	1.061	-0.2368	0.0355
1.062	-0.2312	0.0346	1.040	-0.2590	0.0396	1.036	-0.2319	0.0356	1.092	-0.1252	0.0182
1.092	-0.1313	0.0191	1.085	-0.1008	0.0148	1.090	-0.1066	0.0156	1.115	-0.0293	0.0042
1.115	-0.0330	0.0047	1.114	-0.0300	0.0042	1.115	-0.0316	0.0045	1.161	-0.3156	0.0432
1.120	-0.2873	0.0382	1.161	-0.3156	0.0432	1.161	-0.3154	0.0432	1.191	-0.2934	0.0392
1.161	-0.3157	0.0432	1.203	-0.2825	0.0374	1.193	-0.3111	0.0415	1.335	-0.0617	0.0074
1.347	-0.0828	0.0098	1.346	-0.0786	0.0093	1.333	-0.0551	0.0066	1.376	-0.4003	0.0463
1.376	-0.4003	0.0463	1.376	-0.4003	0.0463	1.377	-0.4025	0.0465	1.409	-0.3257	0.0368
1.409	-0.3251	0.0367	1.409	-0.3246	0.0366	1.409	-0.3259	0.0368	1.718	-0.4635	0.0429
1.720	-0.4620	0.0427	1.710	-0.4528	0.0421	1.716	-0.4621	0.0428	-	-	-

TABLE VI

Oscillation frequency f, real part of the eigenvalue σ and damping ratio ζ extracted from the relevant eigenvalues for the post-fault systems. The total number of states is 82.

Case I			Case II			Case III		
f [Hz]	σ [s^{-1}]	ζ [pu]	f [Hz]	σ [s^{-1}]	ζ [pu]	f [Hz]	σ [s^{-1}]	ζ [pu]
0.057	-0.0905	0.2449	0.050	-0.0519	0.1624	0.042	-0.0302	0.1145
0.162	0.0617	-0.0606	0.415	-0.1513	0.0579	0.330	-0.0072	0.0035
0.457	-0.2254	0.0783	0.554	-0.0830	0.0238	0.440	-0.1194	0.0431
0.563	-0.1028	0.0290	0.607	0.0400	-0.0105	0.636	-0.0695	0.0174
0.715	-0.0957	0.0213	0.715	-0.0967	0.0215	0.972	-0.1083	0.0177
0.963	-0.1063	0.0176	0.871	-0.0990	0.0181	0.982	-0.0799	0.0130
0.968	-0.0522	0.0086	0.973	-0.1177	0.0192	1.061	-0.2368	0.0355
1.038	-0.2546	0.0390	0.981	-0.0631	0.0102	1.092	-0.1252	0.0182
1.088	-0.0863	0.0126	1.086	-0.0951	0.0139	1.115	-0.0293	0.0042
1.124	-0.0945	0.0134	1.110	-0.0296	0.0042	1.161	-0.3156	0.0432
1.160	-0.3070	0.0421	1.159	-0.3068	0.0421	1.191	-0.2934	0.0392
1.201	-0.2818	0.0373	1.198	-0.2792	0.0371	1.335	-0.0617	0.0074
1.337	-0.0460	0.0055	1.341	-0.0527	0.0063	1.376	-0.4003	0.0463
1.377	-0.4025	0.0465	1.375	-0.4011	0.0464	1.409	-0.3257	0.0368
1.414	-0.3082	0.0347	1.414	-0.3066	0.0345	1.718	-0.4635	0.0429
1.682	-0.4430	0.0419	1.716	-0.4622	0.0428	-	-	-

Paper E

A system protection scheme concept to counter inter-area oscillations

M. Jonsson, J. Daalder, M. Begovic

Submitted to IEEE Transactions on Power Delivery

A SYSTEM PROTECTION SCHEME CONCEPT TO COUNTER INTER-AREA OSCILLATIONS

Mattias Jonsson, *Student member IEEE,* Jaap Daalder and Miroslav Begovic, *Senior member IEEE*

Abstract— **This paper introduces a concept of a generator coherency based System Protection Scheme, addressing inter-area oscillation events. The scheme uses wide area generator speed measurements combined with DFT analysis to determine coherency.**

A test case simulated in the NPCC 68 bus system is used to introduce the scheme's operating principle. The test case is also used to investigate the scheme suitability for different well established DSP methods. Further aspects as evolving-/sliding window functions, window size and frequency resolution are analyzed.

For the detection of inter-area modes, parametric DSP methods turned out to be the most feasible. In general evolving windows are faster than sliding windows. However, evolving windows require a trigger and were therefore rejected for the design proposed here. A lower frequency resolution may shorten the response time at the expense of the quality of the estimates of the instantaneous speed deviation and the generator coherency. The design proposed here is based on a high frequency resolution at the cost of a lower respond time.

Keywords— **Coherency determination, DFT analysis, DSP, Inter-area oscillations, System Protection Scheme, Transient instability, Wide Area Protection.**

I. Introduction

OPERATING limits of electrical bulk power systems are continuously stretched due to environmental constraints and deregulation. Different types of power system instability are the immediate threat to power systems. In early years transient stability was the main issue while voltage stability has become important during the last 20 years. Many applications have been developed in order to master voltage stability and to some extent it may be argued that transient stability was given less priority. However, in the Swedish transmission system and likely due to deregulation, the annual number of inter-area events has increased significantly during recent years. In 1996 the annual rate of recorded inter-area oscillation events was about 15 while in 2000 the rate had increased to more than 300 [1]! In fact, in a few cases, operating conditions have occurred where the system was close to its limits (it should be noted that about 30 % of the events recorded in 2000 were related to one specific maintenance job lasting three weeks). As an example, a very serious condition occurred during the evening of New Years Day in 1997. An earth fault on a 400 kV busbar in the South-West part of Sweden combined with an unusual pre-fault loading condition resulted in serious power oscillations (maximum 1100 MW peak to peak) which in its turn led to the loss of a nuclear plant (1700 MW). The system was on the brink of a blackout [2]. The increasing number of power oscillations encourage strong incentives for precise and reliable on-line methods to ensure fast detection and effective counteraction of events involving inter-area modes. Moreover, the fundamental presumption to ensure the most effective corrective actions in case of inter-area events is a well established generator coherency.

System Protection Schemes (SPS) are attractive candidates to improve system performance due to their environmentally friendly character and relatively low cost compared to building new power plants and transmission lines. Recently developed communication and computer based technologies have significantly enhanced the potentials given by SPS.

In [3] a new method for generator coherency determination was introduced which supports SPS applications very well. According to the investigation carried out in [3] the new method defines a more reliable coherency than for example generator angle monitoring. In addition, the investigation indicated that the new method establishes the coherency faster than conventional angle monitoring as it is less sensitive to transient distortion. In this paper some conceptional solutions for this method are introduced. The Digital Signal Processing (DSP) issue is probably the most crucial part in order to obtain a reliable scheme based on the new method. Another important aspect is the technique used for the instantaneous speed (frequency) measurement. Extensive work has been reported in this area, where any opportune technique processing reliable low frequency estimates can be used for the scheme. Examples of methods used for frequency estimation in power networks are polynomial DFT and tracking of zero crossings. These and additional methods are further described in [4] and [5]. Further important issues involve the geographical structure of the scheme, wide area data processing and the counteractive measures. These issues can be solved by fairly conventional solutions, where for example, GPS based Phasor Measurement Units (PMUs) are powerful tools as they are a good example of the equipment that can provide time synchronized wide area speed measurements. In addition they posses the capability to perform extended data processing which make them attractive for this application. However, the main focus in this paper is on the DSP part as it represents the main issue for a practical realization of the scheme.

This work was financially supported by Svenska Kraftnät. M. Jonsson and J. Daalder are both with Chalmers University of Technology, Gothenburg, Sweden. E-mail: mattias.jonsson@elteknik.chalmers.se, jaap.daalder@elteknik.chalmers.se. M. Begovic is with Georgia Institute of Technology, Atlanta, USA. E-mail: miroslav.begovic@ece.gatech.edu

II. GROUPING OF GENERATORS BY SPEED MEASUREMENT AND DFT ANALYSIS

In (1) δ_l corresponds to the angle between the generator stator and rotor flux. Apart from negligible deflections resulting from small load variations the speed deviation ω_l will be zero during normal operation. In case of a disturbance the present value of δ_l will be altered in order to meet the new system conditions. The transition from the pre- to the post-disturbance operating point appears as more or less developed oscillations resulting from the electrical and mechanical torque deviation. Hence ω_l is obviously an authentic reflection of the oscillations present in the system.

$$\dot{\delta}_l = \omega_l \tag{1}$$

By monitoring the generator speed and applying Discrete Fourier Transform (DFT) analysis the fundamental speed will be reflected by the zero frequency spectral component while the speed deviation can be obtained from the non-zero frequency components. Moreover by determining the phase of the dominant non-zero frequency component in time (i.e the dominant oscillation mode present in the system) the swing characteristic for the machine can be obtained. Furthermore, by comparing the phase of the dominant component for all machines the generator coherency can then be acquired. The procedure is given by (2) to (7).

The DFT of the generator speed in time C is obtained according to (2) [6] where k and i are integers such that $-\infty \leq k \leq \infty$ and $0 \leq i \leq n-1$. The parameter ω represents the sampled generator speed signal and h the window function, where h controls the extension of the part of the speed signal used to calculate the frequency spectrum associated with the current time of interest k. In this paper a rectangular window function is adopted defined as $h[m] = 1$ for $0 \leq m \leq l-1$ and otherwise $h[m] = 0$. Furthermore, n are the number of equally spaced spectral components.

$$C[k,i] = \sum_{m=0}^{l-1} \omega[k+m]h[m]e^{-j\frac{2\pi im}{n}} \tag{2}$$

The oscillation modes present in the system are reflected by the peaks given by the spectra including all non-zero frequency components. Based on (2) we can determine a vector $\mathbf{c_k}$ for each time value k (3) which contains the DFT coefficients $c_{k,1} \ldots c_{k,i} \ldots c_{k,n-1}$ separated by the spectral frequency resolution decided by n. These coefficients are complex and denote both the magnitude and phase of each oscillation mode. Note that the zero frequency component is excluded in (3) as it corresponds to the fundamental speed. Theoretically the spectra are limited to a domain given by the Nyquist criterium [6]. However, in case of short sampling intervals the investigated frequency range should be further restricted to the domain relevant to inter-area modes.

$$\mathbf{c_k} = (c_{k,1}, \ldots, c_{k,i}, \ldots, c_{k,n-1}) \tag{3}$$

In order to determine the dominant inter-area mode the DFT coefficient with the largest amplitude $A_{k,dom}$ is identified as given in (4). The index *dom* corresponds to the position in $\mathbf{c_k}$ for the DFT coefficient representing the largest magnitude. As indicated above the theoretical pick-up value for an inter-area mode is immediately above zero. However, to exclude measurement distortion and frequency deviations due to load variations a minimum value for an acceptable (dominant) DFT coefficient is required. Thus the final establishment of a dominant inter-area mode is carried out according to (5) where $A_{pick-up}$ is a pre-defined pick-up value outside the range of these phenomena. Note that the dominant mode may change its frequency as a function of time and can therefore be of a temporary nature.

$$A_{k,dom} = max\{\mid c_{k,1} \mid, \ldots, \mid c_{k,i} \mid, \ldots, \mid c_{k,n-1} \mid\} \tag{4}$$

$$c_{k,dom} = \mathbf{c_k}[dom] \leftrightarrow A_{k,dom} \geq A_{pick-up} \tag{5}$$

Once a dominant inter-area mode has been identified the phase of that mode $arg\{c_{k,dom}\}$ is determined for the involved system generators $1 \ldots l \ldots p$ and a vector is organized including all these phases (6).

$$\begin{aligned} \varphi_{\mathbf{k,dom}} \quad = \quad & (arg\{c_{k,dom,1}\}, \ldots, \\ & arg\{c_{k,dom,l}\}, \ldots, arg\{c_{k,dom,p}\}) \end{aligned} \tag{6}$$

Finally, a phase comparison is performed (7) where one of the generators' phase angle is used as the reference angle φ_{ref}. The generator coherency is then defined by $\mathbf{\Delta}\varphi_{\mathbf{k,dom}}$ where generators having (approximately) the same phase difference with respect to φ_{ref} represent a coherent group. Here $\mathbf{E}$ is a unit vector of length p.

$$\mathbf{\Delta}\varphi_{\mathbf{k,dom}} = \varphi_{\mathrm{ref}} \cdot \mathbf{E} - \varphi_{\mathbf{k,dom}} \tag{7}$$

III. STRUCTURE OF THE ON-LINE GENERATOR COHERENCY GROUPING SCHEME

In this section some structural aspects of the practical realization of the on-line scheme are discussed. However, the scheme is still at an early stage of development, and therefore it should be noted that the case study presented in the next sections is based on post-processing following a disturbance applied on a network simulation.

The most natural choice of structure for the scheme is either the Wide Area Remote or Wide Area Central as defined in [7] and illustrated in Fig.1. Obviously combinations of these two structures are also applicable, although in this report we will address the Wide Area Central structure. In order to obtain the desired performance for any type of high performing wide area protection or monitoring system, GPS based PMUs represent powerful tools as they are a good example of equipment that can provide time synchronized wide area speed (frequency) measurements. In addition they can easily be extended to provide

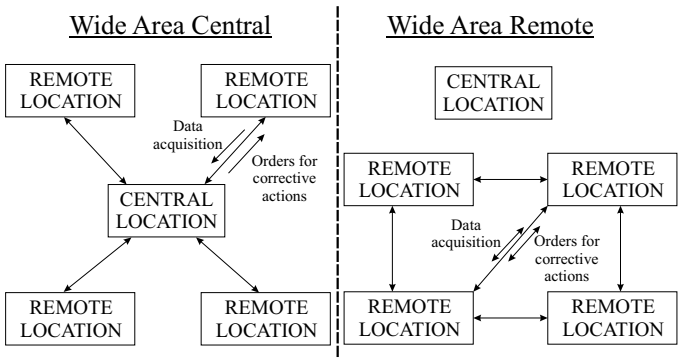

Fig. 1. Wide Area Central and Wide Area Remote structures. In case of the Wide Area Central structure data acquisition, data processing and orders for corrective actions are all carried out centrally. For the Wide Area Remote structure all these actions involve a number of remote stations exclusively.

DFT calculations. Obviously also other equipment providing synchronized speed measurement and data processing may be used for the scheme.

The choice of generators used as sensor locations for this type of scheme is obviously much dependent on the architecture of the power system. However, for any system configuration it may be suitable to locate the data acquisition units at a few "pilot generators" in order to obtain the overall system behavior at minimum cost and an appropriate level of reliability. For lightly meshed systems with localised centres of generation and demand an opportune location of the units is most often straightforward. However, in case of densely meshed systems with dispersed generation and demand an optimal localization may require extensive contemplation. In [8] and [9] methods have been developed to secure optimal sensor/PMU location.

For the Wide Area Central design illustrated in Fig.2, synchronized speed measurement is performed at the pilot generators. Based on the speed measurement the DFT coefficients are calculated locally and continuously sent to the central location. A vital aspect for the practical implementation is that the speed measurements must be obtained using identical algorithms for all remote measurement units. This is to ensure consistent real-time synchronized speed measurement response during transients. At the central location the DFT coefficients are used to identify any dominant mode (4)-(5). In case the central data processing detects an inter-area mode, the generator coherency (7) for that mode is determined and the appropriate orders for corrective measures are sent to the relevant remote locations.

Typically the curative measures initiated by the scheme may involve load shedding, generator rejection, system separation and activation of different FACTS devices. Load shedding, generator shedding and system separation are fast and extensive actions which typically are used as (ultimate) measures to prevent loss of synchronism. Actions involving FACTS devices are mainly used to accelerate the damping of stable modes but obviously they also contribute to the avoidance of loss of synchronism.

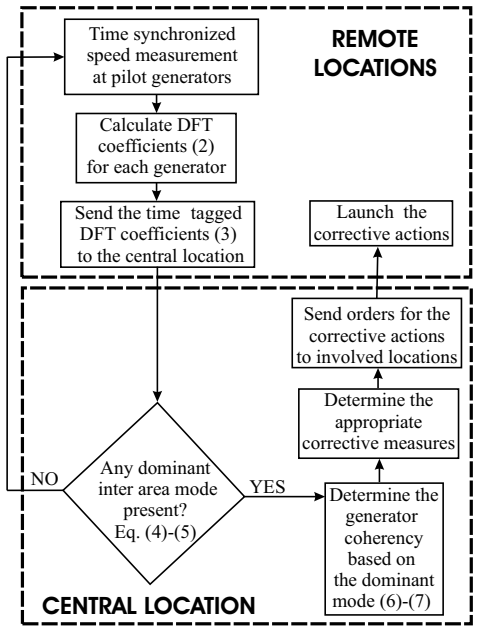

Fig. 2. The block diagram of the scheme paradigm for the Wide Area Central structure. Note that the large box denoted "Remote Locations" in practise represent multiple remote locations as illustrated in Fig.1.

IV. TEST SYSTEM

The test system used here is the 68 bus NPCC network which represents a reduced order model of the New England/New York interconnection about 30 years ago. The system involves 16 generators where generators G13 to G16 represent large generator group equivalents. The frequency control is maintained by G1 to G9 while G10 to G16 are operated at a constant mechanical torque. In Fig.3 the dashed lines indicate the coherent groups as given by Rogers [10] and the thick lines indicate the weak tie-lines interconnecting the different regions. System parameters used for the simulations are based on data given in [10].

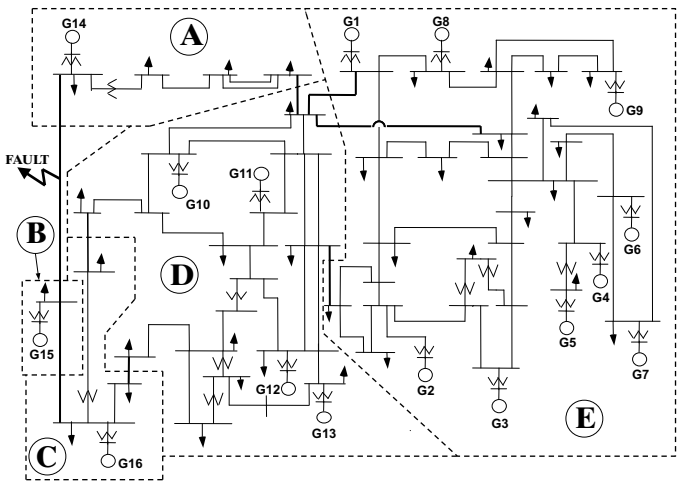

Fig. 3. Test system topology.

V. TEST CASE

Prior to the disturbance all system devices are in operation. Fifteen seconds after the simulation is started a permanent three phase fault occurs on the line indicated in Fig.3. The line is permanently removed and undamped inter-area oscillations in the range of 0.23 Hz arise as region A becomes weakly interconnected to the remaining regions (Fig.4, Fig.5 and Fig.6).

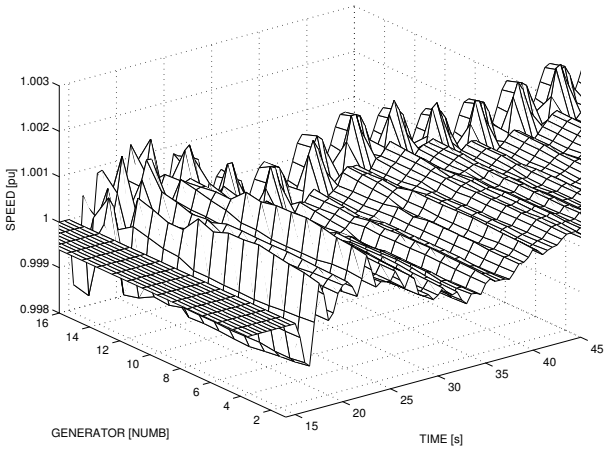

Fig. 4. The speed of all machines.

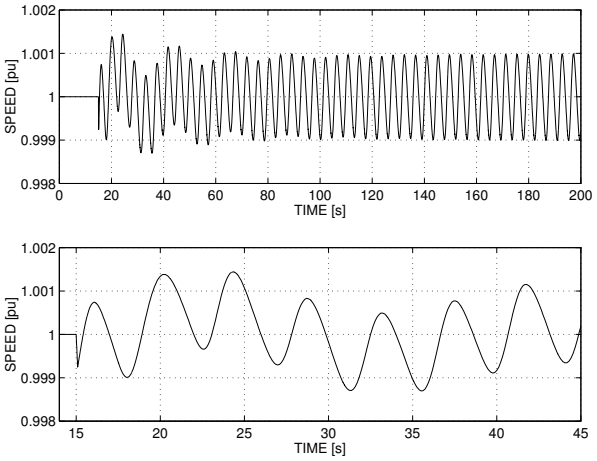

Fig. 5. The speed of G14.

In addition to the undamped inter-area mode two damped modes are present for some time after the disturbance. For generators (e.g G14) which are strongly involved in the undamped mode these additional swing frequencies will have a minor effect on the detection of the dominant mode. However, for generators less involved these additional inter-area frequencies may slightly complicate the distinction between the damped and undamped modes. An example is given in Fig.7 where the magnitude of the DFT coefficients for G5 is illustrated. As can be observed from the figure a reliable discrimination of the unstable 0.23 Hz mode may require some additional time as compared to the example given in Fig.6. Nevertheless when the damped modes have attenuated the dominant unstable mode can easily be discriminated.

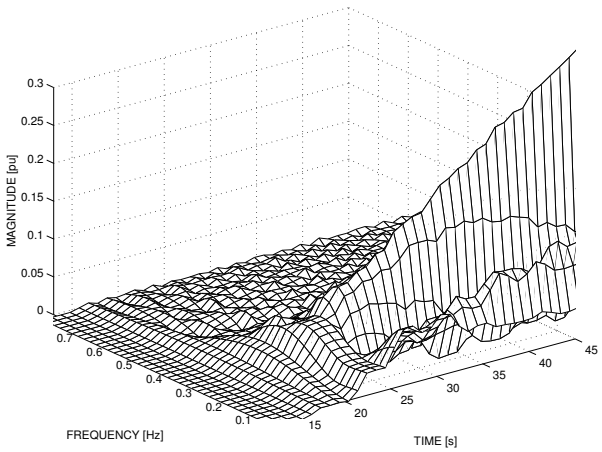

Fig. 6. The magnitude of the DFT coefficients for G14 within the frequency range of inter-area oscillations.

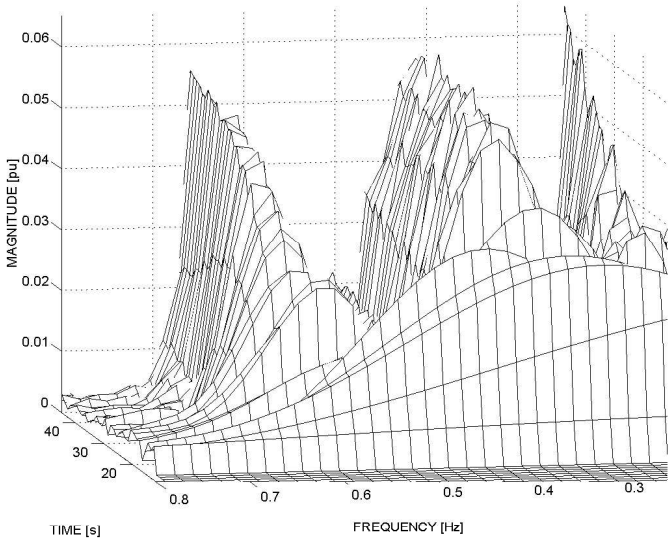

Fig. 7. The magnitude of the DFT coefficients for G5 within the frequency range of inter-area oscillations.

By grouping of the angle graphs Fig.8 illustrates that G14 swings against all other generators. Fig.6, Fig.7 and Fig.8 are all based on a sampling frequency of 20 Hz and a sliding window function corresponding to a time segment of 100 s.

VI. DIGITAL SIGNAL PROCESSING METHODS FOR THE GENERATOR COHERENCY DETERMINATION

The Digital Signal Processing (DSP) requirements for the generator grouping scheme introduced in this paper can be divided into three parts; first the detection and verification of the dominant inter-area mode, then the phase estimation

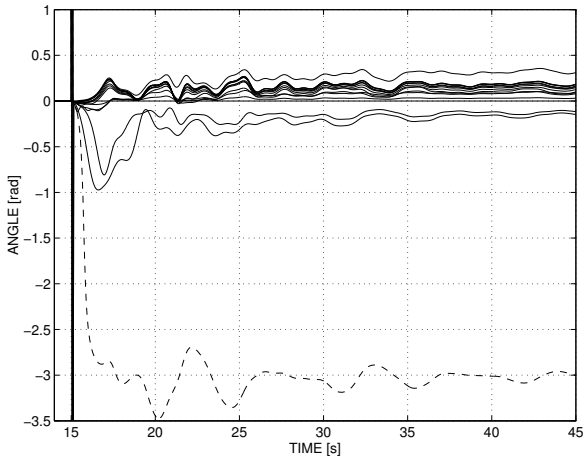

Fig. 8. The phase angles of the 0.23 Hz DFT coefficients for all generators in the case of frequency resolution 0.01 Hz. The dashed line corresponds to G14 while solid lines are used for the remaining generators.

associated with that mode and finally the stable/unstable nature of the mode(s). An accurate and fast distinction between unstable and stable modes is of particular importance in order to obtain successful corrective actions. In some cases and for certain generators more than one mode may initially be present as Fig.7 demonstrates. Obviously this behavior complicates the detection process, nevertheless it is important to successfully resolve these cases and distinguish the dominant mode as quick as possible.

For optimal performance the DFT coefficients should be continuously determined with a high frequency resolution based on data samples corresponding to a very short time segment i.e a high time resolution. The nature of these high requirements for the frequency-time resolution is related to the necessity of an accurate monitoring of the instant system status as this is essential for the detection and the curative process. However, according to the uncertainty principle [12] a trade-off between frequency and time resolution must always be accepted.

The simulation in Section V indicates that a long sliding window function (i.e each window corresponds to a data segment involving a long time period) with its detailed frequency resolution is appropriate for the phase calculation and also for the visual discrimination of a dominant frequency mode. However in order to track mode shifts and obtain the stable/unstable nature of the modes (or in case the frequency estimates are used as control parameters) the time resolution engendered by a long window function may be insufficient. Still for discernment of adjacent multiple modes a high frequency resolution is required, as a poor frequency resolution may lead to a shift of the resulting spectral peak(s). A number of conventional methods provided in the MATLAB SIGNAL PROCESSING TOOLBOX have been tested for the *detection* of the dominant inter-area mode using different window functions. The methods involve classical FFT, non-parametric, parametric and subspace based methods. Additionally a couple of adaptive filter algorithms have also been examined. Apart from Esprit [13] and Pisarenko [13] all other methods are described in MATLAB HELP [14] where further references also are provided.

For the evaluation of the different methods the speed signal of G14 was chosen; Fig.5. The signal contains features that the speed signal typically may involve in case of inter-area modes. For example, damped low frequency transients associated with the frequency control and the obvious undamped inter-area oscillations.

In accordance with realized Wide Area Protection applications [7] 20 Hz was used as the sampling frequency. Different sampling frequencies have been tested, showing negligible improvement of the performance. Two main types of rectangular window functions were used for the investigation; the *sliding* function, where a fixed number of time samples are windowed and supplied to the DSP algorithm and the *evolving* function, where an increasing number of time samples are supplied to the DSP algorithm. The sliding window function is continuously in operation independently of the present power system status while the evolving window function is started in the case of a possible disturbance only. Furthermore the sliding window functions were shifted two samples at the time and thus the frequency components were updated every 100 ms while the evolving functions were updated for each sample.

The definition of detection is here that the dominant frequency component must posses a value at least 5% above the second largest component in order to be detectable. However cases where there are two or three adjacent components which are closely tied together and strongly deviating from the remaining modes have also been treated as detectable at the point where all the immediate modes posses a value larger than 105% of the mode with the next largest magnitude. Moreover and in order to obtain a reliable detection the pick-up value must maintain the 5% margin with respect to the other modes for a time delay corresponding to 300 ms. Initially a time delay of 100 ms was applied, however occasional peaks for some methods in the initial transient stage led to an unreliable detection process for this time delay. In case the margin is lost before the time delay has expired, the timer associated with the pick-up value is reset. Initially a frequency resolution of 0.01 Hz was adopted for all methods. The detection times for the different methods are summarized in Table.I. Also a sliding window function corresponding to a data segment of 1 s was applied on each method, without useful results though. The most encouraging results were obtained for the parametric methods where the covariance method showed the best performance.

The main concern in the case of parametric methods is the requirement of appropriate system modelling. Here an extensive number of model orders were tested involving orders of 1 to 200. The same test range was also used for subspace based methods. The values presented in Table.I all correspond to the model order or subspace dimension giving the best performance for the associated method. Unex-

pectedly many methods worked best for fairly large orders and dimensions.

Sliding window functions using a short data segment proved to be less reliable according to their "peaky" character, although they sometimes provide faster detection. In case of sliding window functions the computational requirements for the subspace based methods were in general more extensive than for the remaining methods.

TABLE I

Detection times, $t_{data\_segment}$, in the case of frequency resolution 0.01 Hz for window functions corresponding to data segments of 100 s, 50 s, 10 s and 5 s, respectively. In addition the detection times, t_{evol}, for evolving functions are also presented. Note that the detection time corresponds to the simulation running time at the moment of detection. For "-" no successful detection was obtained.

Method	t_{100} [s]	t_{50} [s]	t_{10} [s]	t_5 [s]	t_{evol} [s]
FFT	36.6	36.6	-	-	36.2
Chirp	37.1	37.1	-	-	36.7
Periodogram	32.3	32.3	-	-	29.9
Welch	32.5	34.2	-	-	33.1
Multitaper	32.4	32.4	-	-	-
Yule-Walker	26.0	26.0	25.9	-	25.6
Burg	25.3	25.3	23.0	-	23.9
Covariance	23.5	23.5	23.9	22.9	20.4
Modified Covariance	24.8	24.8	24.6	22.0	21.3
Peig	23.8	23.8	23.4	-	22.3
MUSIC	42.5	35.4	-	-	22.4
Pisarenko	-	-	-	-	-
Steiglitz-McBride	27.2	25.3	23.6	-	22.6
Prony	105.8	55.8	23.4	-	23.0
Esprit	42.5	42.8	45.0	-	42.7

Adaptive filters are self-learning applications whose filter coefficients adjust themselves in order to obtain optimal performance. Here the linear prediction sample by sample method was applied and the adaptive filters examined involve a Kalman algorithm, a Recursive Least Square (RLS) algorithm and several Least Mean Squares (LMS) algorithms [14]. To obtain the foremost filter performance extensive parameter tuning was performed in order to encircle the appropriate parameter values. One observation made indicated that the adaptive filters generated very broad spectra in case of high sampling frequency. Thus to facilitate the detection process the sampling frequency was reduced from 20 Hz to 2 Hz.

The shortest detection times obtained for the frequency resolutions 0.01 Hz and 0.1 Hz are presented in Table.II (the 0.1 Hz resolution is further discussed in section IX). Generally the adaptive filters perform worse than parametric methods but similar or slightly worse than non-parametric methods. In general the foremost performance is obtained for a certain model order and is unimproved although the model order is increased. Thus the model orders given in Table.II correspond to the lowest possible model order supporting the presented detection times.

In the case of the RLS method and frequency resolution 0.01 Hz the forgetting factor 0.9 gave the best performance while the forgetting factor value 1 (infinite memory) turned out to be best for the 0.1 Hz resolution. Moreover the results given for the Kalman filter is obtained for the measurement noise variance 0.2 and the process noise covariance 0.01.

TABLE II

Detection times, t_{det}, in case of frequency resolutions 0.1 Hz and 0.01 Hz for adaptive filter algorithms. For the 0.01 Hz resolution only the pick-up of the 0.23 Hz mode is given while the pick-ups for both the 0.2 Hz and 0.3 Hz (within brackets) modes are given for the 0.1 Hz resolution. Note that the detection time corresponds to the simulation running time at the moment of the detection and that "-" corresponds to no pick-up or absence of associated parameter use.

Method	Model order 0.1 Hz res./ 0.01 Hz res.	Step size	t_{det} [s] 0.1 Hz res.	t_{det} [s] 0.01 Hz res.
LMS	15/53	0.05	21.5(18.5)	44.5
Normalized LMS	8/78	$5 \cdot 10^{-5}$	-(20.0)	55.5
Sign-data LMS	11/41	0.05	21.0(18.0)	36.0
Sign-error LMS	10/40	0.005	21.5(18.5)	38.0
Sign-sign LMS	10/48	$5 \cdot 10^{-5}$	21.0(18.0)	41.0
RLS	15/40	-	21.5(18.5)	38.0
Kalman	13/53	-	21.5(18.5)	42.5

VII. OPERATING SCHEME FOR GENERATOR COHERENCY DETERMINATION

Referring to the investigation above no method alone succeeded to provide a satisfactory time-frequency resolution. The adopted frequency resolution was adequate while the resulting time resolution was insufficient. The most promising phase estimations were obtained for long sliding window functions; compare Fig.8, Fig.11, Fig.12 and Fig.13. However by using the long window function the instantaneous behavior of the speed deviation is unrevealed. This is unacceptable both for the verification of the dominant mode and also for the understanding of its unstable/stable nature. Thus an approach involving three different window functions is proposed. First the window function associated with the detection and verification of the dominant mode, then the long window function used for the coherency determination and finally the sliding Fast Fourier Transform (FFT) window with a length corresponding to the dominant mode and used to track the instantaneous nature of the dominant mode. The proposed algorithm for the DSP process at the central location in Fig.2 is illustrated in Fig.9. Apart from the framed sections which involve data from all generators the algorithm should be continuously executed for all generators in parallel.

The algorithm is continuously supplied with the most recent updates of the coefficients $c_{k,1}, \ldots, c_{k,i}, \ldots, c_{k,n-1}$ reflecting the speed deviation. First the algorithm distinguishes any dominant mode in the section SEARCH_FOR_DOMINANT_MODE. This task is carried out by identifying the mode with the largest magnitude $c_{k,dom}$ and then evaluating if $c_{k,dom}$ has a magnitude which is $K_{pick-up}$ times larger than the mode occupying the second largest magnitude. In Fig.9 the magnitude of $c_{k,dom}$

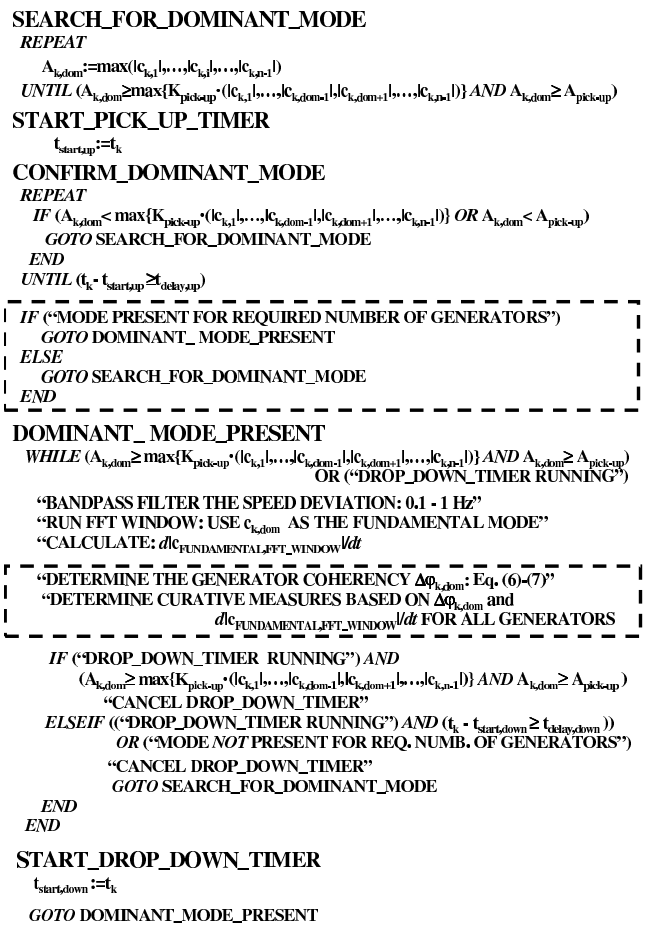

Fig. 9. The generic code for the DSP process at the Central location in Fig.2.

is denoted $A_{k,dom}$. To avoid pick-up due to measurement distortion or load variations an additional verification of $A_{k,dom}$ is carried out with respect to $A_{pick-up}$ where $A_{pick-up}$ is defined in Section II. When the criteria are fulfilled the pick-up timer is started at the instant $t_{start,up}$ and in case $A_{k,dom}$ remains above the pick-up values during a time period of $t_{delay,up}$ the algorithm concludes that a dominant mode is present for the addressed generator (see CONFIRM_DOMINANT_MODE). In case a dominant mode is detected for one generator a verification is required with respect to the remaining generators, i.e the mode must be present for a minimum number of machines before the dominant mode can be completely established (and the algorithm can proceed to DOMINANT_MODE_PRESENT). Typically a short sliding window together with a parametric method can be used for the detection of the dominant mode. The parameter t_k corresponds to the current running time. Note that all quantities with the subscript k are continuously updated as the real-time data reach the algorithm.

When the dominant mode has been identified three parallel processes must be carried out as given in the section DOMINANT_MODE_PRESENT. Those processes embrace the coherency determination based on the dominant mode (6)-(7), the knowledge of the instantaneous behavior of the dominant mode (the FFT window) and the long term verification of the dominant mode (controlled by the *while* statement and the DROP_DOWN_TIMER).

In order to obtain the instantaneous nature of the magnitude of the inter-area mode the speed deviation is bandpass filtered and then a sliding FFT window applying the dominant mode $c_{k,dom}$ as its fundamental is started. Obviously this window cannot be started until the dominant mode is distinguished. However, once this is accomplished the most recent data segment corresponding to that fundamental mode is used to obtain the instantaneous behavior. To establish the stable/unstable nature of the current mode the rate of change of the fundamental mode of the FFT window $d|c_{FUNDAMENTAL,FFT\_WINDOW}|/dt$ is determined. In case the rate of change is positive the magnitude of the mode is of an increasing nature and the mode is unstable while for a negative rate of change the mode is damped. Strictly theoretical the approach based on the FFT window to obtain the instantaneous behavior of the mode is dubious as by definition the FFT method is valid for stationary signals only. However, the method has proven to be applicable also here and was therefore customized. Alternatively, in the case of limited confidence in the FFT method, the method can be replaced by an integrator determining the RMS value based on the data segment corresponding to the cycle time of the dominant mode $c_{k,dom}$.

In case the speed deviation is unfiltered the low frequency modes will affect the determination associated with the instantaneous behavior of the signal. This is true both for the FFT and the RMS methods. For example, for the speed deviation of G14 the frequency components below 0.1 Hz will significantly reduce the availability of the methods while in the case of the filtered signal the performance is completely satisfactory. Fig.10 illustrates the instantaneous behavior of the test signal generated by the adapted FFT window function and the RMS computation, respectively. Here a Chebyshev Infinite Impulse Response filter of order 10 was used for the bandpass filtering.

Based on data from all generators the coherency determination is performed in the lower box in Fig.9. First the phase estimation (6) is carried out for each generator's speed signal based on a long sliding window function applying conventional Fast Fourier Transform. Then the coherency is established according to (7) and as a next step the curative actions are determined based on both the coherency and the stable/unstable nature of the mode.

In addition to the two processes described above a continuous verification of the dominant mode must be performed in order to assure the appropriate input modes to the two other processes. The verification is based on the same window function as the detection. In Fig.9 this verification is accomplished by the logic *while* statement and the DROP_DOWN_TIMER. The dominant mode is continuously monitored to confirm its superior status. In order to give up its supervising function the mode must re-

main below any of the levels $K_{pick-up}$ times the second largest mode or $A_{pick-up}$ during a time period of at least $t_{delay,down}$. In addition a continuous mode verification with respect to the other generators is executed which also can dismiss the dominant mode.

Here we have chosen separate timers for the pick-up and drop down of the dominate mode. The background for this approach is to ensure the drop down of the present mode before the pick-up of the new mode in case of gradual mode shifts. However, only one timer may be applied for this process; i.e immediately after the drop down of one dominant mode and in case of a new mode that is $K_{pick-up}$ larger than the second largest mode, the new dominant mode is immediately established as a dominant mode. The new dominant mode will then immediately be used to establish generator coherency and corrective actions. Practically this is a matter of design where the most appropriate approach for the given implementation should be adopted.

For the evaluation of the different DSP methods in Section VI, $K_{pick-up}$ and $t_{delay,up}$ were given the values 1.05 and 300 ms, respectively. Furthermore, for the generic code given in Fig.9 strictly one mode must contain a value larger than $K_{pick-up}$ times the magnitude of all the remaining modes during the whole process. Alternatively, at least one but up to two or three adjacent modes which all clearly deviate from the other remaining modes may also be an appropriate indicator of a dominant mode as the oscillation may arise as multiple adjacent modes due to leakage. Simulations have indicated that the phase of the adjacent modes are similar and thus any of the adjacent modes is feasible for the generator grouping. Thus in case of an approach accepting two adjacent modes, any mode may be used for the phase calculation where the mode occupying the largest magnitude is probably the most immediate choice, while for the three mode approach the most natural concept is to determine the phase for the mode in the middle. Obviously this is a design option where the single mode approach has been adopted in Fig.9 while the three mode approach was applied for the evaluation of the different DSP methods above.

VIII. THE PERFORMANCE OF THE SCHEME

Here the SPS concept in Fig.2 is illustrated based on the test case given in Section V. A central computer is continuously supplied with the spectral coefficients reflecting the speed signals of all system generators. The generators' coefficients are all processed in parallel on identical replicas of the algorithm in Fig.9. When the algorithm in Fig.9 has identified a dominant mode the three parallel processes below DOMINANT_MODE_PRESENT are started. In case we use the 5 s sliding window function together with the covariance method for the identification of the dominant mode, the three parallel processes are started about 8.0 seconds after the initial three phase fault. In fact G14 is the first generator to pick-up up and consequently the detection time is 7.9 s (Table.I) plus approximately 0.1 s to verify that the 0.23 Hz mode is present for all machines. The verification with respect to the remaining generators

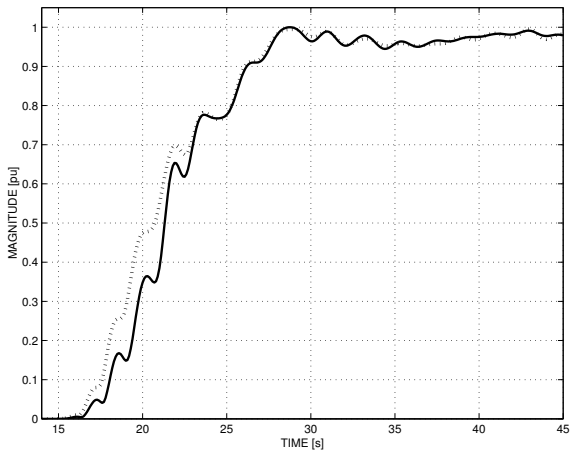

Fig. 10. The magnitude of the fundamental Fourier coefficient 0.23 Hz. Also the "running" RMS value for time segments corresponding to the cycle time of the Fourier coefficient 0.23 Hz is presented. Both graphs are determined from the filtered speed deviation of G14. The 0.23 Hz mode is illustrated by the plain line while the RMS value is given by the dotted line.

is based on spectra showing that the mode is present for all units. Note that the mode is present for most machines, but has not yet picked-up with respect to the given time- and pick-up levels.

When the dominant mode has been established the scheme immediately determines the instantaneous behavior of the oscillation and the generator coherency. Fig.8 indicates that the coherency is well established by this time. Thus based on these data the appropriate corrective measures can be carried out.

Fig.10 shows that the mode is undamped and Fig.8 indicates that G14 is oscillating against the rest of the system. Based on that information generator rescheduling is performed for G14 in order to reduce the power flow on the remaining line between areas A and D. Consequently the oscillations are attenuated. Throughout the whole process the *while* statement in Fig.9 monitors the superior of the 0.23 Hz mode.

IX. DISCUSSION

So far a frequency resolution 0.01 Hz has been applied throughout this paper. However, with respect to the detection time of the dominant mode it may be beneficial to use a lower frequency resolution. The same range of model orders and subspace levels were examined for the 0.1 Hz frequency resolution (Table.III) as for the 0.01 Hz resolution (Table. I). Furthermore, both the pick-up times for the 0.2 Hz and 0.3 Hz modes are given in Table.III as the 0.23 Hz mode is located in between. For all cases the 0.2 Hz mode more or less becomes the dominant mode, although the 0.3 Hz components often give the fastest pick-up times. In general more spurious pick-ups were registered in the case of reduced frequency resolution.

Reduced frequency resolution results in an obstacle, as a less reliable value is obtained for the length of the FFT

window in Fig.9 determining the instantaneous behavior of the speed deviation. Moreover, when Fig.8 is collated to Fig.11, Fig.12 and Fig.13 the relation between reduced frequency resolution and the phase estimation can easily be observed. In case of the reduced resolution the angles of the DFT coefficients vary substantially more, in contrast to the case for the better resolution. Obviously, more pronounced angle variation will lead to less reliable generator coherency determination.

TABLE III

Detection times, $t_{data\_segment}$, in case of frequency resolution 0.1 Hz for window functions corresponding to data segments of 10 s, 5 s and 1 s, respectively. In addition the detection times, t_{evol}, for evolving functions are also presented. Note that the detection time corresponds to the simulation running time at the moment of detection and that the first number corresponds to the pick-up time of the 0.2 Hz mode while the number in brackets is the pick-up time for the 0.3 Hz mode. For "-" no successful detection was obtained.

Method	t_{10} [s]	t_5 [s]	t_1 [s]	t_{evol} [s]
FFT	21.6(18.8)	21.4(18.8)	-(-)	21.2(18.4)
Chirp	21.9(19.0)	21.8(19.0)	-(-)	21.6(18.6)
Periodogram	21.5(18.6)	21.2(18.6)	-(-)	21.1(17.1)
Welch	22.8(19.0)	-(-)	-(-)	21.6(18.3)
Multitaper	21.6(18.8)	21.1(-)	-(-)	20.7(24.6)
Yule-Walker	19.1(20.0)	20.8(-)	-(-)	20.7(17.5)
Burg	18.7(19.5)	18.8(19.6)	-(-)	20.1(-)
Covariance	20.7(19.8)	20.4(18.5)	20.1(16.8)	18.3(18.7)
Modified Covariance	20.7(-)	20.7(18.6)	18.3(17.1)	20.3(-)
Peig	21.0(19.6)	20.6(18.7)	-(-)	20.0(16.4)
MUSIC	21.6(19.0)	-(-)	-(-)	19.9(16.1)
Pisarenko	-(-)	-(-)	-(-)	18.3(-)
Steiglitz-McBride	21.6(18.8)	21.1(30.5)	20.1(16.7)	21.1(16.0)
Prony	21.6(18.8)	20.5(25.7)	-(-)	20.1(16.3)

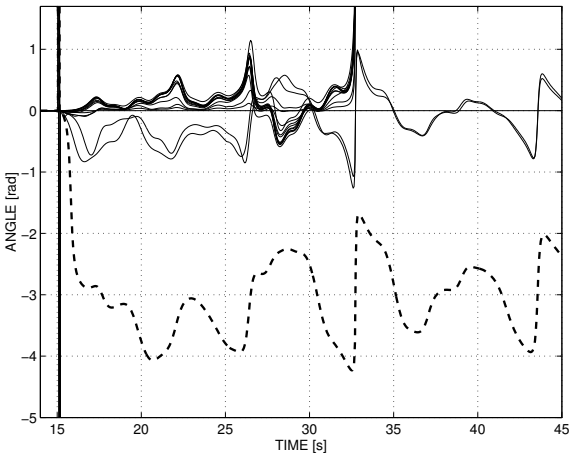

Fig. 11. The phase of the 0.2 Hz mode in the case of frequency resolution 0.1 Hz. The phase of G14 is indicated by the thick dashed line.

In order to reduce the design complexity, the same FFT window as is used for the computation of the instantaneous behavior of the signal can be used for the phase estimation.

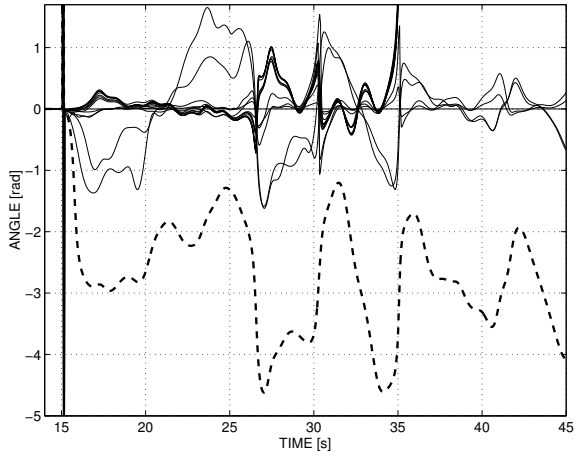

Fig. 12. The phase of the 0.3 Hz mode for frequency resolution 0.1 Hz. The phase of G14 is indicated by the thick dashed line.

However, as mentioned above and as indicated in Fig.13 this approach will obviously suffer from the reduced frequency resolution and consequently generate a less reliable generator coherency.

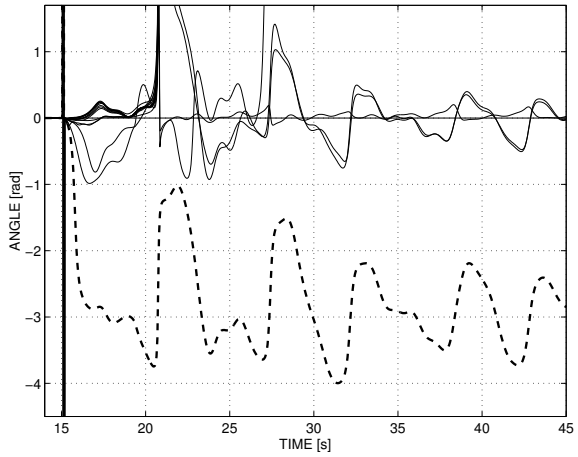

Fig. 13. The phase of the 0.23 Hz mode for all generators in the case of frequency resolution 0.23 Hz. The phase of G14 is indicated by the dashed line.

Here both sliding and evolving window functions have been investigated. There are advantages and disadvantages associated to both approaches. For example, immediately after the disturbance, the sliding window function will be subject to obsolete data. The same is true for an evolving function some time after the initial disturbance in the case of contingencies involving altering system conditions. Obviously the phenomenon may impair the distinction process of the dominant mode. The main obstacle for the evolving window function is the trigger required to (re)start the window at the appropriate moment in order to include the relevant data only. Conventionally, the trigger could be based on a pick-up level associated to any power quantity

or the voltage. However, cases involving altering system conditions cannot be resolved easily by this approach.

Obviously, the ultimate challenge for the scheme introduced here involves changing system conditions at an already critical operating point. For example, a disturbance occurs and an associated group coherency is obtained. Next a subsequent disturbance again leads to a modified grid configuration which in turn may correspond to a new generator coherency. In order to handle this situation, a DSP method with a high frequency- and time resolution is required. Similarly, in the case of emergency situations involving cascading outages, the same requirements are true for the DSP applications. The concept proposed here should support these scenarios. The most crucial part may be the phase estimation based on a long sliding window as obsolete data will affect the current determination of the DFT coefficients. However, as the dominant mode transits from one oscillation frequency to another, only the most recent data will define the phase for the new mode as no previous data can be associated with that new mode. Thus, the long sliding window will also provide a reliable tool for the phase estimation in the case of inter-area mode transitions. A transition from one mode to another and then back to the original mode may lead to difficulties generating the appropriate generator coherency, as data related to the first appearance of the mode will also affect the phase estimation the second time the mode arises. However, the likelihood for such a scenario is very low, in particular that the same mode would occur twice and involve different phase compositions.

According to [3] pronounced multiple modes appear only for generators which are involved in the oscillations to a very limited extent. For the scheme proposed here, the central generator coherency determination based on the phase of the dominant mode is exclusively carried out for the mode *involving all* the generators affected by inter-area oscillations. By that approach examination of the relevant mode is guaranteed. Generators which are uninvolved in the crucial inter-area mode are left out of the coherency investigation as their grouping affiliation must be post-determined in order to avoid subsequent inter-area modes resulting from corrective measures changing the network configuration. Referring to Fig.7 the leakage is especially crucial for cases were multiple modes are involved. However, when the approach given above is applied for multiple modes the associated leakage can be ignored as the mode is anyhow present, with a less developed magnitude though.

X. CONCLUSIONS

This paper introduces a new concept for a System Protection Scheme addressing inter-area oscillation events. To determine generator coherency a method is used based on speed measurements combined with DFT analysis. A number of well established Digital Signal Processing methods have been investigated in order to evaluate their scheme suitability. For the detection of inter-area modes, parametric methods turned out to be the most feasible. Both evolving and sliding window functions have been investigated. Evolving functions generally detect the dominant mode somewhat faster than sliding functions. However, evolving windows require a trigger activated by the presence of an inter-area mode. This trigger may complicate the design of the scheme and thus the design proposed here is based on a sliding window.

The scheme proposed here must be fast. To shorten the detection time of the dominant mode, a reduced frequency resolution can be applied. However, a lower frequency resolution contributes to spectral mode shifts and reduces the quality of the estimate of the instantaneous speed deviation. As a result the discrimination of the unstable/stable nature of the modes is of a lower quality. Also the phase estimation deteriorates which in turn leads to a less reliable generator coherency determination. The design proposed here is therefore based on a high frequency resolution, accepting a somewhat slower response.

The scheme is still at an early stage of development, where the case study used for the analysis in this paper is based on post-processing following a disturbance applied on a network simulation. The next step for implementation should address practical issues supporting real-time operation.

Acknowledgments

The authors would like to thank Svenska Kraftnät for their interest in this research area and for their financial support. The authors also would like to thank ABB Power Systems for providing Simpow. Graham Rogers is acknowledged for his help related to the test system. Professor James H. McClellan, Professor Mats Viberg and Associate Professor Irene Gu are all acknowledged for their help associated to the DSP part. Mattias Jonsson would like to express his sincere gratitude to Professor Miroslav Begovic for accepting him as a visiting scholar in his group during the spring and summer of the year 2002.

References

[1] Wide Area Protection seminar, *Real-Time Monitoring of Fast Dynamic in the Swedish National Grid (Fast RTMS)*, Presentation by Svenska Kraftnät, Västerås, Sweden, April 2, 2001.

[2] Hiskens I.A, Akke M, *Analysis of the Nordel Power Grid Disturbance of January 1, 1997 Using Trajectory Sensitivities*, IEEE Transactions on Power Systems, Vol. 14, No. 3, August 1999, pp. 987 - 993.

[3] Jonsson M, Begovic M, Daalder J, *A new method suitable for real time generator coherency determination*, Submitted to IEEE Transactions on Power Systems.

[4] Begovic M, Djuric P, Dunlap S, Phadke A, *Frequency Tracking in Power Networks in the Presence of Harmonics*, IEEE Transactions on Power Delivery, Vol. 8, No. 2, April 1993, pp. 480 - 486.

[5] Djuric P, Begovic M, *Adaptive Estimation of Frequency in Power Networks*, Proceedings of 1992 International Symposium on Circuits and Systems (ISCAS), San Diego, CA, USA, May 1992, pp. 1024 - 1027.

[6] Oppenheim A.V, Schafer R.W, *Discrete-Time Signal Processing*, 2nd ed, ISBN: 0-13-216292-X, Prentice Hall, 1989.

[7] Jonsson M, *Present Status of System Protection Schemes*, Tech. Report 23R, ISSN 1401-6176, Chalmers University of Technology, Gothenburg, Sweden, 2002.

[8] Sadegh P, Spall J.C, *Optimal sensor configuration for complex systems*, Proceedings of the 1998 American Control Conference, Philadelphia, PA, USA, June 23 - 26, 1998, pp. 3575 - 3579.

[9] Milosovic B, Begovic M, *Nondominated Sorting Genetic Algorithm for Optimal Phasor Measurement Placement*, IEEE Transactions on Power Systems, Vol. 18, No. 1, Feb. 2003, pp. 69 - 75.
[10] Graham Rogers, *Power System Oscillations*, ISBN: 0-7923-7712-5, Kluwer Academic Publisher, 2000.
[11] Fankhauser H.R, Aneros K, A-A Edris. and Torseng S, *Advanced Simulation Techniques for the Analysis of Power System Dynamics*, IEEE Computer Applications in Power, Vol. 3, No. 4, October 1990, pp. 31 - 36.
[12] Qian S, Chen D, *Joint time-frequency analysis - methods and applications*, ISBN: 0-13-254384-2, Prentice-Hall, 1996.
[13] Proakis J.G, Manolakis D.G, *Digital signal processing - principles, algorithms, and applications, third edition*, ISBN: 0-13-394338-9, Prentice-Hall, 1996.
[14] *Matlab Help*, Version 6.1.0.450, Release 12.1 , The MathWorks Inc , 2001.

Mattias Jonsson received his M. Sc. and Lic.Eng from Chalmers University of Technology in 1998 and 2001, respectively. His interest lies in power system stability and power system protection. At present he works towards a Ph.D. thesis.

Jaap Daalder obtained his Ph.D in power engineering from the Eindhoven University of Technology, The Netherlands. He worked there as an Associate Professor until 1984 when he left for Norway to become a Director of Technology and Member of the Board of a subsidiary of the Brown Boveri Company, nowadays ABB. In 1993 he was appointed as full Professor at Chalmers University of Technology. Since 1997 he is heading the Department of Electric Power Engineering. His areas of interest are power systems and environmental issues related to power engineering.

Miroslav Begovic (S'87, M'89, SM'92) is Associate Professor in the School of ECE, Georgia Institute of Technology in Atlanta, Georgia. His interests are in the general area of computer applications in power system monitoring, protection and control, and design and analysis of renewable energy sources. Dr. Begovic chairs the Working Group "Wide Area Protection and Emergency Control" in the Power Systems Relaying Committee of the IEEE Power Engineering Society. Dr. Begovic's work on distributed generation and photovoltaic (PV) systems has resulted in design of the 340 kW PV system on the roof of the Georgia Tech Aquatic Center, which was the largest of its kind at the time of initial deployment. Dr. Begovic is a Senior Member of IEEE's Power Engineering, Circuits and Systems, and Computer Societies, and a member of Sigma Xi, Tau Beta Pi, Eta Kappa Nu, and Phi Kappa Phi.

Paper F

An emergency strategy scheme based on conventional distance protection to avoid complete system collapse

M. Jonsson, J. Daalder, K. Walve

Accepted for
IEEE/PES Transmission and Distribution Conference and Exposition,
September 7 - 12, 2003, Dallas, USA.

An Emergency Strategy Scheme Based on Conventional Distance Protection to Avoid Complete System Collapse

Mattias Jonsson, *Student member, IEEE,* Jaap Daalder and Kenneth Walve

Abstract: An emergency protection scheme which prevents a system collapse in the case of extreme voltage instability is proposed. The scheme is based on conventional distance protection.

The performance of the scheme was analysed using the NORDIC32 test system. The test case confirms that complete system collapse can be prevented when the relevant distance relays are given settings according to the proposed method. As a result the restoration time after a power system breakdown can be significantly reduced.

Keywords: Distance protection, Emergency scheme, Voltage collapse, Wide Area Protection.

I. INTRODUCTION

In the Swedish electrical power system the main load centres are located in the south region while a significant part of the generation is located in the north. The regions are separated by hundreds of miles and thus the Swedish bulk power system involves large power transfers over long distances. Deregulation resulting in the decommission of (small) power plants in the south part of Sweden has further enhanced the radial system characteristic of the system. The possibilities for local generator support in the case of power system instability have obviously been reduced and local reactive supply in the case of voltage instability has deteriorated. In addition an increased variation of power flow directions has been experienced during recent years. Experience has shown that voltage collapse is restricted to the southern regions. However, with respect to the new situation, there is an enhanced risk that a contingency in the southern part will propagate further north affecting an increasing portion of the system. The main concern associated with this scenario obviously is a complete system collapse following an extensive restoration time. Much time can be saved by maintaining the voltage in some part(s) of the system and thereby keeping some generators synchronized. Here we introduce an emergency scheme avoiding complete system collapse as a result of voltage instability. The scheme represents the ultimate “last call action“ and should exclusively be activated when system stability cannot be maintained by any other conventional measure.

This work was financially supported by Svenska Kraftnät.

Mattias Jonsson and Jaap Daalder are both with the Department of Electric Power Engineering, Chalmers University of Technology, 412 96 Gothenburg, Sweden. Their e-mail addresses are mattias.jonsson@elteknik.chalmers.se and jaap.daalder@elteknik.chalmers.se. Kenneth Walve is with Svenska Kraftnät and his e-mail address is kenneth.walve@svk.se

II. THE EMERGENCY SCHEME

The scheme is based on a strategy where the purpose is to maintain voltage stability in a part of the system in order to avoid a complete system breakdown. It should only operate for situations where there is no other way to maintain voltage stability within the complete system by any other means. Hence the scheme is primarily intended for extreme contingencies.

The scheme is based upon conventional Zone 3 distance relays and can have a varying degree of sophistication; e.g stand alone or be a part of an extensive protection strategy including communication equipment. However, in its basic form only local data are utilized and the scheme will function also in emergency situations, where for example communication links are out of service.

In the case of voltage instability lower voltages and increased (reactive) power flows will lead to a reduced apparent impedance as seen by the distance protection. The function of the scheme is obtained by assigning the Zone 3 distance relays for all lines associated to the intersection between the region to be saved, and the remaining system, settings corresponding to the operating point “system beyond recovery“. In the case of an irrevocable collapse the tripping zones for these distance relays are entered. As a result the scheme separates the system part to be saved and a stable operating condition can be established. The separation is simply carried out by tripping the lines interconnecting the region to be saved from the surrounding system. Obviously, the region where stable voltage is secured must be carefully chosen with respect to reliable island operation at the same time as the objective should be to minimize the breakdown

area. The scheme is to a certain extent similar to out-of-step procedures involving system separation, although the scheme proposed here is addressing voltage instability.

III. THE SETTINGS OF THE DISTANCE RELAYS

The aim is to identify the appropriate settings for the Zone 3 distance relays for the transfer section intended for system separation. The main challenge is to accurately determine if the system is operating beyond recovery, and then to identify the corresponding apparent impedances as seen by the relays.

The setting process for the distance relays is given in Fig. 1. First all lines of the transfer section are assumed to be in service (BLOCK 1) and their total line equivalent is established (BLOCK 2). Next the power injected into the interconnection is determined for all relevant operating conditions (BLOCK 3). Lines are modelled as π-equivalents in ARISTO [1] (which is used for our illustration in section IV) and therefore a technique based on the PV-curve is adopted in order to examine the relevant operating conditions (BLOCK 3b). However, more full scale static and dynamic investigations may be required in case of more complicated systems. In BLOCK 3b all stable operating conditions are investigated by examining all possible combinations of relevant sending end voltages, $V_{send,a}$, and receiving end voltages, $V_{rec,j}$, for the line equivalent. Based on system experience of the test system, the injected- and received reactive powers associated to the transfer section have been given the value zero. In case this assumption cannot be adopted, the reactive powers must be a non-fixed variable for the investigation; i.e Q_{rec} is varied between the possible maximum (Q_{max}) and minimum (Q_{min}) reactive power levels.

The equation (5) is solved with respect to the received active power P_{rec} and under the condition given in (6). The α and β variables are defined by (7) - (9). As a next step the corresponding injected power, $P_{injected,a}$, is determined based on loss-summation (10)-(11). The process (5)-(11) is executed for all possible operating conditions $V_{send,a}$ and $V_{rec,j}$, where the resulting powers $P_{injected,a}$ are organized into the matrix $\mathbf{P_{injected,i}}$. In order to determine the relevant operating impedances also the corresponding sending end voltage matrix $\mathbf{V_{send}}$ is established. When all possible active powers to be injected into the transfer section, $\mathbf{P_{injected,i}}$, have been determined they are used together with their corresponding sending end voltages $\mathbf{V_{send}}$ to identify the apparent impedance identifying the operating point "system beyond recovery" (BLOCK 4). Obviously this condition is identified by the smallest possible apparent impedance resulting from the square of the sending end voltage divided by the sending end power (12). In (12) a value ε is subtracted from the smallest apparent impedance in order to assure settings corresponding to unstable operation. As the minimum value resulting from the division in (12) in fact represents the smallest impedance possible for stable operation. The relay setting for the transfer section configuration is determined in (13).

As a next step one line is removed from the transfer section (BLOCK 6) and the same calculations are carried out for the new section configuration (BLOCK 2 - BLOCK 4). During this process, always the longest line (largest impedance) is removed since the scheme should NOT operate for a stable operating condition and priority is given to security. Finally, when the calculations are performed for all possible operating conditions and for all transfer section configurations, the setting for the Zone 3 relays, $R_{3,set}$, is chosen (BLOCK 7). The minimum value is selected since no possible stable condition should lead to tripping of the transfer section.

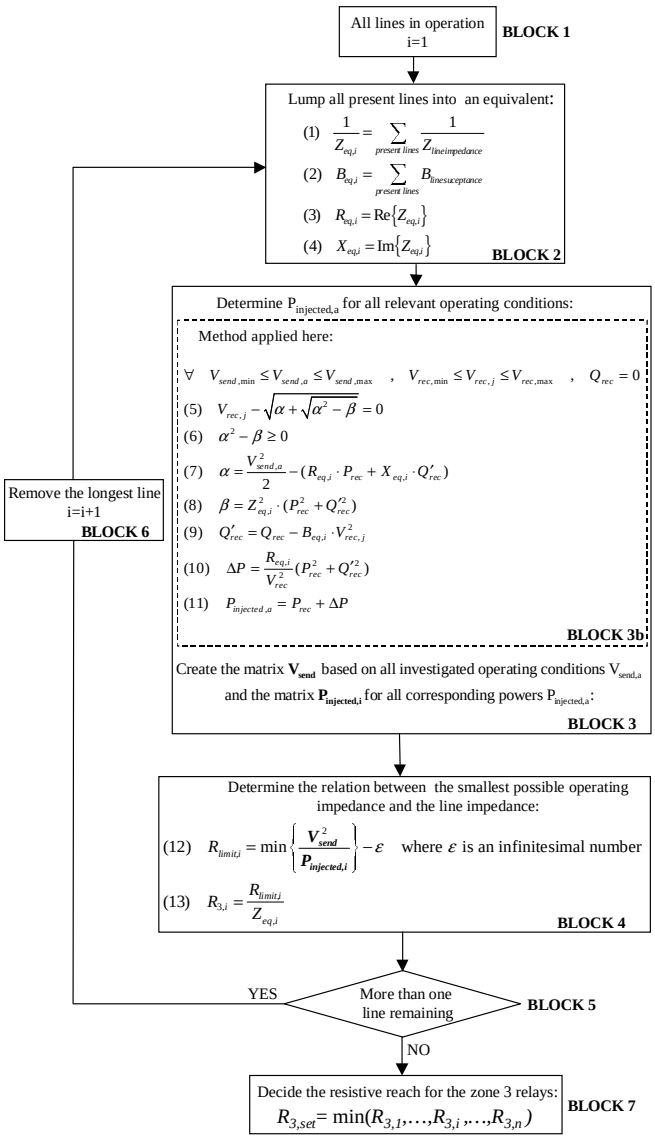

Fig. 1. Flow chart for the setting process. Note that normal variables correspond to real numbers while bold variables represent vectors and matrixes.

The same setting $R_{3,set}$ is used for all lines in order to synchronise the tripping process of all relays. The relays of the longer lines will reach a bit longer in Ω as compared to the relays of the shorter lines but this is compensated by the slightly smaller power flow due to the larger line impedance. As a result the tripping will occur at the same time for all lines. Note that the transfer section is considered as a number of parallel lines, while in reality this assumption is only a fair reflection of the true system. Accordingly, the lines will most likely not trip at exactly the same moment. This is of less importance but the main issue is that no line should trip in case of stable operation. For an unstable case it is sufficient if at least one line is tripped as the resulting power re-distribution after the loss of the first line will accelerate the tripping of the remaining lines.

The reactive reach for distance protection is strongly linked to fault conditions. In addition to the fault resistance the resistive reach has a close relationship to normal operation involving load encroachment. The setting process described here addresses only the resistive reach of the distance protection. The selectivity of the protection system is thereby secured as the resistive settings given by this method will not affect the fault clearing with respect to distance but only with respect to fault resistance.

IV. TEST CASE

The simulation used to illustrate the protection scheme was performed in ARISTIO [1] and the NORDIC32 system [2] displayed in Fig. 2 was applied as the test system. The NORDIC32 network represents a test system with similar dynamic behaviour as the Swedish bulk power system. The system involves large power transfers from the Northern hydro dominated regions to the main load centres in the Central and SouthWest areas. The generation in the Central and SouthWest regions is mainly based on thermal power.

Two test scenarios are given in [2]; a peak load scenario where the n-1 design criteria are completely assured, and an extreme (but possible) load condition where *almost* all n-1 contingencies result in acceptable post-contingency conditions. Extensive (simulation based) studies have indicated that the maximum power transport from the North region towards the Central should be limited to about 2850 MW in order to sustain any n-1 contingency. For the extreme case given in [2] about 3260 MW is transferred between the two regions. In our test case we have a power transport between the two regions of about 3100 MW immediately before a contingency event is launched. The increased power transport as compared to the peak load scenario given in [2] is mainly due to reduced generation (loss of one unit) in the SouthWest region. At the same time the spinning reserve in the Central and SouthWest regions are preserved at an acceptable level. Note that in contrast to the n-1 contingency illustrated below, most n-1 contingencies lead to acceptable post-contingency conditions also for a load condition of 3100 MW.

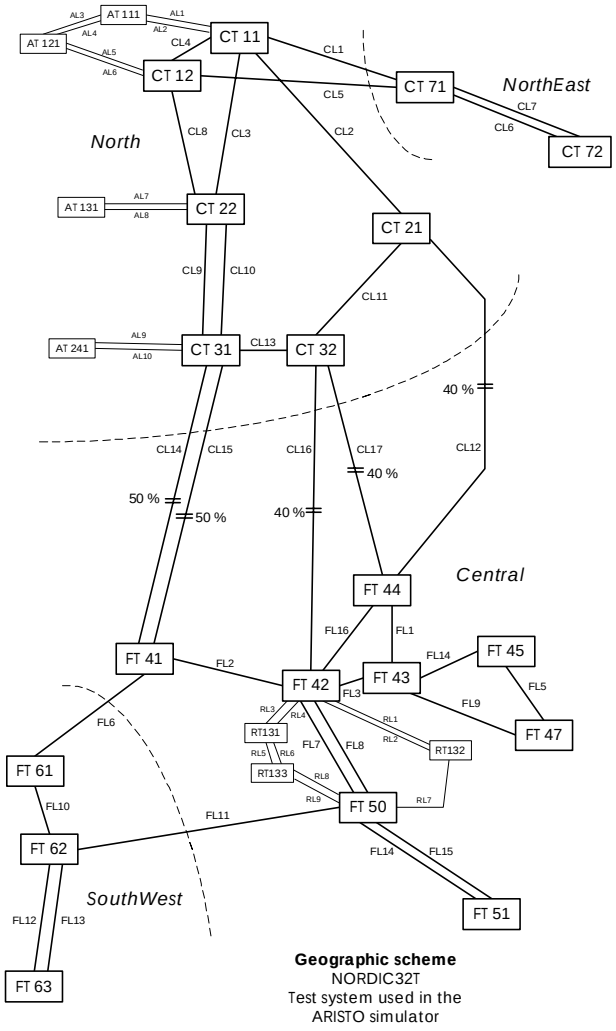

Fig. 2. The NORDIC32 test system.

The triggering event for the contingency is the permanent loss of one generation unit in station FT63. The unit tripping leads to a further increased power transfer over the North-Central interconnection. Consequently, a long term voltage collapse is initiated in the SouthWest and Central regions where the voltages are continuously decreasing resulting in a propagating voltage reduction affecting the Northern regions as well. About 160 s after the initial generator loss a complete system blackout is a fact, although automatic schemes involving shunt switching and load shedding were initiated. The interconnecting lines CL14 and CL15 were never tripped and the Northern regions were never separated from the remaining system. This is one of the main reasons for the complete

system collapse. The original distance protection settings for the transfer section are given in Table 1.

Table 1. Original Zone 3 settings in the resistive direction. The reach of the relay is obtained from the product of the setting factor R_3 and the line reactance.

Line	R_3 [pu]
CL12	1.1
CL14, CL15	0.6
CL16, CL17	0.72

Next, the distance protection for stations located in the North region and associated to the North-Central interconnection were given settings according to the method proposed in section III. First the active powers, P_{rec}, were obtained for all possible operating conditions (5)-(9). The non-linear equations were solved by conventional numerical methods and as a next step the relevant settings were determined from (10)-(13). Finally, when the relay settings had been determined for all possible system configurations, the appropriate Zone 3 setting could be selected. The settings obtained from (13) for each loop i in the setting process of Fig. 1 are given in Table 2. For illustration also the setting factors for the cases where the shortest lines were removed are given. Table 2 confirms that the case to be used for the relay settings is the one where the longest lines are removed since the restricting settings are then obtained.

Table 2. Zone 3 setting factors for different network configurations determined from (13) in Fig. 1.

Number of lines in service between the North and Central regions.	$R_{3,i}$ [pu] (longest line removed)	$R_{3,i}$ [pu] (shortest line removed)
All lines (i=1)	1.0091	1.0091
4 lines (i=2)	1.0072	1.0105
3 lines (i=3)	1.0074	1.0132
2 lines (i=4)	1.0051	1.0153
1 line (i=5)	1.0056	1.0213

For the setting process the voltages were varied in steps of 0.01 pu where V_{min} and V_{max} corresponded to 0.8 pu and 1.05 pu. The max and min values were selected with respect to the settings of the remaining system devices. For example, all Generator UnderVoltage Protection schemes operate at voltages of 0.82 pu or higher. From Table 2 the setting factor 1.0 pu was decided to be an appropriate choice for the relay settings which means that the resistive reach had to be increased for all relays, apart from the CL12 device. The distance protection used in ARISTO is of box form and accordingly all distance relays in the North region and associated to the interconnection were given the resistive reach 1 pu with respect to its own line reactance. Note, according to the implementation of the distance relays in ARISTO $Z_{eq,i}$ is here replaced by $X_{eq,i}$ in (13) for the setting process. Consequently, the resistive reach of the relays are given with respect to their line reactance and not their total line impedances.

The test case was investigated with the new relay settings. About 143 s after the initial generator loss CL12, CL14, CL15 and CL 16 are tripped by their distance protection. Seven seconds later also the relay of CL 17 operates and the North and NorthEast regions are completely separated from the remaining regions. Consequently, the northern regions are protected and immediately recover to a normal operating condition, while the Central and SouthWest regions are subjected to a collapse.

Immediately after the first four lines are tripped the voltage in the Central and SouthWest regions drops rapidly which in turn initiates load shedding. The tripping of CL 17 is delayed by this load shedding as the power through the transfer section is reduced. Additionally, some generator shedding is required in the North region in order to avoid over-frequency after the initial line tripping. Also the generator shedding will reduce the power transfer over the interconnection and contribute to the delay of the tripping of CL17. Generator shedding is required since the NORDIC32 system is relatively small and there is insufficient system capacity to absorb the surplus power within an acceptable time frame.

If communication equipment is used the co-ordination of the line tripping can be further improved by adding a device that trips all lines when e.g three out of five lines are out of service as there is no practical possibility that the system will remain stable for such an operating condition.

V. DISCUSSION

Today duplicated main protection is often used for transmission lines, and the Zone 3 relays can conveniently be used for the emergency scheme proposed here. Distance relays usually provide more than three tripping zones and thus the scheme can also be operated for systems applying remote back-up or reversed tripping schemes based on communication. For certain relay characteristics (e.g mho) the settings in the resistive and reactive direction are dependent on each other. When those relays are used for transfer sections relevant to the emergency scheme the associated conventional remote back-up zones most likely require a longer reach than the relay settings

required by the scheme due to the very large line impedances involved. Thus, the traditional remote back-up protection may inherently provide a function where regions are separated in the case of abnormal operating conditions; the separation will be carried out in an unforeseen manner though. However, conventional long remote back-up settings should be prevented as they may lead to mal-trips due to load encroachment which in turn may significantly increase the probability of instability [3]. On the other hand the separation principle based on load encroachment by distance protection can be adopted, but the system separation should be accomplished in a controlled and pre-determined manner.

According to the nature of the scheme, caution should be given to the setting process as inappropriate settings can be detrimental. In order to obtain an overall reliable performance with respect to both the scheme and normal fault clearing, only distance relays offering separated setting-mechanisms in the resistive and reactive direction should be used. The scheme should be used together with Out-of-Step protection in order to obstruct the increased mal-trip possibility resulting from increased tripping zones.

In the case of systems operating at line loading levels below Surge Impedance Loading, as the NORDIC32, reversed distance protection reach may be required. However, as the time delay of the Zone 3 elements are much larger than the time delays of the interacting forward reach Zones 1 and 2, the selectivity should be unaffected. For the test case in section IV the reversed approach was rejected. Nevertheless, by applying this technique the tripping co-ordination time for CL 17 will be significantly improved and the time gap between the tripping of the first four lines and CL 17 is accordingly reduced.

In the case where a shorter reach is obtained for the Zone 3 element than for the Zone 1 and 2 elements, i.e the reach obtained is less than the required fault resistance, priority must obviously be given to the fault resistance. However, with respect to relevant system and fault data this scenario is highly unlikely.

To restrict the number of lines removed in the case of a contingency, the distance protection settings obtained for the scheme can also be used for remote control of load shedding and other conventional corrective measures. However, the scheme should primarily be an extremely reliable final measure to avoid a complete collapse and should therefore be independent of long distance communication.

VI. CONCLUSIONS

An emergency scheme based on conventional Zone 3 distance protection has been proposed where the scheme avoids a complete system collapse in the case of severe voltage instability. The scheme is simple in its nature and easy to implement as it is using relays which are already in service. The main incentive for the scheme is to avoid a complete breakdown as this leads to an extremely time consuming restoration process. Furthermore, the scheme is intended to be a robust and final corrective measure for situations when there is no way to maintain voltage within the entire system.

The performance of the scheme has been illustrated from a test case based on the NORDIC32 system. The scheme showed an encouraging performance. A complete system collapse as in the case of original relay settings was restricted to a partial collapse when the scheme was applied.

If long distance communication applications are introduced the method can also be utilized for a more extensive Wide Area Protection System. Examples are supervising remote control of load- and/or generator shedding.

VII. ACKNOWLEDGEMENTS

The authors would like to thank Svenska Kraftnät for their interest in this research area and for their financial support.

VIII. REFERENCES.

[1] Edström A, Walve K, ”A Highly Interactive Fast Simulator Covering Transients Stability and Long Term Dynamics in Large Power Systems”, CIGRÉ Report 38-204, Paris, August 28-September 3, 1994.

[2] CIGRÉ TF 38-02-08, ”Long Term Dynamics Phase II”, 1995.

[3] Jonsson M, ”Line Protection and Power System Collapse”, Technical Report No. 393L, Chalmers University of Technology, Sweden, 2001.

IX. BIOGRAPHIES

Mattias Jonsson received his M. Sc. and Lic.Eng from Chalmers University of Technology in 1998 and 2001, respectively. His interest lies in power system stability and power system protection. At present he works towards a Ph.D. thesis.

Jaap E. Daalder obtained his Ph.D in power engineering from the Eindhoven University of Technology, The Netherlands. He worked there as an Associate Professor until 1984 when he left for Norway to become a Director of Technology and Member of the Board of a subsidiary of the Brown Boveri Company, nowadays ABB. In 1993 he was appointed as full Professor at Chalmers University of Technology. Since 1997 he is heading the Department of Electric Power Engineering. His areas of interest are power systems and environmental issues related to power engineering.

Kenneth Walve received his M. Sc. from the Royal Institute of Technology, Stockholm in 1969. For many years he worked at Vattenfall (The Swedish State Power Board) and since 1992 at Svenska Kraftnät (Swedish National Grid). His tasks has been power system analysis and now he is working mainly with operator training and special projects.